NAVAL POSTGRADUATE SCHOOL

MONTEREY, CALIFORNIA

THESIS

GEOLOCATION OF SOURCE INTERFERENCE FROM A SINGLE SATELLITE WITH MULTIPLE ANTENNAS

by

Brian C. Fredrick

March 2014

Thesis Advisor: Charles M. Racoosin
Second Reader: Daniel W. Bursch

Approved for public release; distribution is unlimited

THIS PAGE INTENTIONALLY LEFT BLANK

REPORT DOCUMENTATION PAGE

Form Approved OMB No. 0704-0188

1. AGENCY USE ONLY *(Leave blank)*	**2. REPORT DATE** March 2014	**3. REPORT TYPE AND DATES COVERED** Master's Thesis

4. TITLE AND SUBTITLE
GEOLOCATION OF SOURCE INTERFERENCE FROM A SINGLE SATELLITE WITH MULTIPLE ANTENNAS

5. FUNDING NUMBERS

6. AUTHOR(S) Brian C. Fredrick

7. PERFORMING ORGANIZATION NAME(S) AND ADDRESS(ES)
Naval Postgraduate School
Monterey, CA 93943-5000

8. PERFORMING ORGANIZATION REPORT NUMBER

9. SPONSORING /MONITORING AGENCY NAME(S) AND ADDRESS(ES)
N/A

10. SPONSORING/MONITORING AGENCY REPORT NUMBER

11. SUPPLEMENTARY NOTES The views expressed in this thesis are those of the author and do not reflect the official policy or position of the Department of Defense or the U.S. Government. IRB Protocol number ____N/A____.

12a. DISTRIBUTION / AVAILABILITY STATEMENT
Approved for public release; distribution is unlimited

12b. DISTRIBUTION CODE

13. ABSTRACT (maximum 200 words)

Interference of satellite communications is a frequent and ongoing concern for both DoD and civilian enterprises. Geolocation of the interfering source is an essential step in mitigating or eliminating the interference and restoring operation of the communications service. Existing techniques to locate sources of such interference are not applicable to newer satellite communications systems.

This thesis offers an innovative method for locating interference that takes advantage of modern multi-antenna satellites. The location of a source of radio frequency interference can be determined by comparing the received signal strength across multiple antennas on the same satellite. The difference between signal strength—as received by the satellite antennas—can be computed and plotted as lines of position on the surface of the Earth. The intersection of two or more lines of position represents the location of the interfering transmitter.

An advantage of this method is that it is completely passive and can be done in real time. The size and accuracy of the resultant geolocation area are a function of a number of different factors, including terrestrial latitude of the interfering transmitter, the accuracy of the signal strength measurement, and the geometry of the intersecting lines of position.

14. SUBJECT TERMS RF Interference Geolocation, Single Satellite Geolocation, Multiple Antenna Geolocation, Ka Geolocation	**15. NUMBER OF PAGES** 181
	16. PRICE CODE

17. SECURITY CLASSIFICATION OF REPORT	**18. SECURITY CLASSIFICATION OF THIS PAGE**	**19. SECURITY CLASSIFICATION OF ABSTRACT**	**20. LIMITATION OF ABSTRACT**
Unclassified	Unclassified	Unclassified	UU

NSN 7540-01-280-5500

Standard Form 298 (Rev. 2-89)
Prescribed by ANSI Std. 239-18

THIS PAGE INTENTIONALLY LEFT BLANK

Approved for public release; distribution is unlimited

GEOLOCATION OF SOURCE INTERFERENCE FROM A SINGLE SATELLITE WITH MULTIPLE ANTENNAS

Brian C. Fredrick
Lieutenant Commander, United States Navy
B.S., Carnegie Mellon University, 2002

Submitted in partial fulfillment of the
requirements for the degree of

MASTER OF SCIENCE IN SPACE SYSTEMS OPERATIONS

from the

NAVAL POSTGRADUATE SCHOOL
March 2014

Author: Brian C. Fredrick

Approved by: Charles M. Racoosin
Thesis Advisor

Daniel W. Bursch
Second Reader

Rudolf Panholzer
Chair, Space Systems Academic Group

THIS PAGE INTENTIONALLY LEFT BLANK

ABSTRACT

Interference of satellite communications is a frequent and ongoing concern for both DoD and civilian enterprises. Geolocation of the interfering source is an essential step in mitigating or eliminating the interference and restoring operation of the communications service. Existing techniques to locate sources of such interference are not applicable to newer satellite communications systems.

This thesis offers an innovative method for locating interference that takes advantage of modern multi-antenna satellites. The location of a source of radio frequency interference can be determined by comparing the received signal strength across multiple antennas on the same satellite. The difference between signal strength—as received by the satellite antennas—can be computed and plotted as lines of position on the surface of the Earth. The intersection of two or more lines of position represents the location of the interfering transmitter.

An advantage of this method is that it is completely passive and can be done in real time. The size and accuracy of the resultant geolocation area are a function of a number of different factors, including terrestrial latitude of the interfering transmitter, the accuracy of the signal strength measurement, and the geometry of the intersecting lines of position.

THIS PAGE INTENTIONALLY LEFT BLANK

TABLE OF CONTENTS

THIS PAGE INTENTIONALLY LEFT BLANK

LIST OF FIGURES

THIS PAGE INTENTIONALLY LEFT BLANK

LIST OF TABLES

THIS PAGE INTENTIONALLY LEFT BLANK

LIST OF ACRONYMS AND ABBREVIATIONS

2D	two dimensional
3D	three dimensional
AOI	area of interest
AOP	area of probability
BPF	bandpass filter
CCI	co-channel interference
dB	decibel
DoD	Department of Defense
EIRP	effective isotropic radiated power
EM	electromagnetic
EMI	electromagnetic interference
FDOA	frequency difference of arrival
FOM	figure of merit
FOV	field of view
GEO	geosynchronous Earth orbit
G_R	gain of receiving antenna
G_T	gain of transmitting antenna
IF	intermediate frequency
JSIR	joint spectrum interference resolution
km^2	square kilometers
L_{FS}	free space loss
LNA	low noise amplifier
L_T	losses associated with a transmitting antenna
MUOS	mobile user objective system
NCA	narrow coverage antenna
sq mi	square miles
QPSK	quadrature phase-shift keying
P_T	power transmitted
RF	radio frequency
RFI	radio frequency interference

SATCOM	satellite communications
SSP	subsatellite point
STK	Systems Tool Kit
TDOA	time difference of arrival
WGS	wideband global SATCOM

ACKNOWLEDGMENTS

This thesis would not have been possible without significant assistance from a number of very special people. First, thank you to my thesis advisor, Charles Racoosin, for everything. There are not enough words, paragraphs, or pages to express how grateful I am for your patience, guidance, and support over the past year. This thesis has been an unparalleled learning opportunity that could not have happened without you.

Thank you to Dan Bursch, both for your valuable inputs as second reader and for the numerous occasions where you have provided perspective and career advice. I sincerely hope that one day I will be asking you for house hunting tips in Houston.

Thank you to Herschel Loomis, Jim Newman, Rudy Panholzer, and Al Scott for volunteering your time to "murder board" this thesis. Your suggestions and critiques have significantly improved the quality of this research.

Thank you to Frank Kragh for providing his knowledge and assistance in researching the concepts relating to the signal flow of a communications satellite.

Thank you to Major Sarah Alcaide for selflessly testing the STK tutorial and providing feedback on areas requiring improvement.

Finally, and most significantly, thank you to all of my girls, Jenn, Taylor, Madeline, and Emma, for your unconditional love and support throughout this process. Thank you Jenn for being my partner and best friend; nothing in my life would be possible without you. Thank you to Taylor, Mads, and Emma for always being there to pick me up when I was down, to make me smile when I was sad, and to make me silly when I was serious. I love all of you, and I cannot wait to celebrate completing this thesis with you!

THIS PAGE INTENTIONALLY LEFT BLANK

I. INTRODUCTION

This thesis offers an innovative method for locating interference that takes advantage of modern multi-antenna satellites. The thesis is organized into five chapters. Chapter I discusses the foundational material for the new geolocation method. The first part of Chapter I is introductory material essential to the thesis. Chapter I then identifies signal interference as a common problem that arises in satellite communications and explains why it is crucial to find a means of locating the source of such interference. Next, a brief history of past geolocation methods leads into an explanation of current geolocation techniques. This discussion will show why a new method of geolocation is needed and how modern communications satellites have enabled such a method.

Throughout the thesis it is mostly assumed that the reader has a basic familiarity with concepts relating to orbital mechanics, satellite communications, and associated terminology. However, many concepts from these areas are explained in detail because they focus the reader's attention on ideas that are integral to the geolocation method.

Chapter II explains the new geolocation method in detail. It includes a conceptual review of antenna gain, antenna field of view (or footprint), and how antenna gain patterns can be used in the new geolocation method. Next, Chapter II introduces the signal strength equation and explains how EIRP and free space loss can be canceled despite being unknown quantities. Then, Chapter II explains the concept of difference contours and how the intersection of difference lines of position form the geolocation area. Finally, Chapter II concludes with a discussion of the advantages of the geolocation model, as well as assumptions made in developing the method.

Chapter III thoroughly covers the use of Systems Tool Kit (STK) software to setup and model the new geolocation technique. This includes the use of pertinent STK objects and manipulation of STK functionality to calculate the elements required for successfully modeling and employing the geolocation method.

Chapter IV discusses the initial proof of the geolocation method, testing the method in four different regions of latitude, and an analysis of the results in each group.

Chapter IV also includes a collection of graphics produced by conducting the geolocation method for emitters in varying locations in each region of latitude. Chapter IV finishes with an analysis of any conclusions that can be reached after analyzing the data produced from testing the method in each latitude region.

Chapter V is the concluding chapter. It compiles all of the conclusions made in this thesis and discusses potential applications of the geolocation method. It also recommends possible areas for future research that were beyond the scope of this thesis.

A. BASIC SATELLITE COMMUNICATIONS SYSTEM

A generic communications system is composed of three parts: a space segment, a ground segment, and a control segment [1, pp. 4-5]. The space segment is the satellite(s) used in the communications system, the ground segment consists of any user, facility, ship, aircraft, etc., that is passing traffic through the communications system, and the control segment includes any ground facilities tasked with controlling and monitoring the satellite(s).

Within that arrangement, there are three main components of the *communications link* that allow for the transfer of information between segments of the communications system: a transmitter, a receiver, and the physical distance between them [2, p. 406]. This basic relationship is shown in Figure 1.

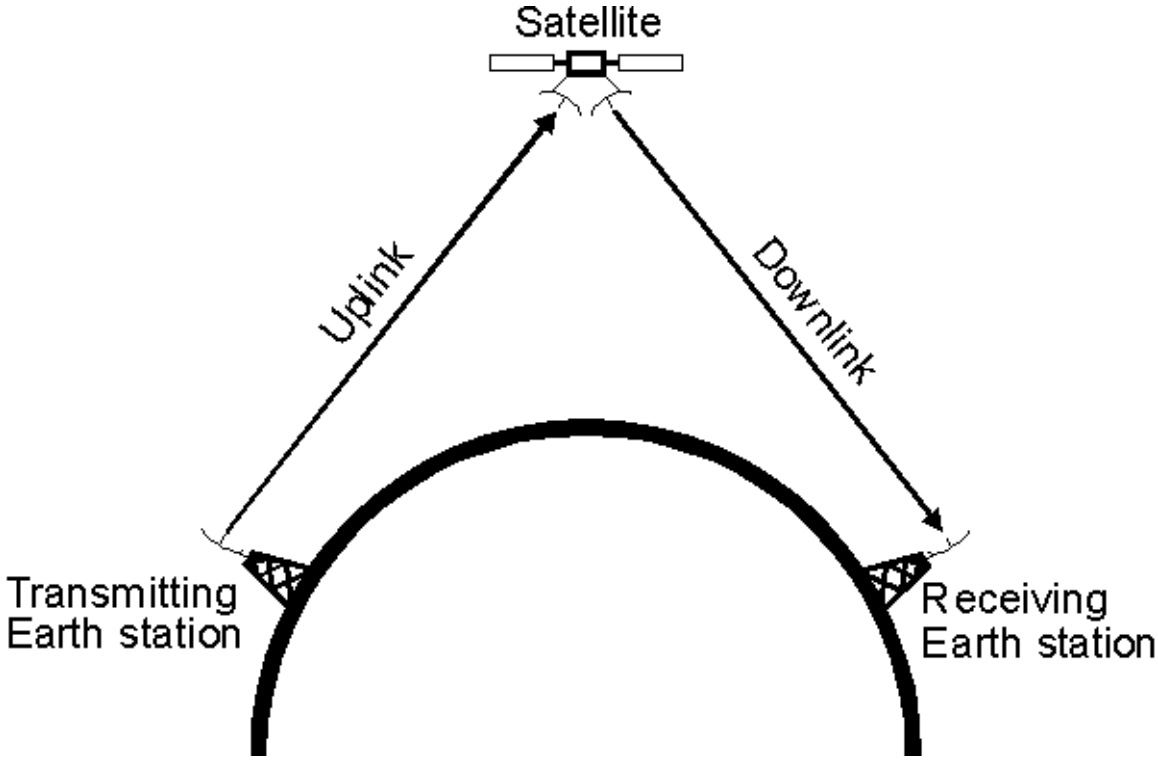

Figure 1. Basic Satellite Communications System (from [3]).

The *uplink* of a communications link is the portion that involves transmitting a signal from Earth to the satellite. More specifically, a transmitting antenna on Earth is sending information that is received by a receiving antenna on the satellite in orbit. The object that is transmitting can be any number of different platforms. Examples include ground facilities, mobile users, cars, ships, aircraft, etc. The *downlink* is the portion of the communications link that involves transmitting a signal from the satellite to a receive antenna on Earth. The receiving antenna can also be a ground facility, mobile user, aircraft, etc. In both of these cases, the distance covered by the signal (from transmitter to receiver) is known as the *free space*.

B. THE PROBLEM

The concept of communicating via satellites in geosynchronous orbit was described by Arthur C. Clarke in 1945 and first put into practice in the early 1960s [4]. Since that time, satellite communications have grown into a large and vital industry used by both military and civilian practices worldwide. The 21st century has seen the U.S.

Government become increasingly reliant on global satellite communications (SATCOM) services, especially with prolonged military operations in Iraq and Afghanistan [5, p. ES-1].

Continuing and growing demand for these services has led to an increase in both the number of communications satellites on orbit and the volume of voice/data/video transiting satellite communication links. The commercial satellite communications industry has significantly expanded its role in supplying a myraid of services to support the increased demand. In 2009, commerical satellite systems provided over 85 percent of the Department of Defense's (DoD) global SATCOM [5, p. 1].

This growth has contributed to increased congestion within the finite electromagnetic (EM) spectrum allocated for satellite communications as users and providers alike seek additional capacity and a greater geographic reach for these services. This in turn has led to an increase in the opportunity for and susceptibility to electromagnetic interference (EMI) from undesired radio frequency (RF) signals [6].

EMI is defined as "any EM disturbance that interrupts, obstructs, or otherwise degrades or limits the effective performance of electronics or electrical equipment." [7, p. A–1] Satellite communications interference can be attributed to a variety of sources, including human error, adjacent satellite interference, terrestrial interference, equipment failure, and intentional interference [5, pp. 21–25]. Human error, adjacent satellite interference, and equipment issues can all be alleviated with proper SATCOM system planning, testing, and training. Once these issues are handled, the two potential sources of interference that remain can either be classified as unintentional or intentional interference. These are transmissions originating from within the effective field of view (FOV) of the receiving (uplink) antenna on the geostationary (GEO) satellite which corrupt or deny the intended communication [7, p. A–4]. The concept of antenna FOV is explained in greater detail in Chapter II.

Most current GEO communications satellites employ transponded payloads which receive a signal within a particular RF band, amplify it, translate it to a different frequency for downlinking, and retransmit the signal down to a ground station (or ground

user) [8, pp. 204–205]. These transponded systems have no way of distinguishing an interfering signal from a legitimate signal and thus have no means of removing it. Therefore, the transponded system will propagate an unwanted signal as if it were legitimate. This signal interference can lead to overall communication degradation, disruption, or complete denial of service, regardless of whether interference is deliberate or unintentional.

The Chairman of the Joint Chiefs of Staff Manual 3320.02D (3 June 2013) was published with the specific goal of establishing standardized techniques, tactics, and procedures for resolving EMI. Within that publication, the *geolocation* of an interfering source is identified as an essential step in mitigating or eliminating the interference and restoring operation of the satellite communications service [7, p. A–2].

C. CURRENT GEOLOCATION METHODS

The geolocation of emitters of electromagnetic energy is typically accomplished by proven techniques such as time difference of arrival (TDOA) and/or frequency difference of arrival (FDOA) of the waveform at the receiving platform [9], [10]. These techniques require that at least two geostationary satellities simultaneously observe the same interfering signal. Then, a ground station with access to downlinks from both satellites, can compute the time and frequency difference information based on the separate paths the signal takes through the two satellites. Figure 2 shows this geometry. The total path lengths from the interfering source, through the two different satellites, and finally to the ground station are not the same. As such, the time of arrival at the ground station of the signal from the interfering source differs for each satellite. This difference can be used to generate a line of position (LOP) which passes through the location of the interfering source.

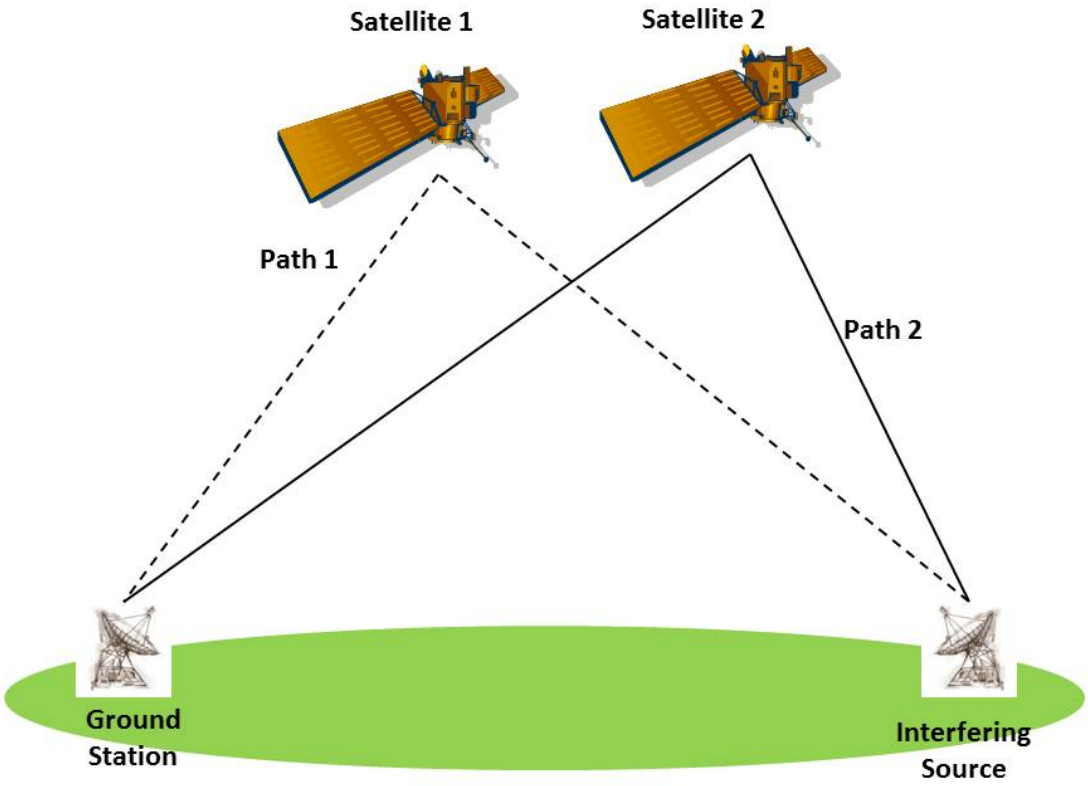

Figure 2. TDOA and FDOA Geometry.

In a similar fashion, the motion of the two satellites and/or changes to the signal as it moves through the RF electronics of the different satellites causes a doppler (frequency) shift of the interfering signal. This doppler shift can be translated into a second LOP which also passes through the location of the interfering source. The intersection of the TDOA and FDOA LOPs reveals the position of the interfering transmitter [9].

D. WHY A NEW METHOD IS NEEDED

Traditional communications satellites employ antennas that create large footprints on the surface of the Earth; these footprints cover large swaths, potentially entire continents [5, p. 23]. As a result, the TDOA/FDOA dual constraint that both satellites simultaneously receive the interfering signal, and that a single ground station receive downlinks transmitted by both satellites is relatively easy to satisfy. This also enables a

single ground station to have access to downlinks from multiple satellites with overlapping coverage areas in order to employ the TDOA and FDOA geolocation techniques mentioned in Part C. However, a consequence of these large antenna footprints operated by older satellites, is that a source of interference located anywhere within the receiving field of view can potentially degrade or interrupt intended communications.

Figure 3 and Figure 4 show examples of the transmit/receive footprint resulting from a large, area-coverage antenna. Figure 3 shows the effective isotropic radiated power (EIRP – explained in Chapter II) contours for a C-band (4-8 GHz) antenna on the Telstar 10 satellite. Figure 4 shows the EIRP contours for a Ku-band (12-18 GHz) antenna on the Telstar 5 satellite. These antenna patterns are representative of older systems operating in these RF bands.

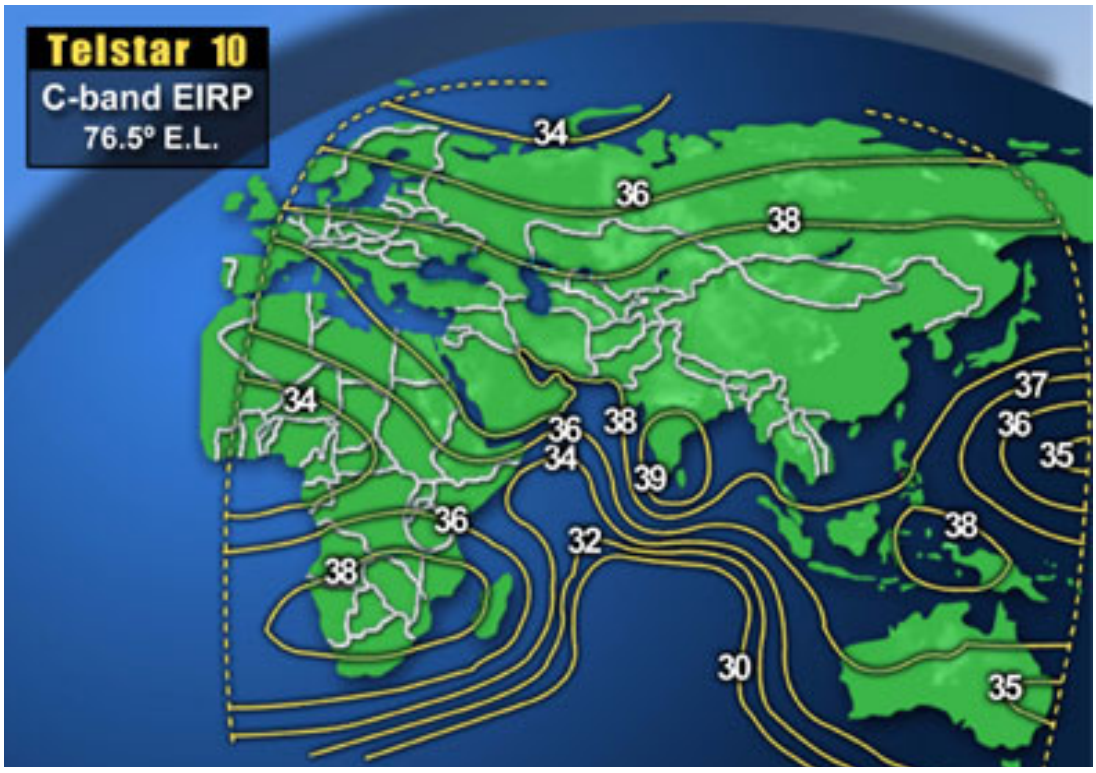

Figure 3. C Band Single Antenna Footprint (from [11]).

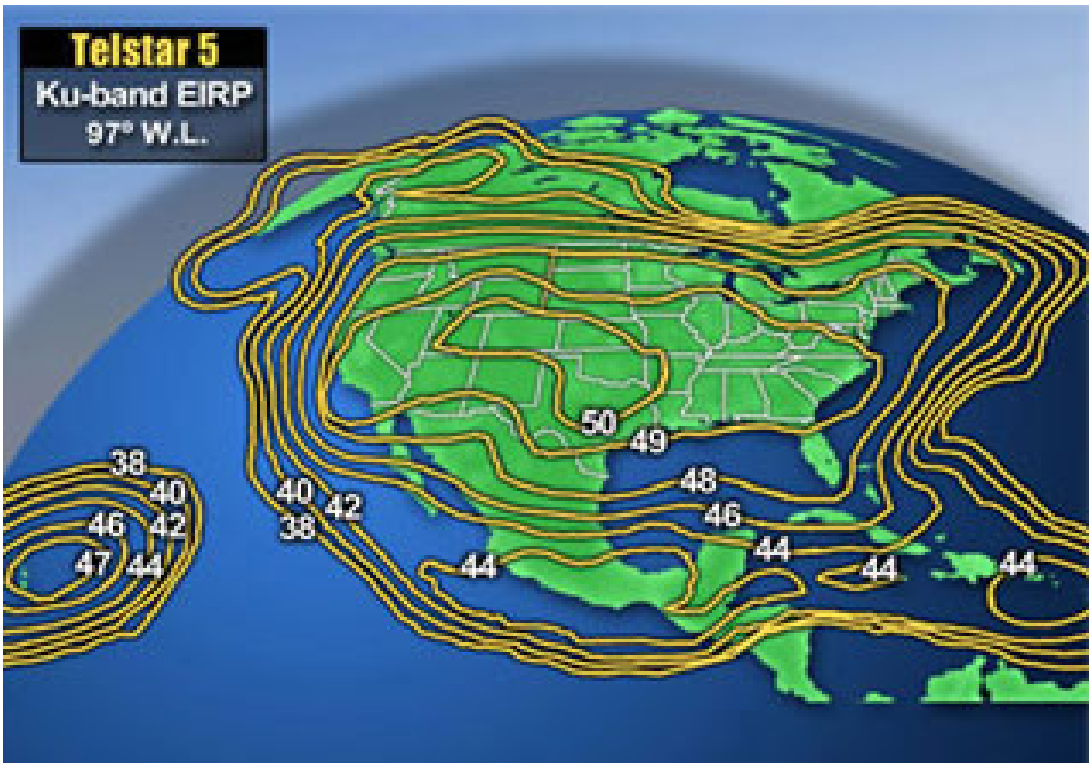

Figure 4. Ku Band Single Antenna Footprint (from [12]).

The global increase in demand for satellite communications services and capacity has outstripped the finite capacity of systems operating in these traditional bands (C and Ku). As such, modern satellite communications systems have started to move into higher regions of the RF spectrum such as Ka-band (17.3-31 GHz) [13]. Higher and less utilized regions of the RF spectrum offer less congestion, and therefore, less overall interference, as well as greater available bandwidth to accommodate higher data-rate services [14].

One consequence of operating in these higher frequencies is that more power is required either to overcome atmospheric and weather-related attenuation or to support the higher data rates required of modern services (such as high definition television). Although the transmitted power can be increased, another practical approach to providing this increase in signal strength is to increase the gain of the transmitting and receiving antennas. At the shorter wavelengths associated with these high frequencies, very high gains can be achieved with reasonably sized antennas for both the ground terminal and

satellite [1, pp. 529–530]. The resulting antenna beam width, however, is narrower and the footprint on the ground can be considerably smaller than shown in Figure 3 and Figure 4. This will also be true for the transmitting terminal on the ground—the angular extent of its transmitted signal will be less likely to spread over a region occupied by multiple satellites. Additionally, with very few satellites currently on orbit operating in Ka-band [14], the constraint of two satellites simultaneously receiving interference from a single source, and a single ground station in view of both satellite downlinks is now very unlikely—rendering the proven TDOA and FDOA geolocation techniques unsuitable.

E. HOW MODERN COMMUNICATIONS SATELLITES ENABLE A NEW METHOD

Improved satellite communications technology coupled with a shift of operation into the Ka frequency band has also led to the employment of innovative antenna systems. As shown in Part D, traditional, lower frequency antenna systems often employed few, large area-coverage beams. Newer, high frequency systems are using multiple antennas to form clusters of spot beams that provide high power, high data rate services over large areas [5, pp. 28–29].

This multiple spot beam configuration offers many advantages over older systems. First, the higher antenna gain and associated EIRP resulting from more focused beams allows for an increased overall throughput. Second, the higher antenna gain also adds an improved ability to overcome atmospheric and weather related attenuation seen at higher frequencies. Third, improved antenna gain on the satellite enables service to smaller user terminals than previously available. Fourth, multiple spot beams isolate geographic regions on the surface of the Earth which allows for frequency re-use in a number of the beams in the overall coverage pattern. This arrangement increases the overall system capacity within the allocated bandwidth [1, p. 530]. And finally, multiple spot beams placed ajacent to each other in a cellular-like pattern can produce a service area as broad as that formed by large area-coverage antennas - with high power, high data rate services.

Figure 5 shows an example of a system employing this sort of antenna system. This image is from INMARSAT's planned Global Xpress system. Shown is the expected coverage provided by three Global Xpress satellites located in geostationary orbit (Atlantic, Indian Ocean and Pacific orbital slots):

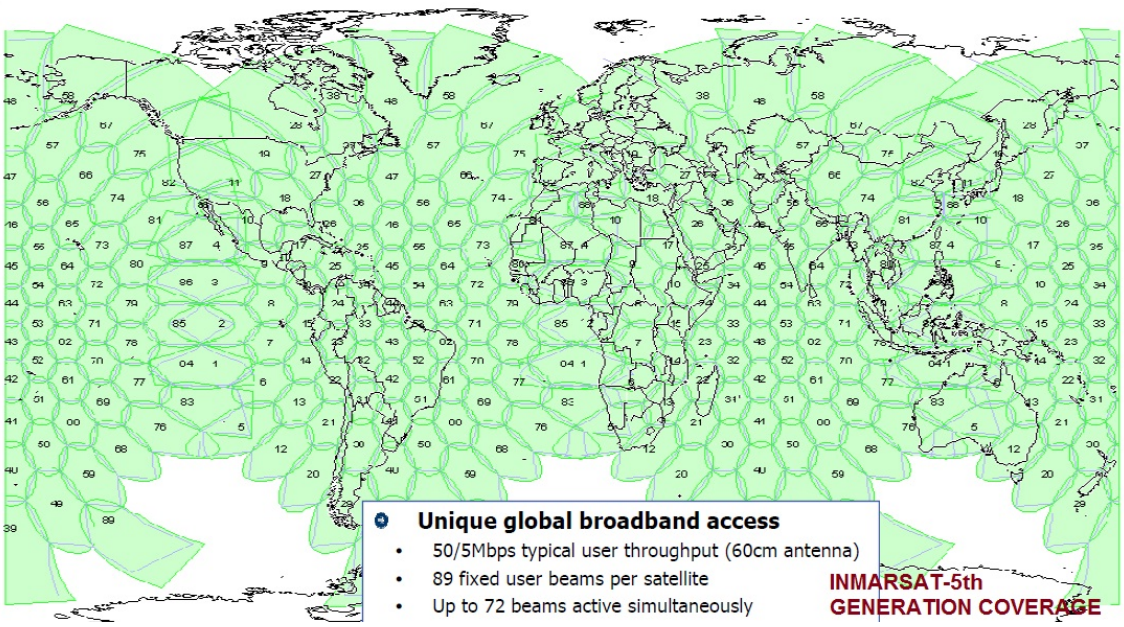

Figure 5. INMARSAT Global Xpress Coverage (from [15]).

F. CHAPTER I CONCLUSION

In conclusion, satellite communications is a global enterprise that will continue to grow. Increased growth has lead to an increase in congestion in the available frequencies currently used by satellites. Congestion leads to RF interference, which is highly undesirable to all parties involved in a communications system.

Emerging technologies are being developed for satellite communications systems with new configurations and being operated in new regions of the RF spectrum. These modern systems with narrow antenna beam designs and sparse satellite population preclude the use of TDOA and FDOA methods to locate sources of RF interference. However, the pattern of many spot beams hosted on a single satellite enables a new method that no longer relies on a second satellite.

II. SINGLE SATELLITE, MULTIPLE ANTENNA GEOLOCATION

A. CHAPTER II INTRODUCTION

Chapter I established two main concepts. First, current methods of geolocating RF interference are not suitable for use by modern communications satellite systems. Therefore, a new process for locating the source of interference is needed. Second, improved satellite communications technology combined with an operational shift into higher frequency bands has enabled a novel method for locating interference.

In Chapter II, the geolocation method is thoroughly explained in three sections. Part B reviews concepts essential to the setup of the geolocation method. Part 0 introduces the signal strength equations and shows how the antenna gain characteristics from Part B can be exploited to produce a new geolocation method. Part D will discuss the distinct advantages offered by this geolocation method as well as the assumptions made while developing it.

B. ANTENNA GAIN CONCEPTUAL REVIEW

1. Antenna Gain Equation

The *gain* of an antenna is a measure of its ability to amplify the signal it is transmitting or receiving. Antenna gain for a circular aperture antenna (like a parabolic reflector used to create the spot beams shown in Figure 5) can be calculated using Equation (2.1):

$$G = \eta\left(\pi D \frac{f}{c}\right)^2 \tag{2.1}$$

where η is a dimensionless antenna efficiency factor, D is the diameter (m) of the aperture, f is the frequency of the signal (Hz), and c is the speed of light. Antenna gain can also be described as the measure of the ability of an antenna to focus energy in a specific direction. The peak of the focused antenna energy is called the *boresight* of the antenna. The antenna gain in decibels (dB) can be displayed graphically as a function of the angular distance either side of boresight to produce a pattern. Figure 6 shows the

antenna gain pattern plotted as a function of angle off boresight for a 25 GHz (Ka band) antenna out to 90 degrees either side of antenna boresight.

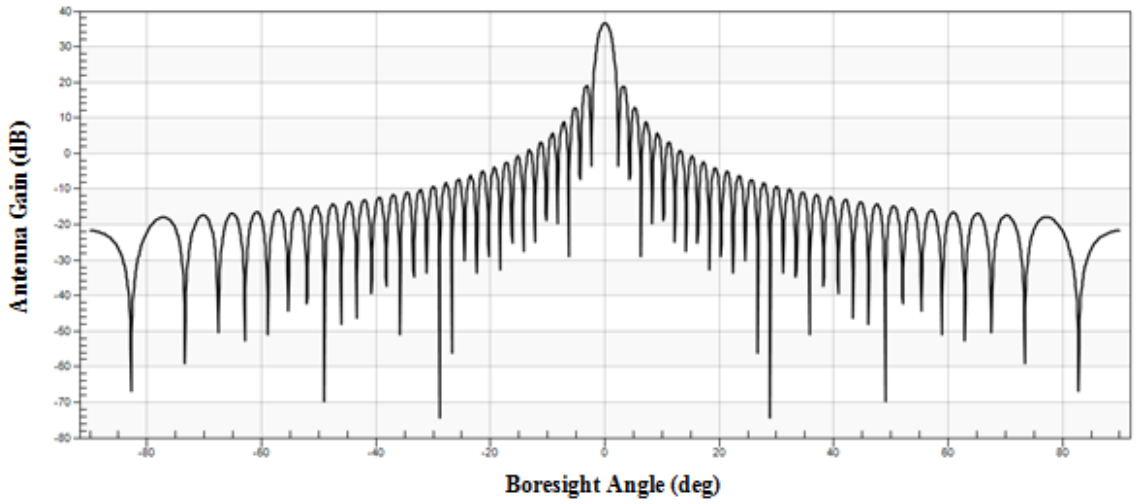

Figure 6. 25 GHz Antenna Gain Pattern (Total Field of View).

2. Antenna Field of View

The peak of the gain from this antenna (37 dB) is focused along the boresight and then decreases as the angle increases. There is positive gain as far as approximately 10 degrees from boresight in either direction. The effective field of view (FOV) of an antenna is typically defined as the area where the antenna gain is within 3 dB (50%) of the boresight. This area is called the half-power beamwidth and can be approximated for a circular aperture by Equation (2.2):

$$\theta = \frac{21}{fD} \tag{2.2}$$

where θ is the half-power beamwidth, f is the frequency (GHz), and D is the diameter (m). Figure 7 details the antenna pattern six degrees either side of boresight for an antenna designed to operate at 25 GHz with a two degree half-power beam width. It is important to note that there is still substantial gain within the main lobe found outside of the half-power beamwidth. This extra gain will be exploited to complete the geolocation method.

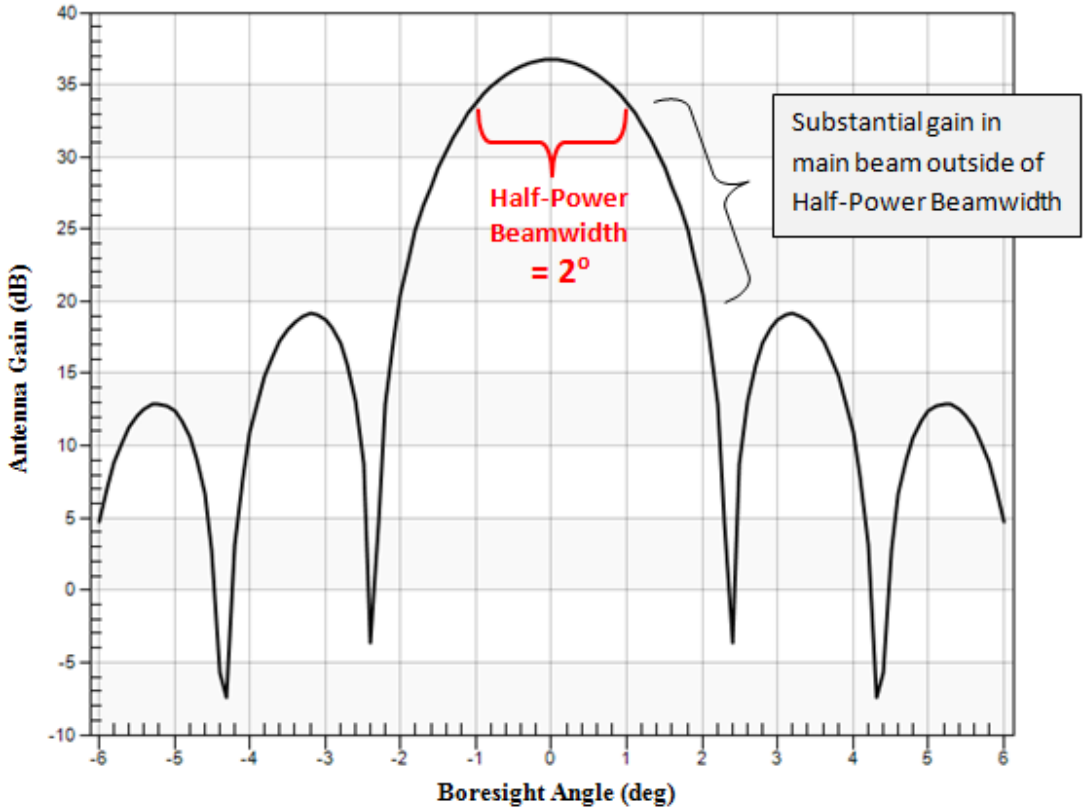

Figure 7. Antenna Gain Pattern Effective Field of View.

As the antenna gain pattern intersects the curvature of the Earth it forms concentric contours on the surface referred to as the antenna "footprint." The shape of the footprint is characterized by the angle of the axis of the boresight and a plane tangential to the surface of the Earth. If the boresight axis is perpendicular to the plane, a circular aperture will produce a circular footprint. If the boresight is not perpendicular – as it points away from the point directly below the satellite, the footprint of a circular aperture will appear elliptical as it intersects the surface of the approximately spherical Earth [1, p. 519].

3. Antenna Gain Pattern Intersecting Earth's Surface

Figure 8 depicts a close-up of the region on the Earth's surface covered by the FOV of three, 2° spot beams, all originating from a single satellite in geostationary orbit located above the equator over South America. A white X represents each antenna

boresight and the green circles represent the half-power beamwidth contours as they intersect the surface of the Earth. The boresights are oriented slightly less than 2° apart to prevent gaps in coverage.

Figure 8. Three Slightly Overlapping 2 Degree Beamwidth Antenna Patterns.

Note that all of the antennas in Figure 8 (but especially Antenna 1) exhibit the slightly elliptical shape described above. These antennas possess boresight axes close to perpendicular to a plane tangential to the surface of the Earth. The antennas in Figure 9 further demonstrate the elliptical appearance of the antenna footprint as its boresight points farther away from perpendicular. Notice that two of the antennas appear to have incomplete footprints. In these cases, the size of the footprint is limited by the curvature of the Earth because they are beyond the horizon of the antenna.

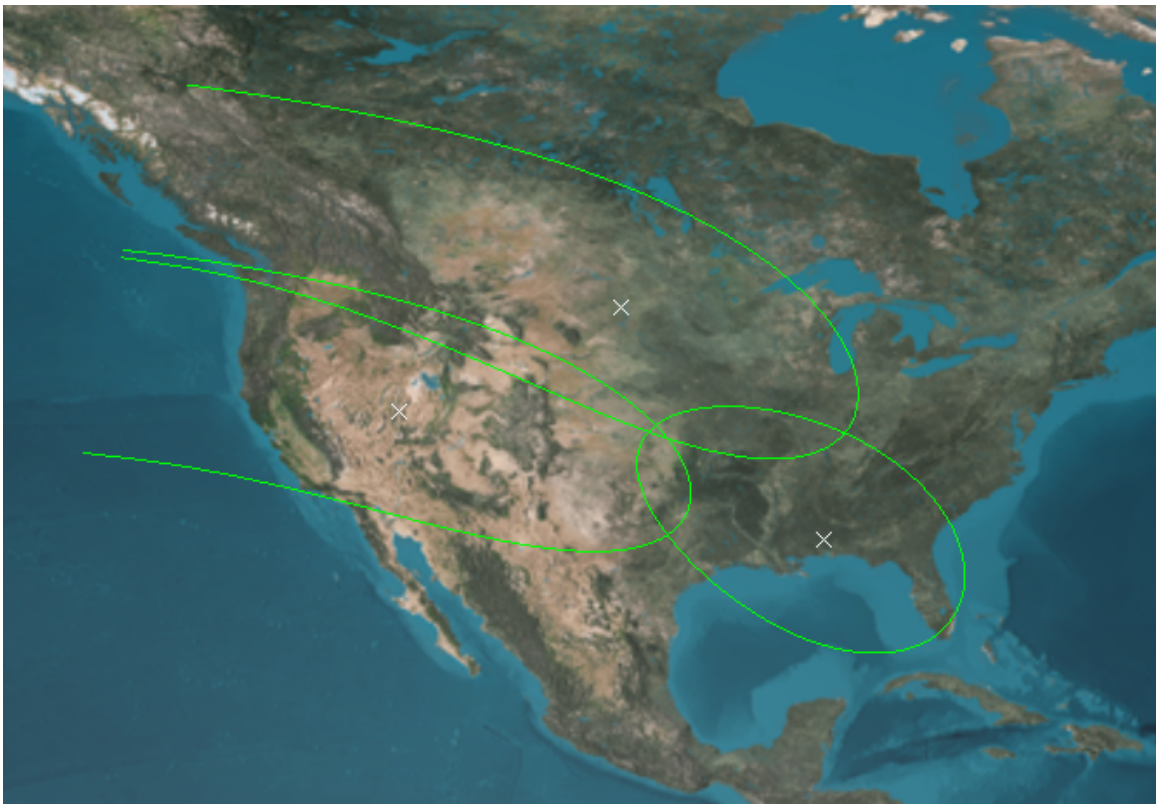

Figure 9. Three Antenna Footprints Intersecting Curvature of Earth in 2D.

This concept is better seen in the 3D graphics in Figure 10 and Figure 11. In Figure 10, the satellite orbit is shown in white and the satellite position is represented by the white node at the bottom of the graphic. Shown in this figure is the view of the surface of the Earth from the perspective of the geostiatonary satellite. It is clear from this vantage point why certain antenna orientations produce elliptical or incomplete antenna footprints intersecting with the surface of the Earth.

Note, the configurations in Figure 8 and Figure 9–Figure 11 are simplified models of portions of the Global Xpress system shown in Figure 5.

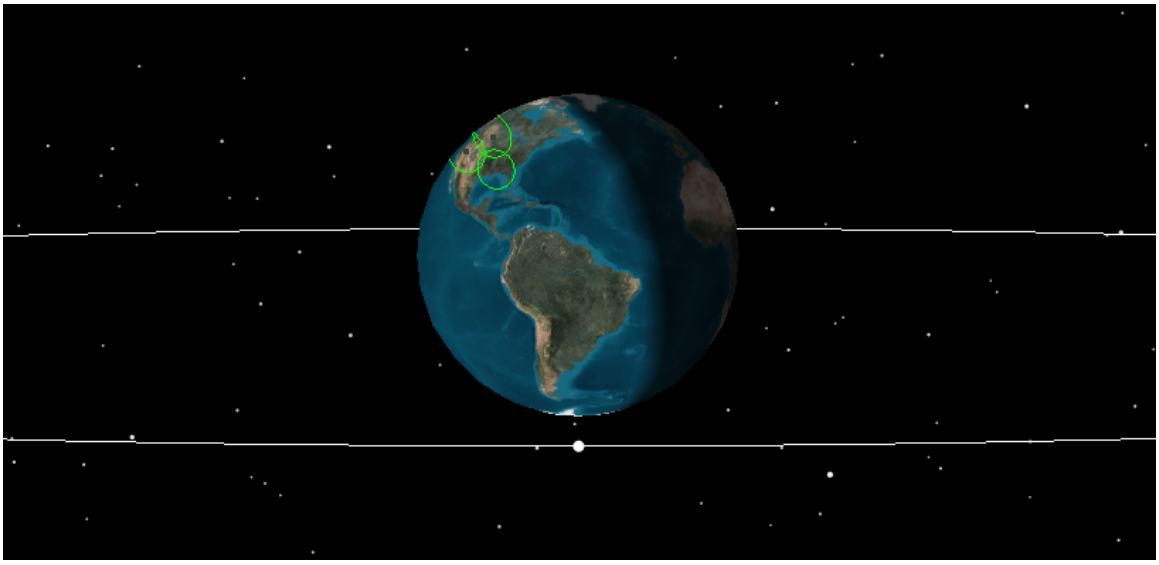

Figure 10. Three Antenna Footprints Intersecting Curvature of Earth in 3D.

Figure 11. Zoom of Three Antenna Footprints Intersecting Curvature of Earth in 3D.

Figure 12 and Figure 13 illustrate the contours generated by a single antenna footprint. The center contour (green) represents the half-power beamwidth and includes all gain values greater than or equal to 34 dB. The remainder of the contours represent

the gain available outside the main beam of the antenna and are displayed at 2 dB intervals (to reduce clutter) down to the 20 dB contour, displayed in red.

The contours are stopped at 20 dB because this is the approximate gain available immediately before the first null in the antenna. A null is an area where the antenna will produce a significantly reduced amount of gain to the signal it is meant to amplify. In Figure 7, all azimuths outside of ±2° produce gain values < 20 dB. Azimuth ranges immediately centered around ±2.3° and ±4.3° have gain values < 0 dB.

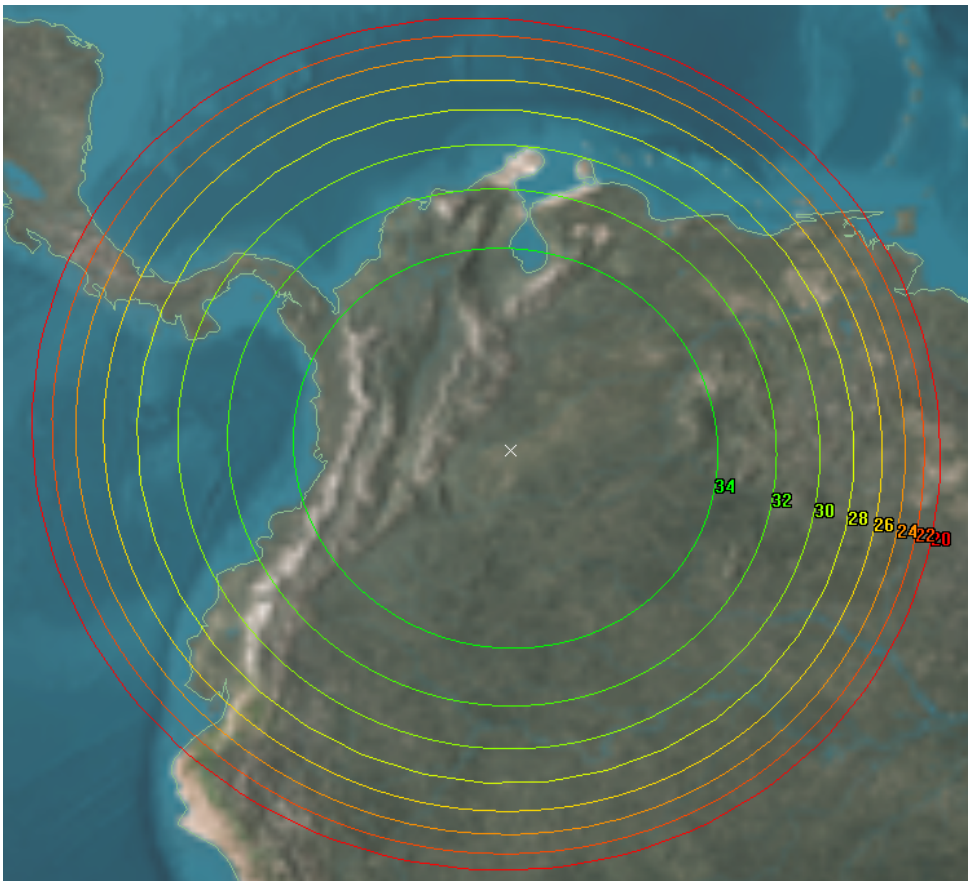

Figure 12. Single Antenna Gain Pattern at 25 GHz down to 20 dB.

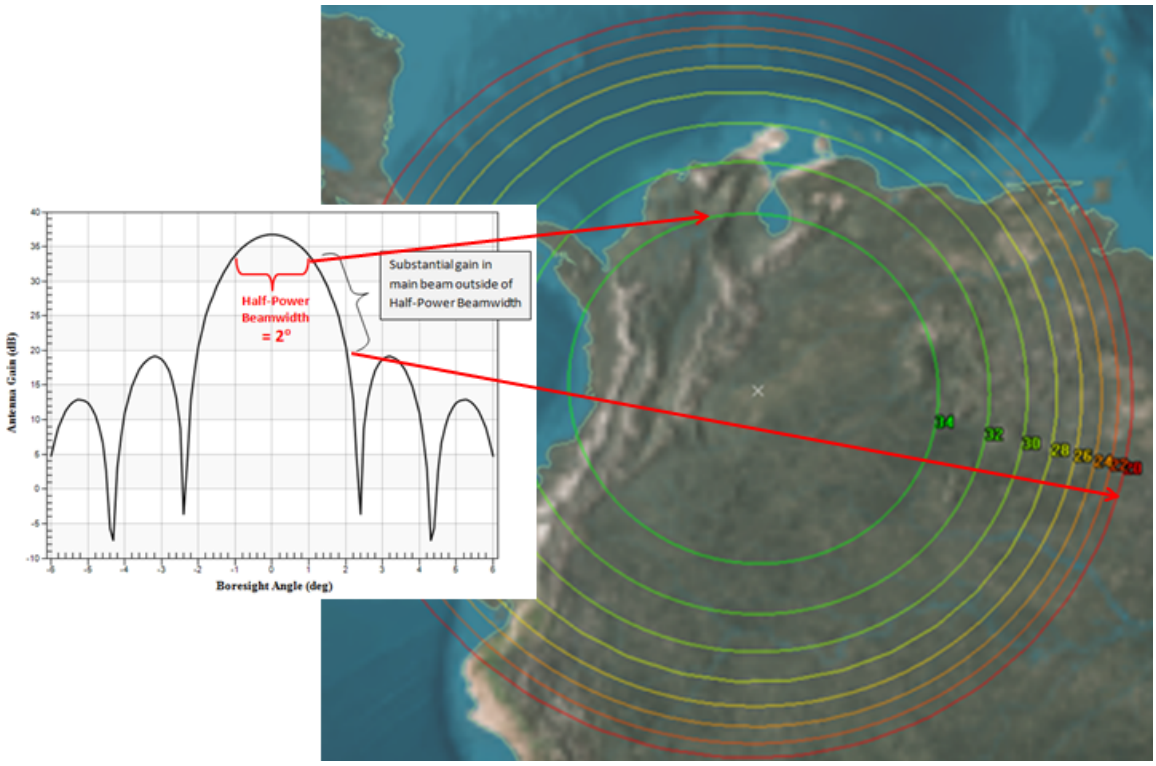

Figure 13. Half Power Beamwidth Overlaid on Single Antenna Gain Pattern at 25 GHz down to 20 dB.

4. Antenna Gain Patterns Intersecting Each Other

Figure 14, Figure 15, and Figure 16 display pairs of antenna gain contour patterns. The boresight of each antenna is represented by a white X and the green circles represent the main field of view of the antennas. These graphics are a combination of the gain patterns from boresight down to 20 dB (as shown in Figure 12) for each combination of the antennas shown in Figure 8. The gain associated with antenna 1 will be referred to as G_1; the gain associated with antenna 2 will be G_2; and the gain associated with antenna 3 will be G_3.

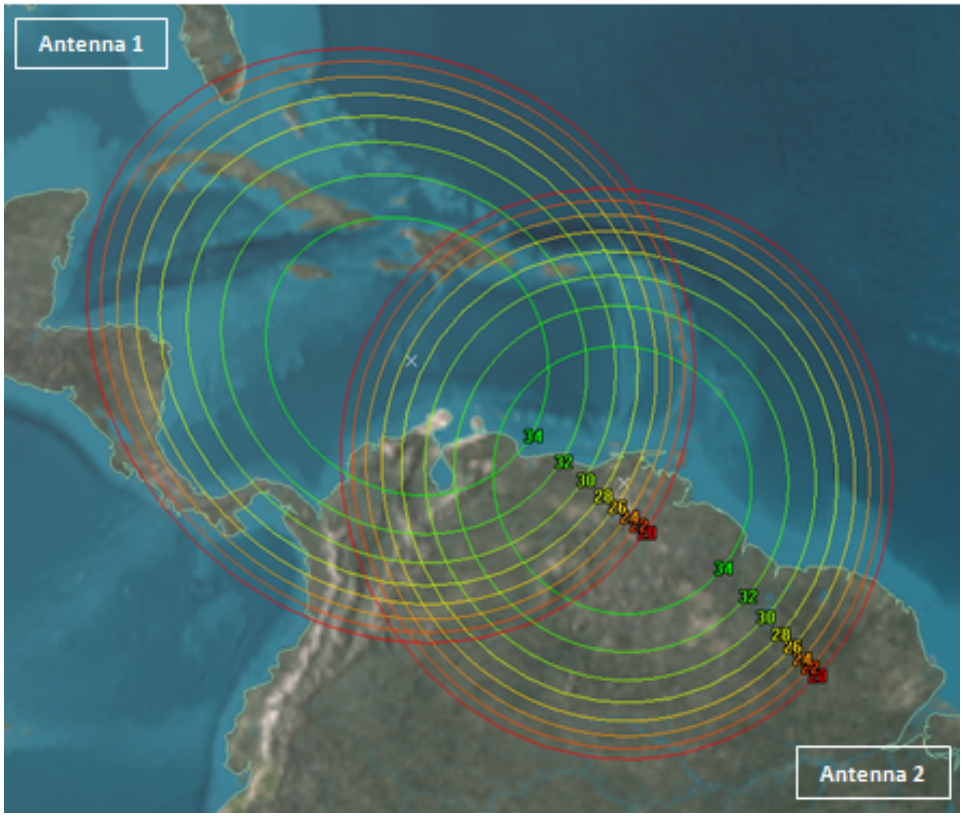

Figure 14. Two Adjacent 25 GHz Antenna Patterns Down to 20 dB (G_1 and G_2).

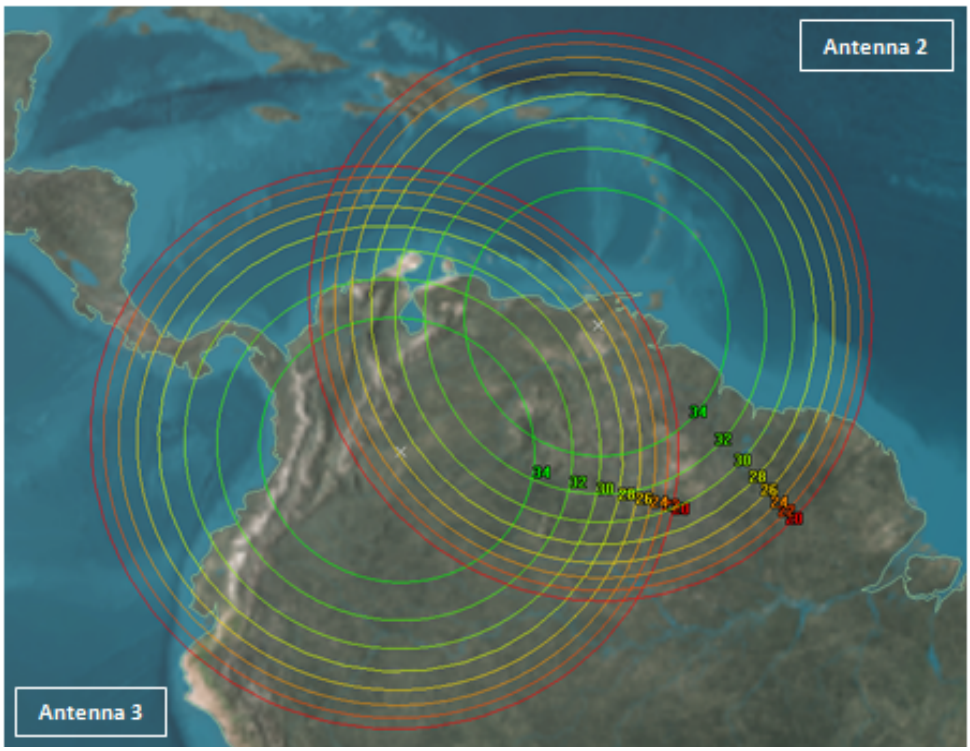

Figure 15. Two Adjacent 25 GHz Antenna Patterns Down to 20 dB (G_2 and G_3).

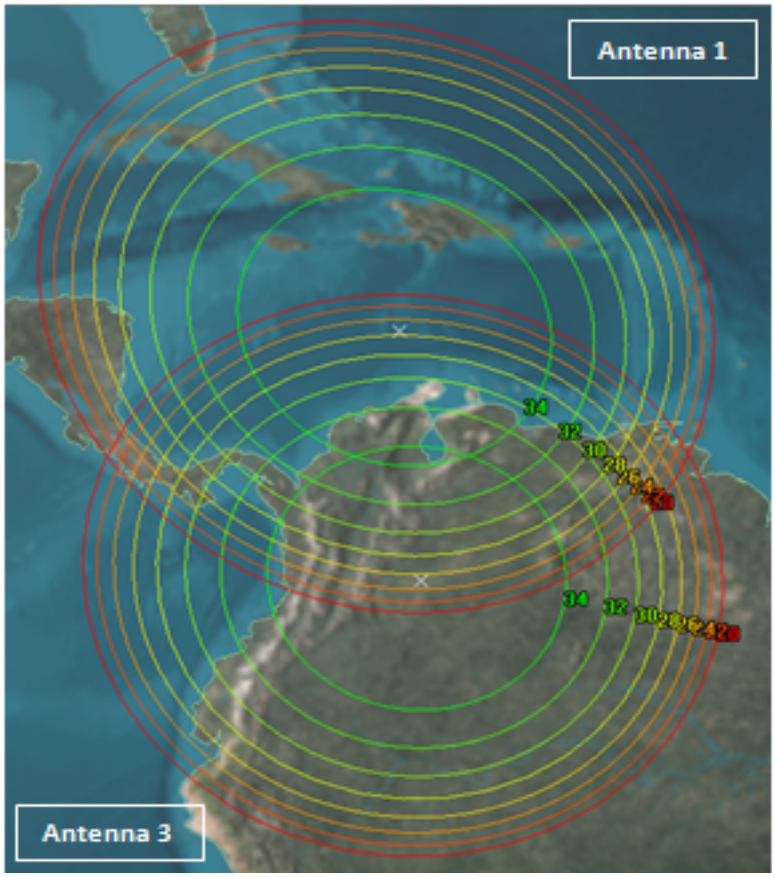

Figure 16. Two Adjacent 25 GHz Antenna Patterns Down to 20 dB (G_1 and G_3).

In Figure 17, the white box approximates the area bounded by each of the three antenna boresights. This region is within the FOV of at least two, and for the most part, all three of the antennas. In this region, it is reasonable that an interfering signal would be seen simultaneously by all three separate antennas. This region will be referred to as the Area of Interest (AOI).

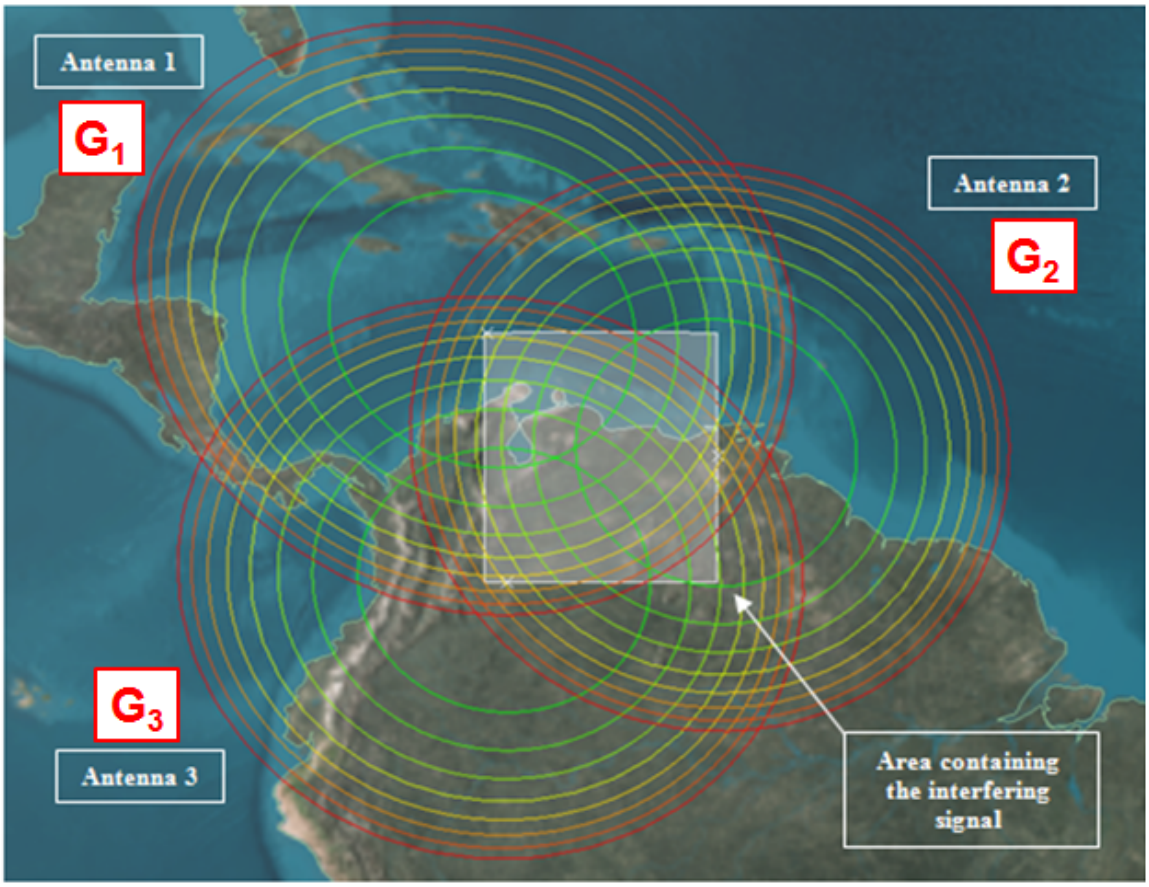

Figure 17. Three Adjacent Antenna Patterns (G_1, G_2, and G_3).

C. GEOLOCATION

1. Signal Strength Equation

Chapter I described the three main components of a communication link: the interfering transmitter located somewhere on the surface of the Earth, the receiver located on the satellite, and the EM signal that propogates between them. These components can be expressed mathematically in order to calculate the total power of a signal (in decibels) received by an antenna on a satellite:

$$S = P_T + G_T - L_T - L_{FS} + G_R \tag{2.3}$$

S is the power of the signal at the receiver, P_T is the power radiated from the terrestrial transmitter, G_T is the gain of the transmitting antenna, L_T includes any losses associated with the transmitting antenna (such as losses associated with output transmission lines and other hardware connecting the transmitter and antenna), L_{FS} represents the free space loss (a summation of losses experienced as the signal travels from transmitting antenna to receiving antenna), and G_R is the gain of the receiving antenna.

2. EIRP Equation

The terms in Equation (2.3) associated with the transmitting source (P_T, G_T, L_T) are commonly referred to as the Equivalent Isotropic Radiated Power (EIRP). They are expressed in Equation (2.4):

$$EIRP = P_T + G_T - L_T \tag{2.4}$$

Equation (2.3) can now be simplified:

$$S = EIRP - L_{FS} + G_R \tag{2.5}$$

As discussed in Figure 17, the interfering signal originating in the area bounded by the three antenna boresights would be received by each distinct antenna. Since each antenna is simultaneously receiving the same interfering signal from the transmitting source, the EIRP is the same for each antenna.

3. Free Space Loss Equation

Similarly, it is reasonable to assume that the signal that reaches the receive antennas will experience the same combination of atmospheric and attenuation losses. These losses are referred to as the free space loss and can be calculated with Equation (2.6):

$$L_{FS} = \left(\frac{4\pi rf}{c} \right)^2 \tag{2.6}$$

r is the distance between the transmit and receive antennas, *f* is the frequency of the signal, and *c* is the speed of light. Admittedly, there will be some physical separation between the feeds for each receive antenna on the satellite. The exact distance that separates the antennas on the satellite will vary uniquely for each satellite design. However, when considering the distance from Earth to geostationary orbit, the free space loss figure can be shown to be negligible.

a. Free Space Loss Proof

Using Equation (2.6) let *r1* = 35,786,000 m (the standard distance associated with GEO); let *r2* = 35,786,001 m (allows for a conservative difference of 1 meter in total distance between antennas); let *f* = 25 GHz (a sample frequency from the Ka region of the RF spectrum); and compute the free space loss for both distances. L_{FS1} will equal the free space loss experienced between a transmitter and a receiver separated by the standard distance associated with GEO and L_{FS2} will represent the free space loss for a distance 1 meter greater than the distance used in L_{FS1}. Note that both free space loss results are converted to dB for final comparison.

$$L_{FS_1} = \left(\frac{4\pi r_1 f}{c} \right)^2 = 1.4063217 \times 10^{21} = 211.48084679 \text{ dB} \tag{2.7}$$

$$L_{FS_2} = \left(\frac{4\pi r_2 f}{c} \right)^2 = 1.4063216 \times 10^{21} = 211.48084655 \text{ dB} \tag{2.8}$$

$$L_{FS_1} - L_{FS_2} = 2.4 \times 10^{-7} \text{ dB} \tag{2.9}$$

The resultant difference between the two possible free space losses is small enough to be assumed to be zero.

4. Signal Strength Equations for Three Antennas

Since the interfering signal received by each of the three antennas was transmitted by the same source (same EIRP), and experienced the same free space loss as it traveled to the satellite, the power of the signal received at each antenna (in dB) is now written:

$$S_1 = EIRP - L_{FS} + G_1 \tag{2.10}$$

$$S_2 = EIRP - L_{FS} + G_2 \tag{2.11}$$

$$S_3 = EIRP - L_{FS} + G_3 \tag{2.12}$$

where S_1, S_2, and S_3 represent the power of the signal received at antennas 1, 2, and 3 respectively; and G_1, G_2, and G_3 are the gains associated with antennas 1, 2, and 3 respectively.

5. Signal Strength Difference Equations

As EIRP and L_{FS} are common to Equations (2.10), (2.11), and (2.12), any difference in the received signal strength between the three antennas can be attributed solely to the difference in the gain provided to the signal as a function of the transmitters location within the antenna gain pattern. The EIRP and Free Space Loss are unknown quantities, but they are the same for each receive antenna. Therefore, the differences between the power of the signal received at each antenna can be calculated to cancel out the unknown terms (EIRP and L_{FS}):

$$S_1 - S_2 = (\text{EIRP} - L_{FS} + G_1) - (EIRP - L_{FS} + G_2) = G_1 - G_2 \tag{2.13}$$

$$S_2 - S_3 = (\text{EIRP} - L_{FS} + G_2) - (EIRP - L_{FS} + G_3) = G_2 - G_3 \tag{2.14}$$

$$S_1 - S_3 = (\text{EIRP} - L_{FS} + G_1) - (EIRP - L_{FS} + G_3) = G_1 - G_3 \tag{2.15}$$

Equations (2.13), (2.14), and (2.15) show that the difference in received signal strength at each antenna on the satellite is due solely to the difference in gain provided to the signal by the associated receive antennas.

$$S_1 - S_2 = G_1 - G_2 \tag{2.16}$$

$$S_2 - S_3 = G_2 - G_3 \tag{2.17}$$

$$S_1 - S_3 = G_1 - G_3 \tag{2.18}$$

6. Antenna Gain Difference Contours

As described in Equation (2.1), the gain characteristics of each receive antenna are a function of the antenna configuration and operating frequency. Also, the location of the antenna gain contours on the surface of the Earth (Figure 17) are a function of the satellite location and antenna orientation. Given that all of these parameters are known by the satellite manufacturers and/or satellite operators, the $G_x - G_y$ values can be computed relative to the surface of the Earth upon the commencement of satellite operation.

As $G_x - G_y$ values are computed for each possible point on the surface of the Earth (and within the associated antenna fields of view), regions of similar net values become evident. These values can be plotted on the surface of the Earth to form patterns of difference contours. These contours should not be confused with the antenna gain contours from Figure 17. An example of $G_x - G_y$ contours is depicted in Figure 18.

In Figure 18, the boresights of antenna 1 and antenna 2 are represented with a white X. The gain contours for antenna 1 and antenna 2 are shown via the thin green, yellow, and red concentric lines. The area of interest is also identified by the white box. The thick bands of color ranging from purple to dark grey and then back to purple are the $G_1 - G_2$ contours. Each band of similar color represents the region where the $G_1 - G_2$ value is approximately the same.

For example, the dark grey contour in the center of Figure 18 represents all points where $G_1 - G_2$ is equal to 0 dB. In other words, $G_1 = G_2$. This is logical as the dark grey band represents an area that is equidistant from the boresights of both antennas. The dark blue contours represent a $G_1 - G_2$ value of either 8 dB or -8 dB. A value of 8 dB indicates the interfering transmitter is located on the dark blue contour closer to G_1 while a value of -8 dB indicates the interfering transmitter is located on the dark blue contour closer to G_2. Of note, Figure 18 is only displaying the contours ranging from 10 to -10 dB. This was done to maximize the clarity of the graphic. Contours that cover the remainder of the region of interest are calculated but not displayed.

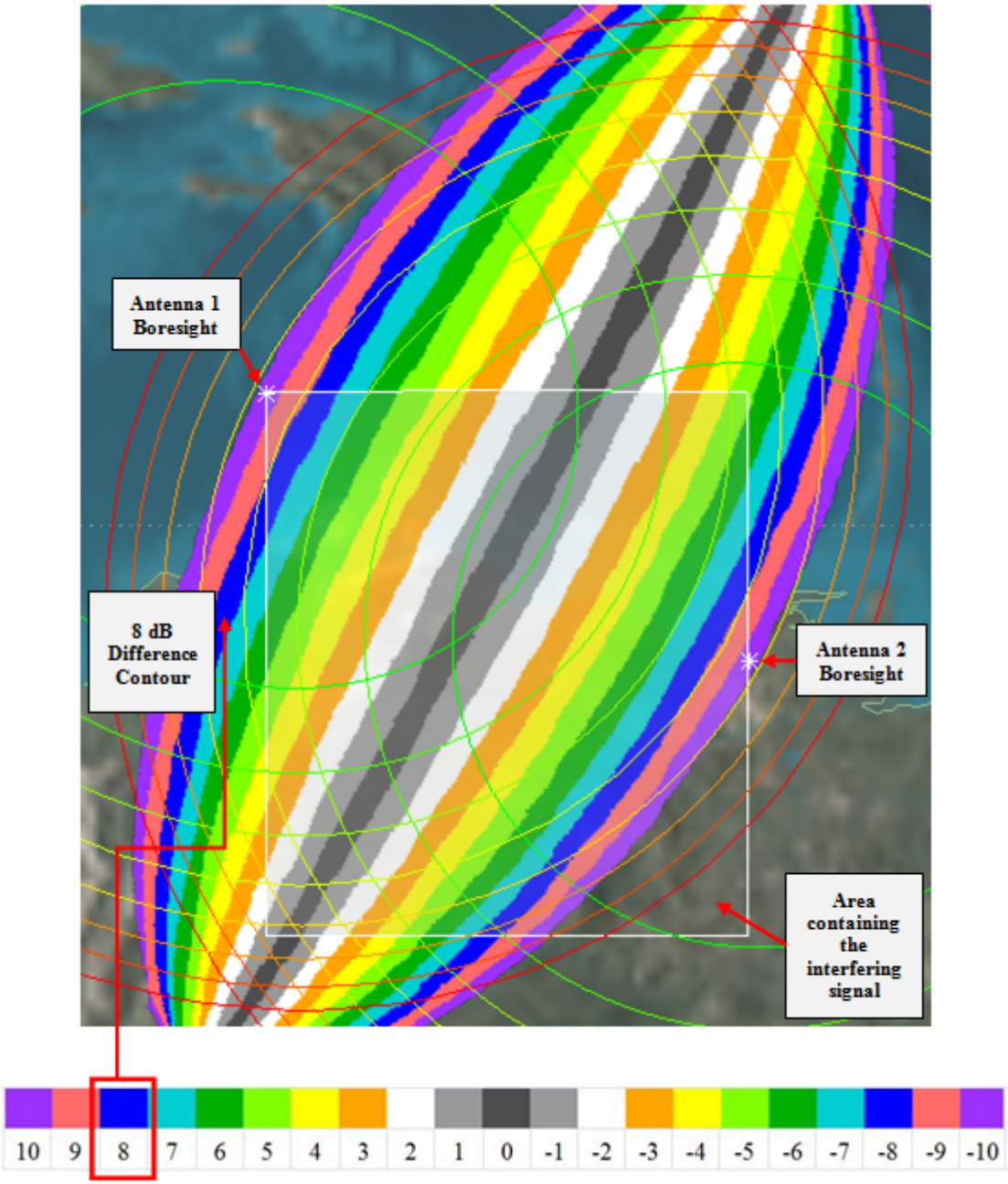

Figure 18. Color Coded Values (dB) of $G_1 - G_2$ Antenna Gain Difference Contours.

Figure 20, Figure 21, and Figure 23 show the calculated difference contours in the area of interest for $G_1 - G_2$, $G_2 - G_3$, and $G_1 - G_3$, respectively.

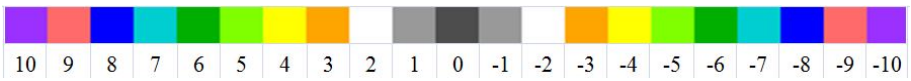

Figure 19. Color Coded Values (dB) for $G_1 - G_2$ Contours.

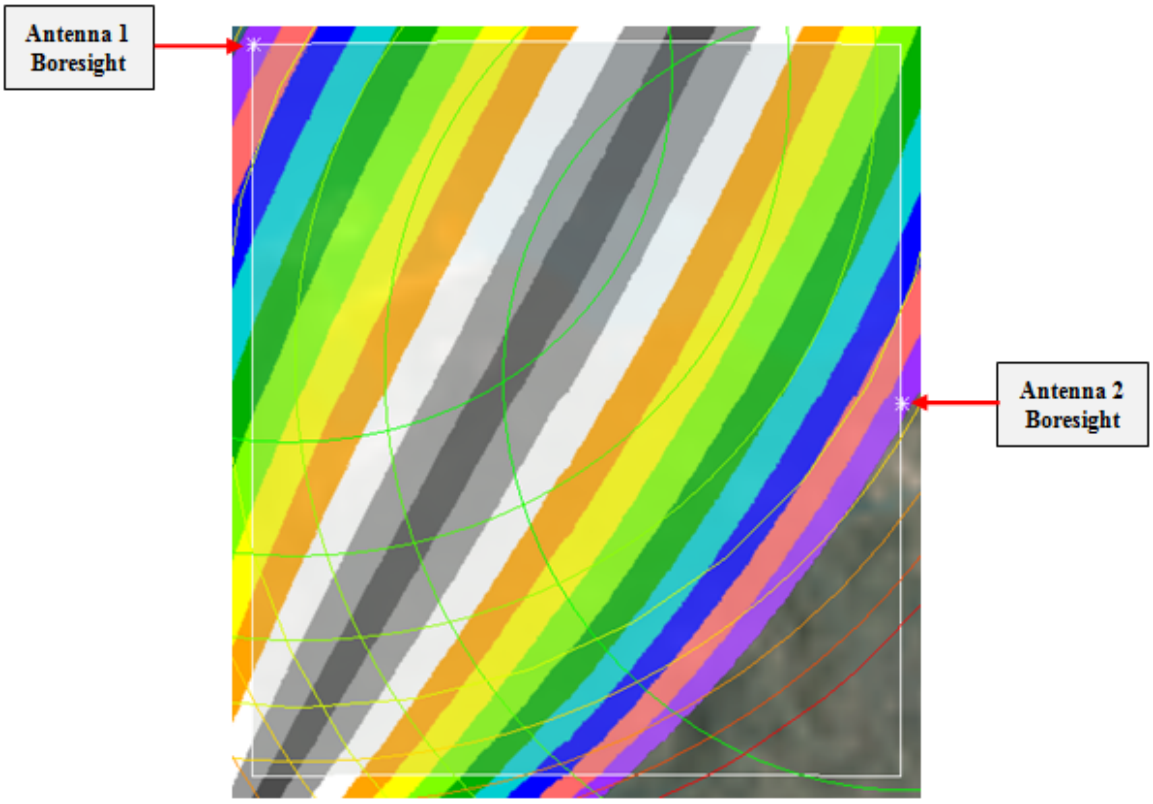

Figure 20. Antenna Gain Difference Contours (G_1 - G_2).

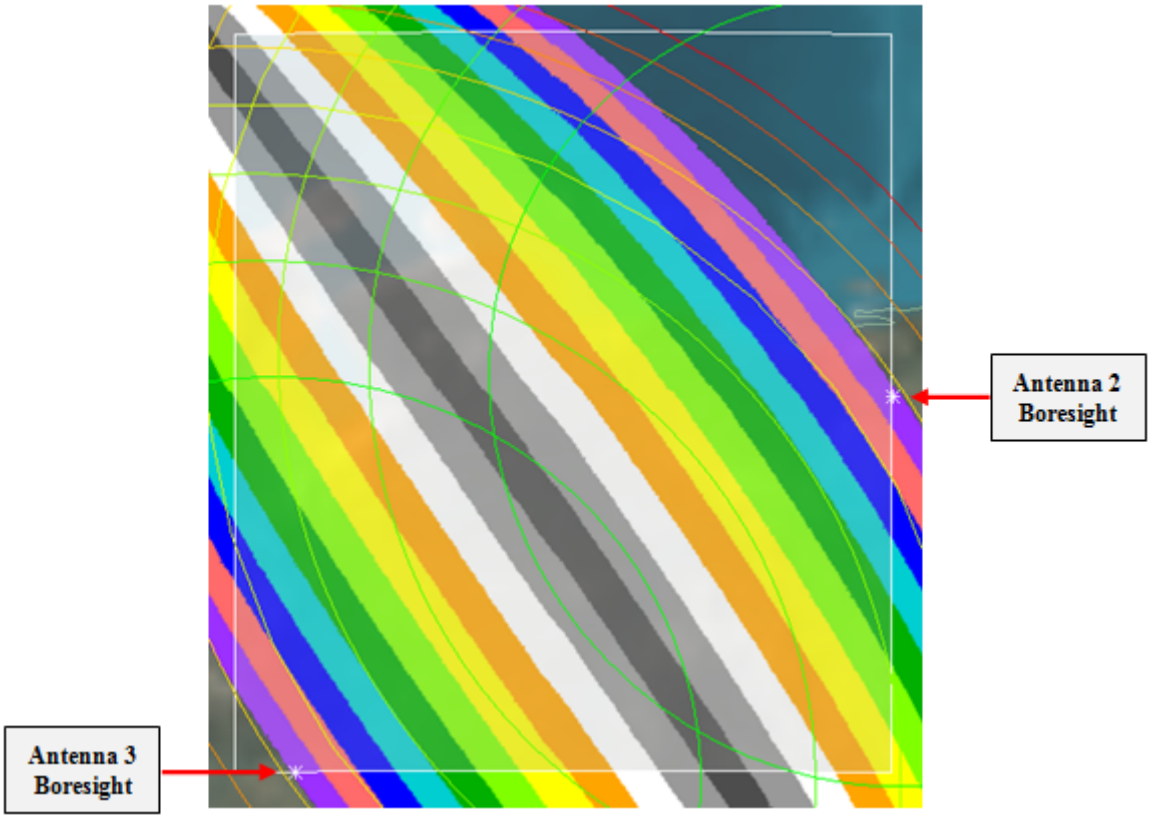

Figure 21. Antenna Gain Difference Contours (G_2 - G_3).

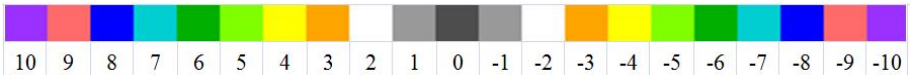

Figure 22. Color Coded Values (dB) for $G_2 - G_3$ Contours.

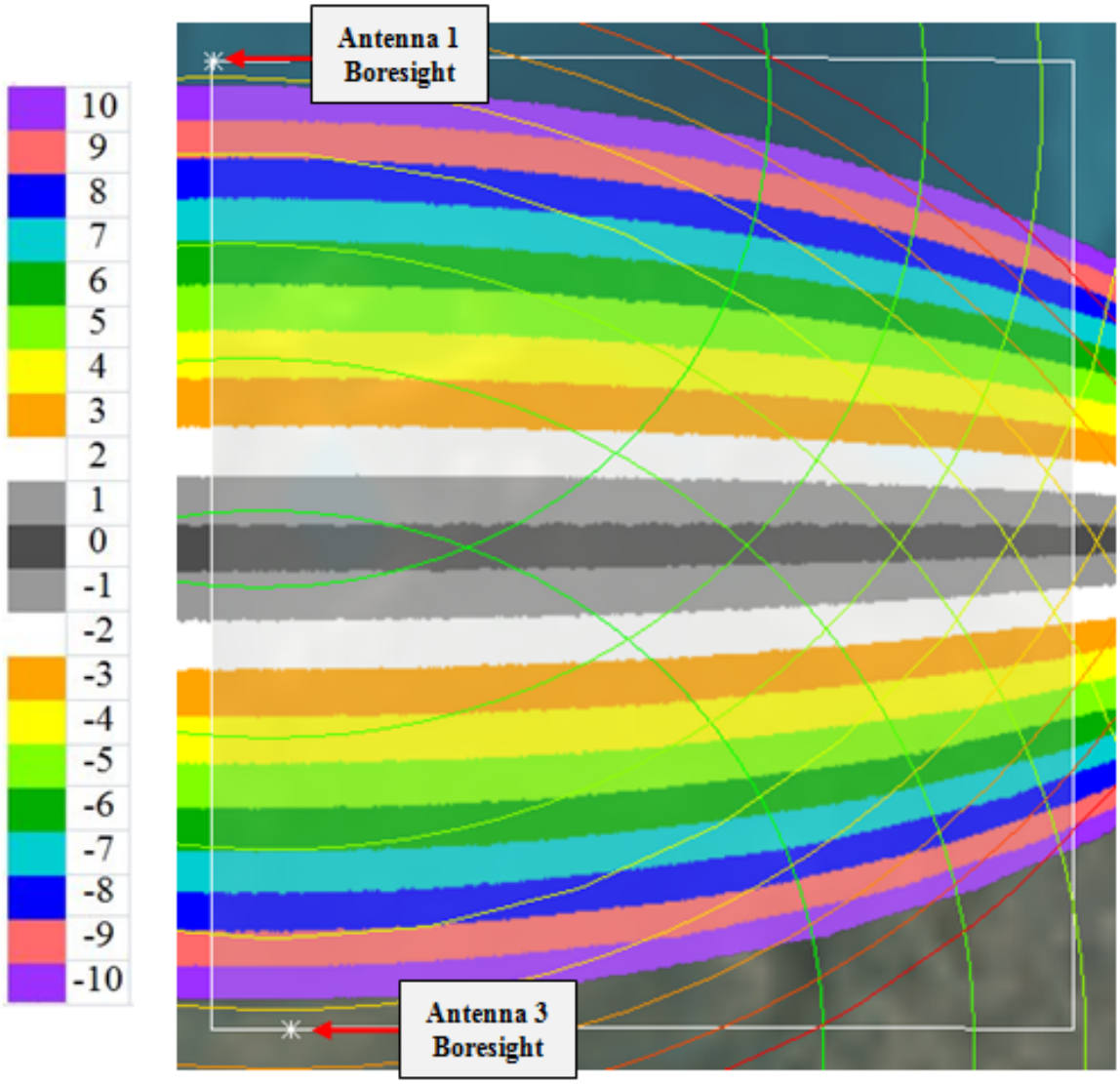

Figure 23. Antenna Gain Difference Contours (G_1 - G_3).

7. Signal Strength Measurements

With the antenna gain difference contours calculated at the onset of satellite operation, the satellite can proceed to normal operations. If an interfering signal is detected during satellite operation, the strength of the signal received by the multiple receive antennas can be measured and the difference in the signal strengths can be computed. The computed difference for each antenna pair produces the difference contour that now represents a line of possible positions (LOP) where the source of interference must be located. The area of intersection of the LOPs represents the region

on the surface of the Earth that correlates to the signal strength measurements taken at the time of detected interference. Therefore, the interfering transmitter is geolocated to the area of intersection of the computed LOPs.

8. Example Geolocation

For example, assume interference is detected and the following signal strength measurements are made:

Antenna	Signal Strength Measurement
G_1	7 dB
G_2	10 dB
G_3	5 dB

Table 1 Example Antenna Signal Strength Measurements

The example signal strength measurements from Table 1 yield the signal strength difference contours compiled in Table 2:

Antenna Pair	Signal Strength Difference Contour
$G_1 – G_2$	-3 dB
$G_2 – G_3$	5 dB
$G_1 – G_3$	2 dB

Table 2 Example Calculated Antenna Gain Difference Contours

Recall that the antenna gain difference contours for all possible antenna pairs were previously calculated and displayed in Figure 20, Figure 21, and Figure 23. Table 2

now isolates the specific difference contours that represent the LOPs that must contain the interfering transmitter. The geolocation is completed by plotting the LOPs from Table 2 and identifying the area of intersection.

Figure 24 represents the LOP where the signal difference (and therefore the signal strength difference $G_1 - G_2$) was calculated to be -3 dB. The value is negative if $G_2 > G_1$, indicating that the source of interference is located in an area where the gain for antenna 2 is greater than the gain for antenna 1. The interfering signal is located somewhere on the -3 dB LOP.

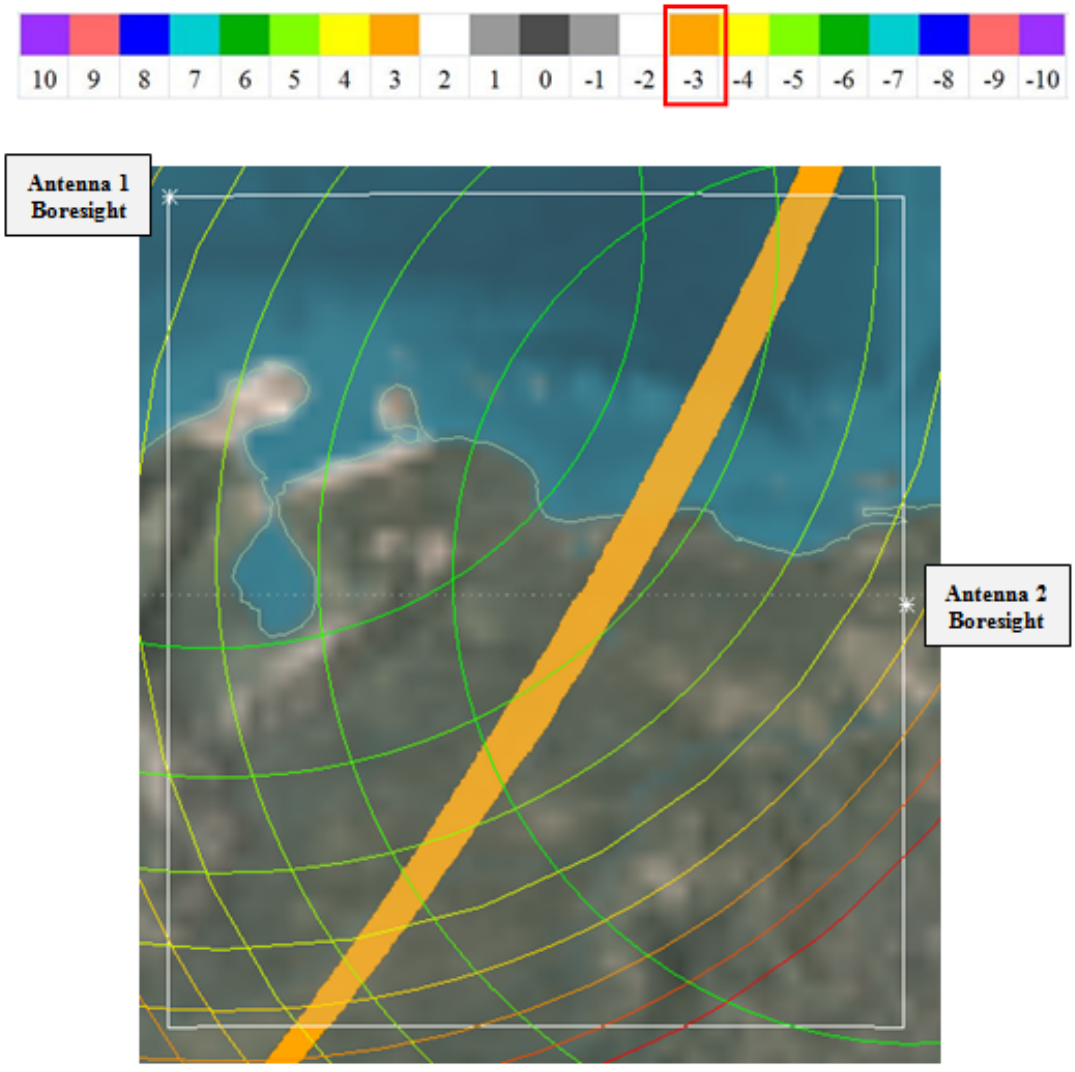

Figure 24. Single Difference Contour (G1 - G2).

Similarly, Figure 25 shows the 5 dB ($G_2 > G_3$) LOP associated with the G_2 and G_3 pair of antennas. The interfering source must be located both on this LOP and the LOP from Figure 24.

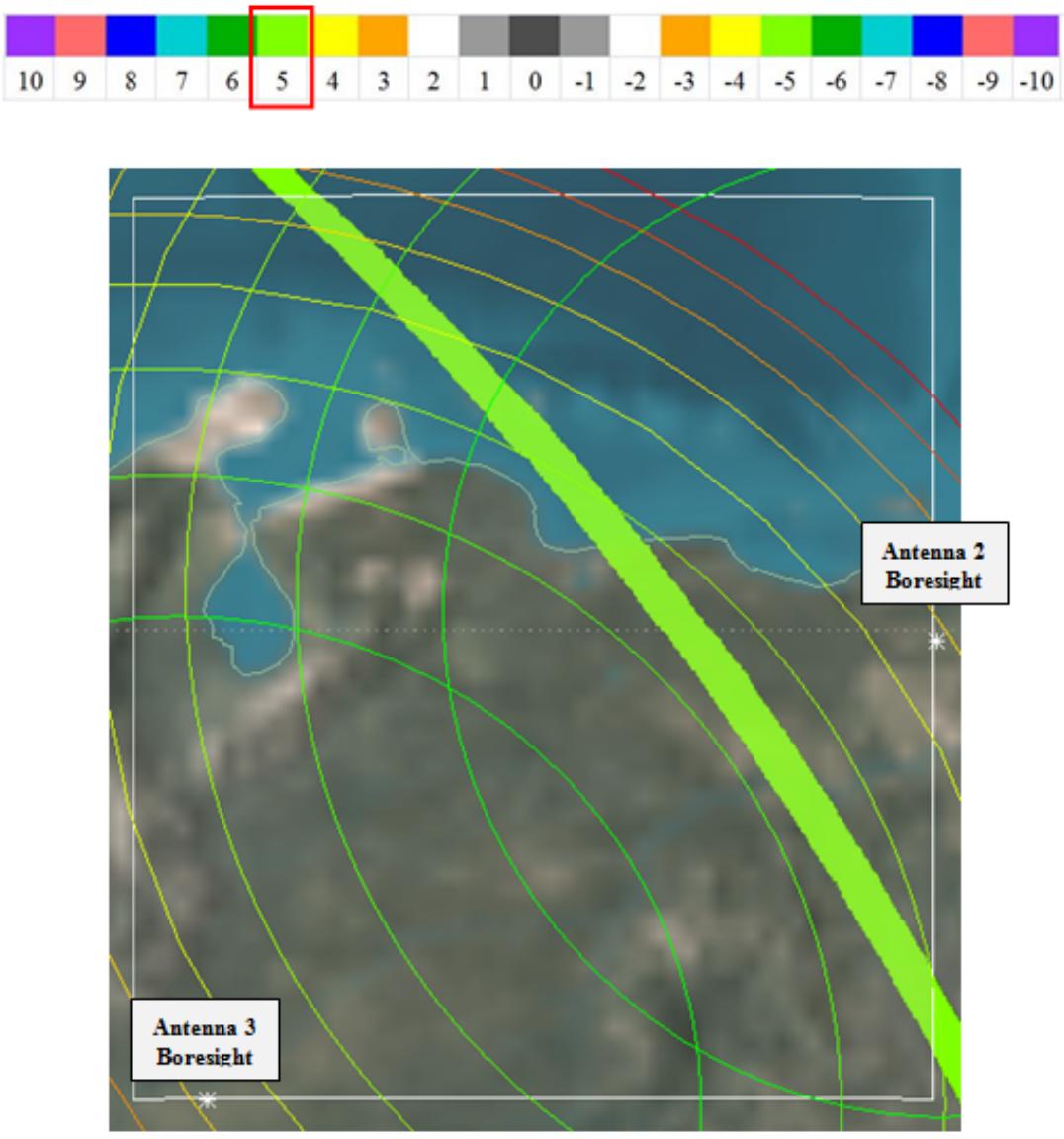

Figure 25. Single Difference Contour (G2 - G3).

The intersection of the LOP from Figure 24 and the LOP from Figure 25 represents the area that simultaneously satiesfies both sets of signal strength difference conditions. This area is the geolocation of the source of interference and is shown in Figure 26.

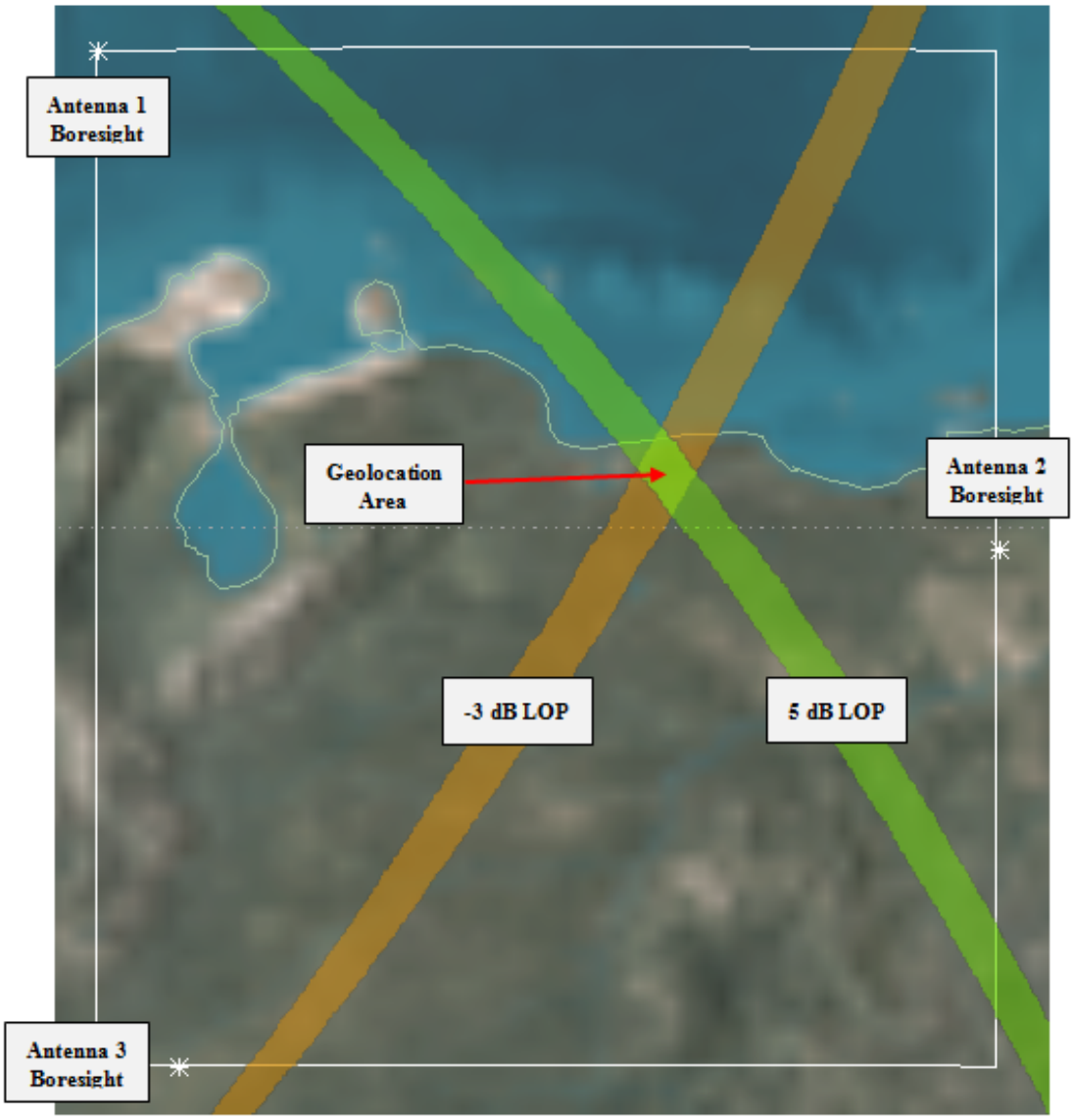

Figure 26. Geolocation.

Figure 27 shows the 2 dB ($G_1 > G_3$) LOP generated from the G_1 and G_3 pair of antennas. The addition of a third LOP that also represents an area that must contain the interfering source serves to further reduce the total area containing the interfering source (Figure 28 and Figure 29).

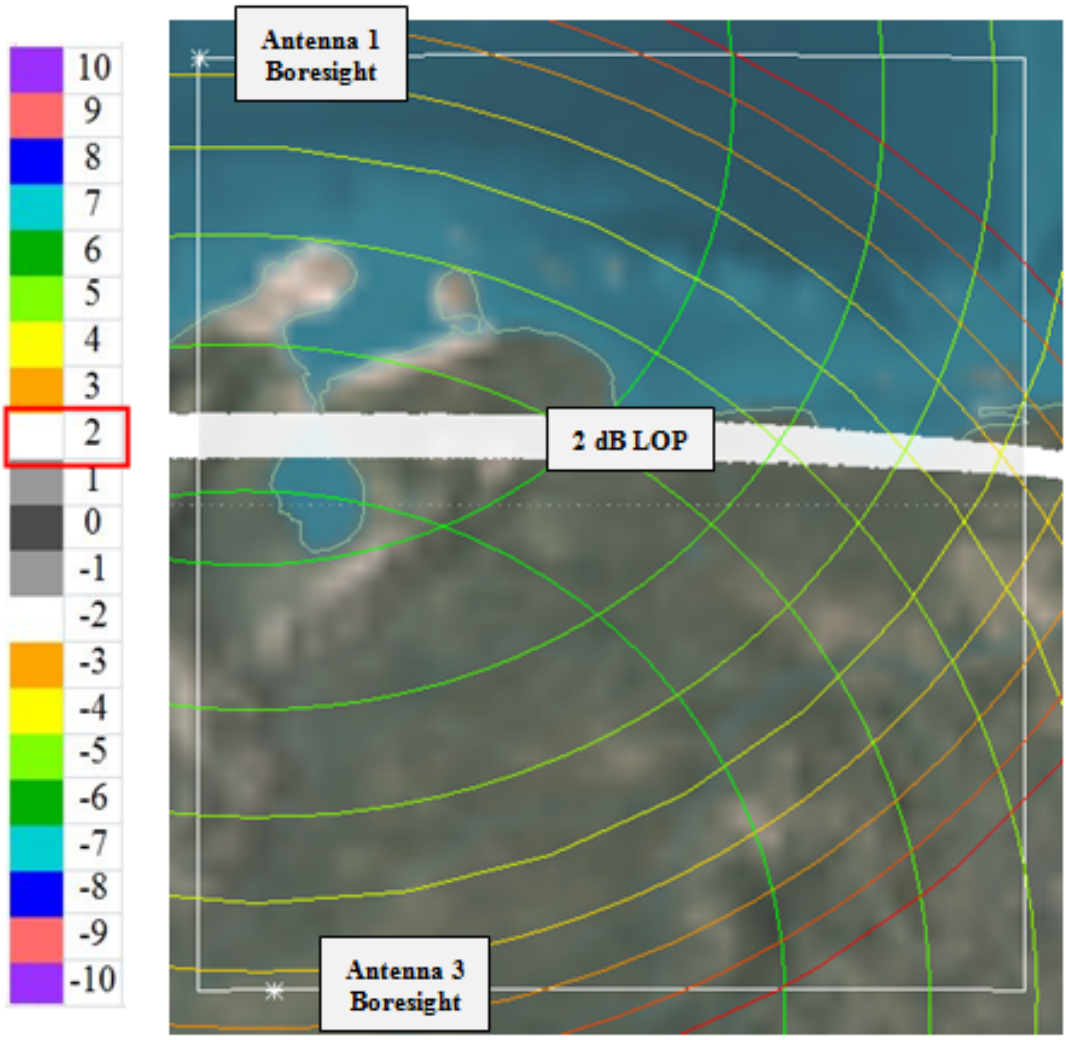

Figure 27. Single Gain Difference Contour (G_1 - G_3).

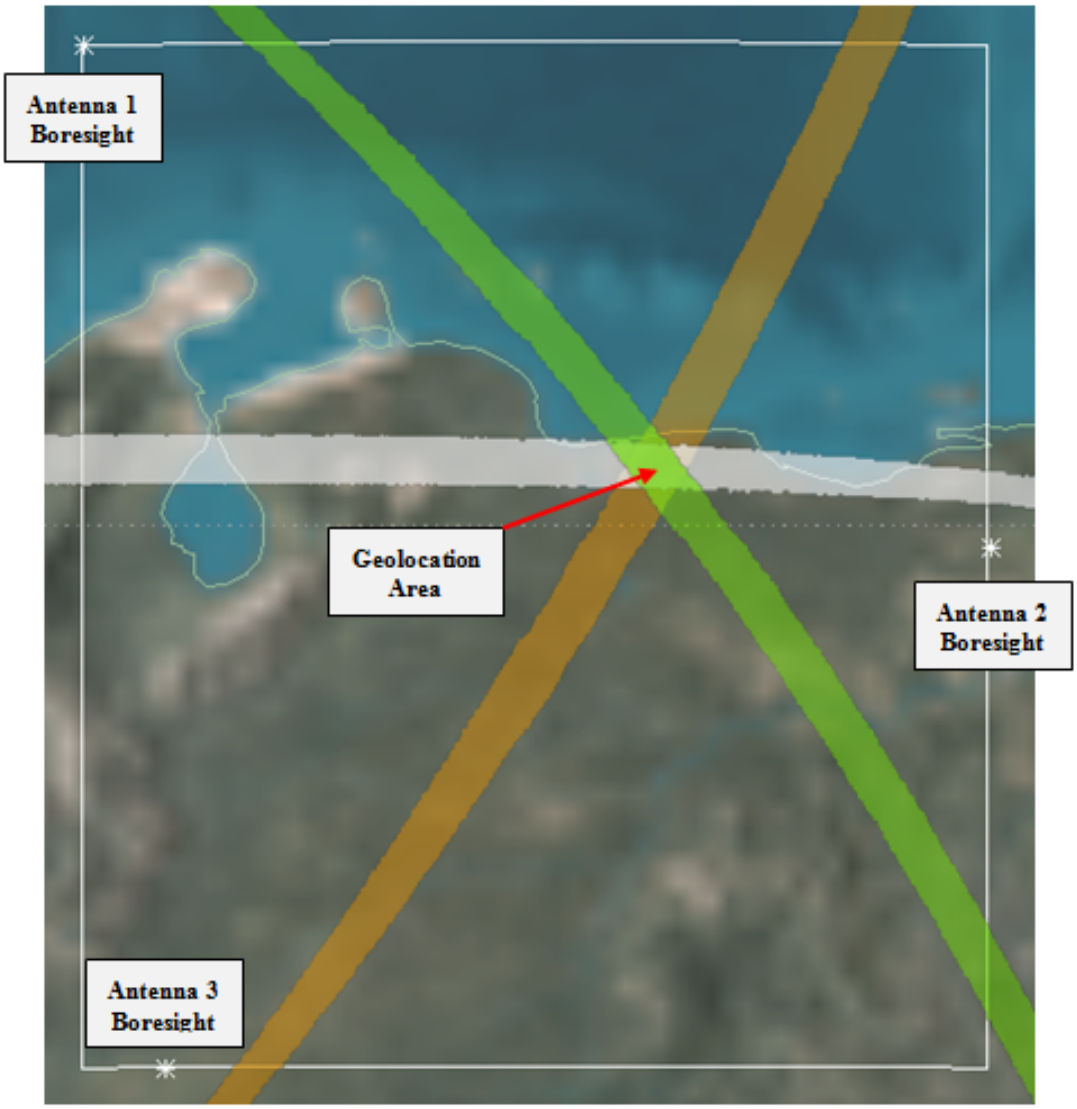

Figure 28. Geolocation Area Produced by Three LOPs.

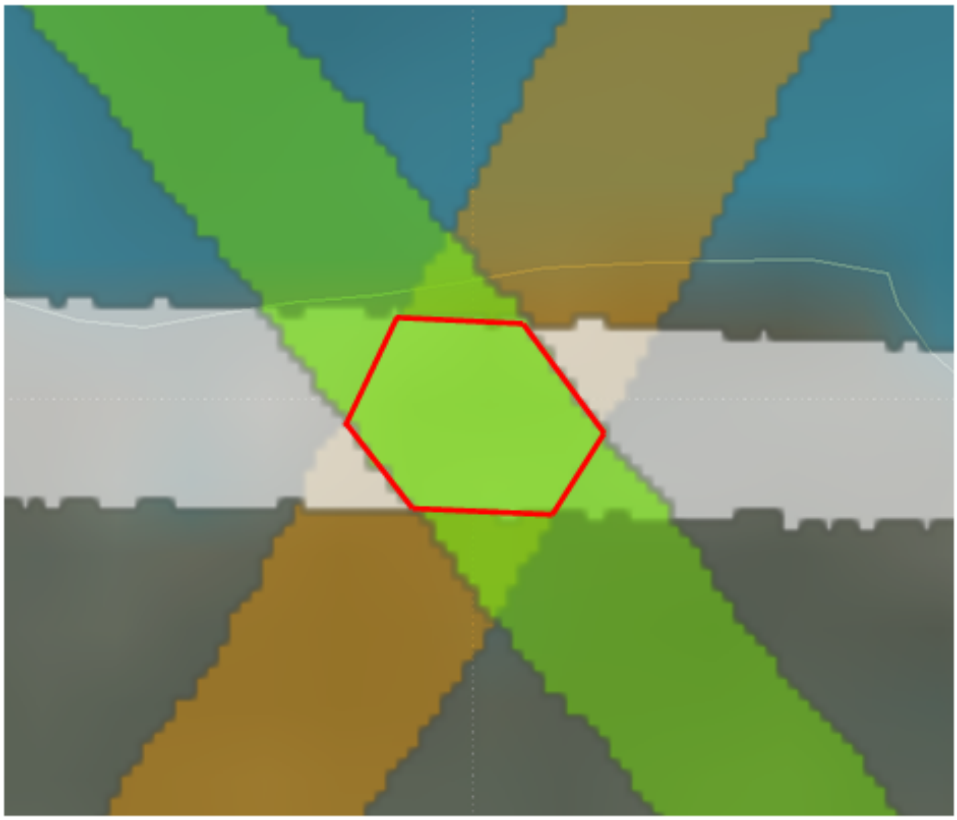

Figure 29. Zoom of Geolocation Area.

D. ADVANTAGES AND ASSUMPTIONS

1. Advantages

a. Single Satellite Geolocation

This innovative means of geolocation offers a number of distinct advantages over previous methods. First and most obvious, it can be completed from a single geostationary satellite with multiple antennas. This feature is in sharp contrast with other geolocation methods that require two or more satellites for geolocation. This is an especially attractive feature when operating in a fiscally restrictive environment.

b. Geolocation Can be Done in Real Time

A second advantage of this geolocation method is the potential that it can be processed in real time. The antenna gain difference contours could be computed at the onset of satellite operation and possibly stored for later use. At the instant interference is

detected, the geolocation can be completed as quickly as the satellite operator can measure the strength of the interfering signal at each receive antenna, compute the differences, and identify the difference contours that contain the interfering source.

A tutorial that teaches the user how to setup and conduct the geolocation method in STK 10 is included in the Appendix. Any latency in geolocating the interfering source will most likely be a result of the time it takes the user/operator to recognize interference plus the time it takes the user/operator to run the geolocation algorithm.

c. Passive Geolocation

A third advantage of this geolocation method is that is entirely passive and self contained. It works entirely by reading and interpreting information available to the satellite operator; it does not, in any way, emit any type of signal that could be detected by the interfering source. During satellite operations, if interference is detected, the geolocation method can be used to mitigate and/or eliminate the interference without alerting the interfering source in any way. This can be especially beneficial if the detected interference is malicious or intentional in nature.

Along those same lines, the geolocation method is self contained. It should be possible to apply the technique without the need for additional equipment on the ground or onboard the spacecraft. This idea will be discussed in greater detail in Part 2.e.

2. Assumptions

a. Satellite Ephemeris is Accurate

The geolocation method requires that the satellite employing the method is positioned in geostationary orbit. This requirement carries with it the assumption that the interfering source is within the FOV of multiple adjacent antennas and that the signal strength measurements are taken as a snapshot in time when interference is detected. No changes in power measurements attributed to movemements of the satellite are used in this geolocation method.

Moreover, the exact location of the spacecraft is assumed to be known to the satellite operator at all times. The satellite may drift between station keeping maneuvers

due to orbital perturbations but it is assumed that the satellite operator can maintain accurate positional data throughout. Any errors in the determination of the satellite position would affect the accuracy of the geolocation method.

b. Minimal Pointing Errors

Along with the assumption that satellite position is known comes the assumption that there are no errors in pointing each of the three antennas. It is assumed that the satellite operator knows the precise parameters of each antenna and can accurately plot the location of the boresight and associated contours. Errors associated with inaccurate pointing data would add positional error when calculating the associated LOPs. Also, inaccuracies associated with the LOPs themselves would add positional error into the plot of the geolocation AOP. The summation of these errors in the final geolocation solution would have an unknown effect on the validity of the product. It is possible that these errors could cancel each other out, but it is equally possible that they compound each other to produce a noticeably erroneous geolocation.

c. Antennas Tuned to Same Frequency

Thus far, it has been assumed that all antennas were operating at the same frequency. This assumption is supported in Chapter I where it was shown that an advantage of newer satellites that create spot beams is frequency re-use. It is therefore possible that adjacent antennas on a satellite are operating at the same frequency.

This is an important assumption for the geolocation method. In order for the math in Equations (2.13), (2.14), and (2.15) to remain valid, all of the antennas being used in the geolocation method must be tuned to the same frequency. This is due to the fact that both the antenna gain equation (2.1) and the free space loss equation (2.6) depend on the frequency of the signal. The difference contours cannot be calculated for the three receive antennas signal strength measurements if the antennas are not opearating at the same frequency.

While it is possible that the antennas are operating at the same frequency at the time interference is detected, it is more likely that adjacent antennas are operating at

different frequencies. This is done to prevent co-channel interference (CCI), which occurs when a user signal transmitted from one footprint is received in the side lobe of an antenna controlling an adjacent footprint [1, p. 337]. The signal from the adjacent footprint is received with much lower gain but, since it is operating on the same frequency, it is superimposed on top of the signals received in the main lobe. The net effect is added noise to the signals in the main beam (CCI). Ironically, this concept is exactly what enables the geolocation method in this thesis, except that the power seen from an intentionally interfering source is likely much greater than the power from CCI. The exact channelization plan for each antenna on a satellite will vary depending on the requirements of the communications satellite system and its associated users.

In this arrangement, a constraint on the geolocation method is that the operating bandwidth of the antenna transponders must include adjacent frequencies. If a receive antenna is able to see/measure an interfering signal in an adjacent footprint, even if it is not providing service at that frequency, the geolocation method should still apply. This is plausible if the channelization design of the satellite provides for overlap in the operating frequency range of adjacent antennas [1, pp. 334-336], [2, pp. 458-459], and [8, pp. 209-211].

Alternatively, the geolocation should still work if the satellite operator is able to re-tune the adjacent antennas to the same frequency (that is being affected by the interference). If the interference is still evident after the antennas are operating at the same frequency, the signal strength at each antenna can be measured to conduct the geolocation method. This would assume that the CCI can be characterized and any disruption of service to users in adjacent footprints is acceptable for the time required to complete the geolocation method.

d. Interfering Source Located in FOV of Three Neighboring Antennas

This assumption is simple to satisfy with a system like the INMARSAT Global Xpress system (Figure 5) that provides worldwide coverage with spot beams. In a similar fashion, the geolocation method should work for any system that employs spot beams in a manner that creates an overlap in FOV that could reasonably contain the interfering

transmitter. Alternatively, it is feasible that the geolocation method could also be accomplished with fewer antennas provided they could be steered to provide the necessary signal strength difference measurements.

For example, a satellite utilizing only two spot beams detects interference in the FOV of the antennas. At a minimum, the signal strength measurements from the antennas can be used to compute a single LOP based on the difference of the two measurements. This alone might be enough information to mitigate the interference and restore functionality to the user; or it could be combined with other known information (such as land masses or bodies of water) to infer a geolocation estimate. If one or both of the antennas are steerable, an antenna can be re-oriented to create the three spot beam geometry shown throughout Chapter I. A possible drawback to this approach could be error induced by the time required to change the orientation of the antenna boresight and to take a new measurement.

Similarly, a satellite with a single steerable spot beam could theoretically complete this geolocation method. This would require trial and error by the satellite operator since the starting condition would only be a single signal strength measurement at the time of interference. Assuming the interference is stationary and continues long enough to obtain additional measurements, the satellite operator could systematically change the orientation of the antenna and record signal strength measurements to generate LOPs. It is unclear whether the time required for this version of the method would hinder the ability to produce a reliable geolocation AOP.

e. Signal Strength is Measurable

A critical assumption in this thesis is that the strength of the signal received by the satellite antennas can be measured. Ideally, the received signal strength is measured immediately at each receive antenna. In this location, the value of the received signal strength is the most accurate representation of the relationship between the interfering transmitter and the satellite antenna. Performing the geolocation technique with the measurements taken at this location will result in the most accurate geolocation AOP.

Figure 30 depicts a simplified model of a possible satellite receiver system. The parabolic line represents the parabolic receive antenna. The "Gain" signifies the ideal location to measure the power of the signal as it is received by the antenna.

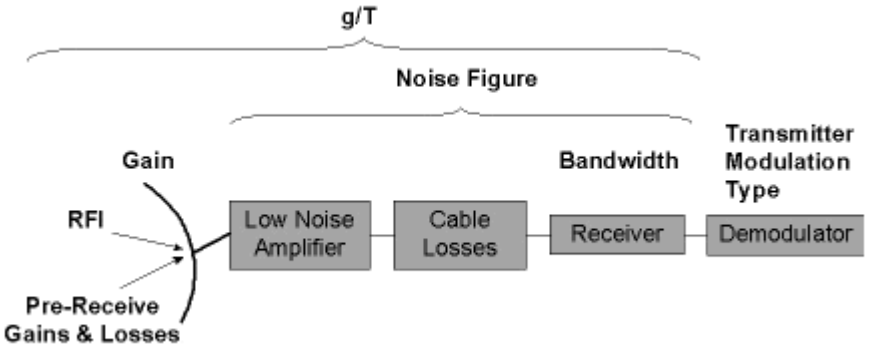

Figure 30. Simplified Diagram of a Satellite Receiver System (from [16]).

If the received power cannot be measured immediately at the receive antennas, then the path the signal follows until it can be measured must be characterized with the highest degree of accuracy. This is due to the fact that, in addition to the availability of the measurement, the accuracy with which the signal strength measurement can be made for each antenna is also essential to the geolocation method. If the signal strength can be measured to ± 0.1 dB, it will likely produce a better geolocation AOP than a signal that can only be measured to ± 1 dB. Along those same lines, if each component in the path of the signal adds ± 0.1 dB of uncertainty to the signal strength before it can be measured, a significant amount of error may be induced in the resultant AOP.

For example, in Figure 30, after the signal is received by the antenna, it goes through a Low Noise Amplifier (LNA) to boost the signal strength, it experiences losses as it travels along transmission lines, then enters the satellite receiver hardware. Once inside the receiver, the signal may go through a Bandpass Filter (BPF) to verify it is in the correct frequency range before continuing on to any number of other components inside the satellite. Any of these components that apply unknown changes to the signal strength, such as amplifications or losses, affect the integrity of the original relationships between the three measurements and induce error in the geolocation AOP.

Similarly, as Figure 30 only depicts a single receive antenna, it is important to understand how each signal received at each antenna flows through the satellite. Does each signal flow through a separate but identical path? Do they merge at some point and follow the same path and experience the same changes in signal strength? Do they experience any potentially different changes to signal strength anywhere in the signal flow scheme? These questions could have different answers for different communications satellites.

Figure 31 illustrates the communications payload signal flow for Boeing's Wideband Global SATCOM (WGS) satellites. The bottom half of the figure shows eight narrow coverage antennas (NCAs) that travel along separate paths through the entirety of the payload. Each signal has a dedicated LNA, and then each signal goes through the intermediate frequency (IF) down converter, a channelizer, an up converter, another dedicated amplifer, and then out a transmit antenna. This schematic suggests that a signal received by each antenna follows a separate path, with separate amplification devices, but experiences identical alterations made in the digital signal processing components (down-converter, channelizer, up-converter).

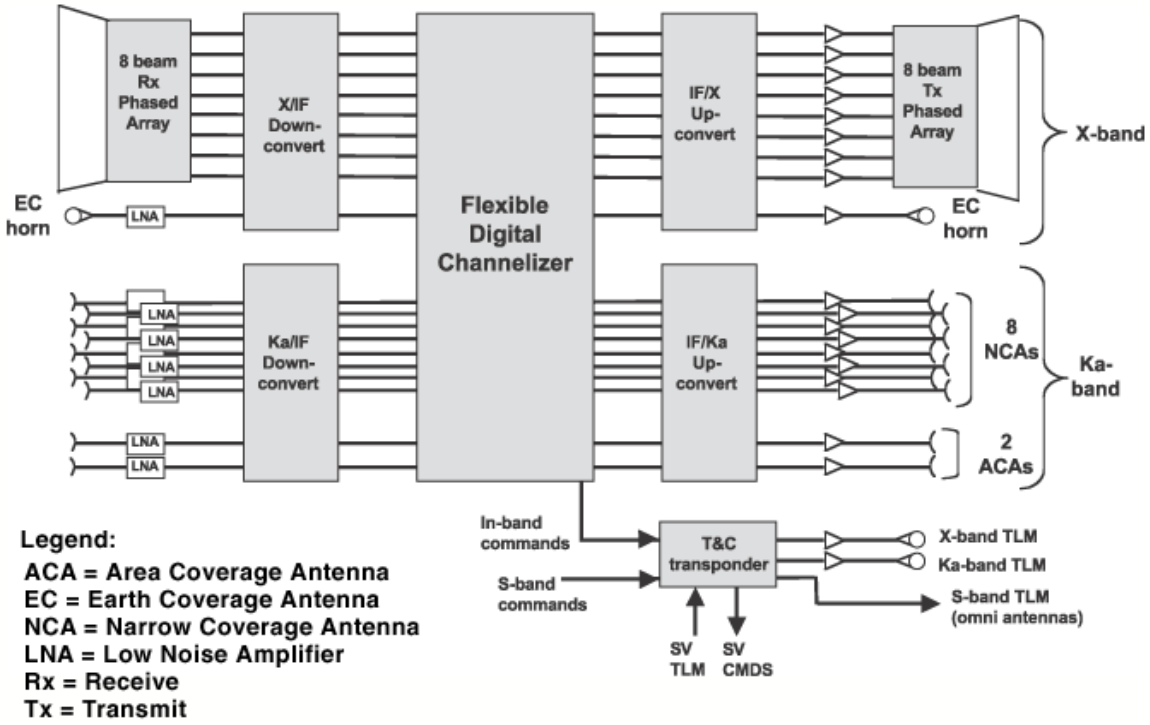

Figure 31. WGS Payload Block Diagram (from [17]).

All of these uncertainties surrounding the signal strength measurement leave a number of potential scenarios that can affect the geolocation method. What is certain is that any error in the accuracy of the signal strength measurement directly results in error in the associated geolocation AOP. Therefore, the best possible scenario is that the signal power is measured immediately at the antenna and it is measured with a high degree of accuracy. This scenario would produce the best geolocation AOP. The next best scenario is that the signal strength is measured as soon as possible in the satellite components, that it is measured with a high degree of accuracy, and any changes made to the signal before it is measured are characterized with a high degree of accuracy. This scenario would theoretically produce a very good geolocation AOP, even if the signal strength is not read until it reaches a ground control station via telemetry data. As long as the changes applied to the signal while onboard the satellite are known, a good geolocation AOP can be created.

Undesirable scenarios result when the signal strength cannot be measured with accuracy, or changes made to the signal strength are not known with accuracy. These

scenarious would induce an unkown but probably significant amount of error in the geolocation AOP. But, these scenarios can potentially be mitigated through the use of a calibration (or reference) signal.

A calibration signal is a signal that originates from a known location, with known parameters (EIRP) [18]. Since the transmit parameters of the signal equation are known, a calibration signal can be used to calculate what the gain should be at the receive antenna. The satellite operator can then use this knowledge to map the signal flow through the satellite until the signal strength can be measured, which then allows the satellite operator to correct for any changes found in the signal when it is finally measured.

For example, Satellite X is not equipped to measure the signal strength of each of its three receive antennas, but those measurement are reported in telemetry data to the ground station controlling Satellite X. A calibration signal is used to show that a signal passing through Satellite X will always end up 0.25 dB lower for G_1, 0.15 dB lower for G_2, and 0.2 dB lower for G_3, than the calculated value expected at the receive antenna. The satellite operator would simply apply these corrections to the signal strength received in the telemetry data to find the true power measurement for the receive antennas. The satellite operator would then calculate the differences in these measurements to find the LOPs to conduct the geolocation.

E. CHAPTER II CONCLUSION

In summary, Chapter II has detailed a fresh approach to geolocating the source of RF interference using a single satellite with multiple antennas. The gain patterns produced by a satellite's unique antenna configuration as they intersect the surface of the Earth are known by the satellite manufacturer/operator. Once the satellite reaches geostationary orbit, the differences in antenna gain for various points on the surface of the Earth within the antenna fields of view can be computed and plotted. These difference contours remain constant as the satellite conducts operations because they were computed using the values of the gain from each antenna, which does not change based on the signals received.

As soon as interference is detected, the strength of the signal received at each antenna is recorded. The differences in these measurements for each pair of antennas is calculated to identify which of the previously computed contours are also the LOP for the interfering source. The intersection of these LOPs reveals the geographic area that contains the interfering transmitter.

The theory of the geolocation technique is sound and highly tenable. But, the quality of the product produced by the method very much depends on the quality of the system employing it. In an ideal scenario, the geolocation technique will locate the interfering source with a high degree of accuracy. Inaccuracies due to potential satellite positioning errors, antenna pointing errors, and antenna gain contour plotting errors can only serve to degrade the potential of the geolocation product. Moreover, the biggest unknown currently surrounding this geolocation method is the availability of the signal strength measurement. The accuracy with which the signal strength measurement can be made will play a major role in the formulation of the final geolocation area.

III. MODELING THE GEOLOCATION METHOD

A. CHAPTER III INTRODUCTION

To test the feasibility of the single satellite multiple antenna geolocation method, it was necessary to create a model with as much real world fidelity as possible. The first step in creating such a model was defining the essential requirements needed to facilitate its creation. The geolocation method required the ability to simulate complex relationships between a single satellite with multiple antennas and a terrestrial transmitter. It also required the ability to graphically represent the computed difference contours in order to facilitate the explanation of the method.

Microsoft Excel, MATLAB, and Systems Tool Kit (STK) were all considered for use as the modeling software. Ultimately STK, created by Analytical Graphics, Inc. was chosen for the model due to its superior ability to meet the two main requirements of the model. "STK is an extremely powerful and highly adaptable physics-based software engine capable of accurately displaying and analyzing land, sea, air, and space assets in real or simulated time" [16].

Furthermore, STK possesses a myriad of capabilities that make it an ideal candidate for modeling the geolocation method. STK can model various vehicle positions and orientations dynamically over a user defined period of time, and offers a number of propagation algorithms for the vehicles. It also allows external input of user defined algorithms. STK can model a variety of characteristics of sensors, communications components, or other payloads assigned to a vehicle or asset. Additionally, it can model spatial relationships between assets and other objects being considered in the scenario. All of these relationships can then be further assessed for quality over defined regions, communications links, and/or a multitude of other factors. STK can accurately account for environmental effects, such as sun position, rain, and other weather on sensor visibility or communication link quality. And finally, STK can precisely display all of the aforementioned models in 2D, 3D, and/or with a plethora of analytical reports and graphs.

Chapter III is organized into three main sections. Part B addresses the initialization of the model, the importance of the Receiver object, the Transmitter object, and a discussion of how both objects were employed in the model. Part C covers the manipulation of various STK tools to generate the calculations required for setting up the geolocation. Part D details the graphical display of difference contours and the geolocation of the interfering source. As mentioned in Chapter I, an STK 10 step-by-step tutorial for modeling the single satellite multiple antenna geolocation method is included in the Appendix. The tutorial guides the user through setting up a sample scenario and then provides instructions that allow the user to perform the geolocation method in a real world application.

B. MODEL INITIALIZATION

1. Satellite Setup

The geolocation technique was modeled using STK version 10.0.2 (released July 2013). To begin model development, a blank scenario was created and initialized with the default time period of 24 hours. From there, it was necessary to first build the single satellite, multi-antenna configuration. For this purpose, a Satellite object was inserted at subsatellite point (SSP) 305° with 0° inclination and a geosynchronous orbital period. These inputs are shown in Figure 32. This setup simulates a geostationary satellite located such that a vector drawn from the center of Earth to the spacecraft would intersect the surface of the Earth at 0° latitude and 305° longitude. The STK model uses J2 perturbation with no other constraints imposed.

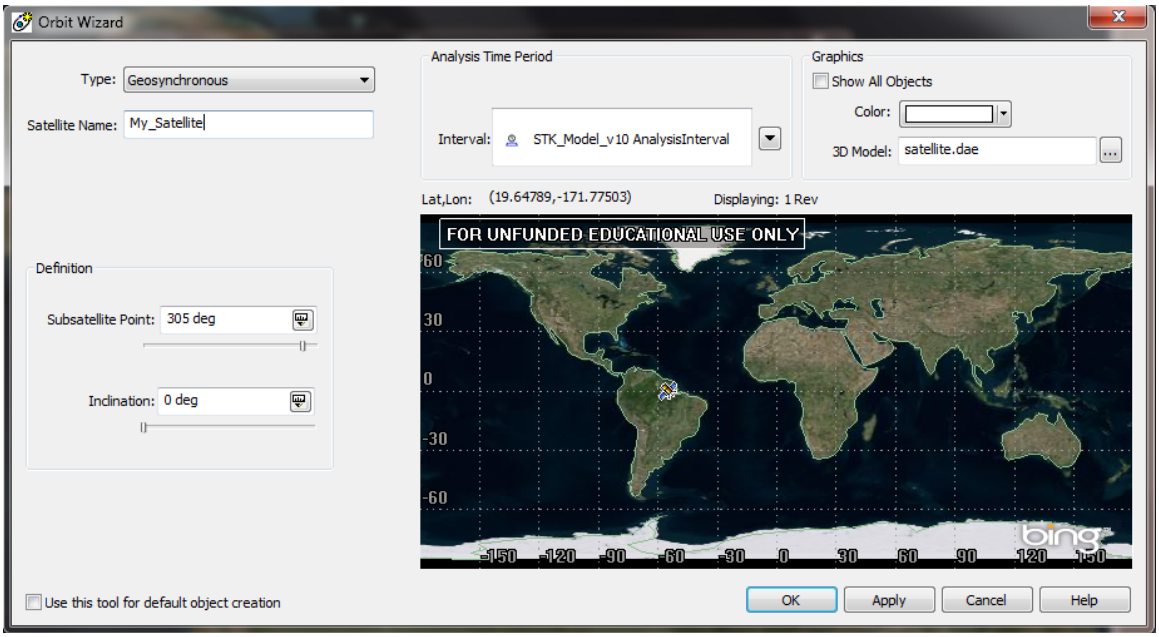

Figure 32. Modeling a Geostationary Satellite in STK.

2. Antenna and Receiver Configuration

The next step was adding three antennas on the satellite. The Receiver object in STK 10 offers a highly configurable representation of all "receive specific" components found on a typical communications satellite. Examples of Receiver components that can be modified include LNA line loss, LNA Gain, LNA to receiver line loss, antenna parameters, noise temperature components, demodulator type, etc.

Recall that for the ideal execution of the geolocation technique, the signal strength should be measured immediately as it is received at the satellite receive antenna. This location in the communications satellite received signal flow is represented by the 'Gain' term in Figure 30. This term is referred to as "Receiver Gain" in STK specific objects, reports, and graphs.

a. Antenna Parameters

The frequency for the geolocation model is set at 25 GHz (Ka band). The parameters used to define the receive antenna are embedded in the STK 10 Receiver object. Each of the three antennas was configured as a parabolic reflector operating at 25

GHz, 2° beamwidth, and 55% antenna efficiency (η). The resultant peak antenna gain of each antenna is 36.7372 dB. These values are shown in Figure 33.

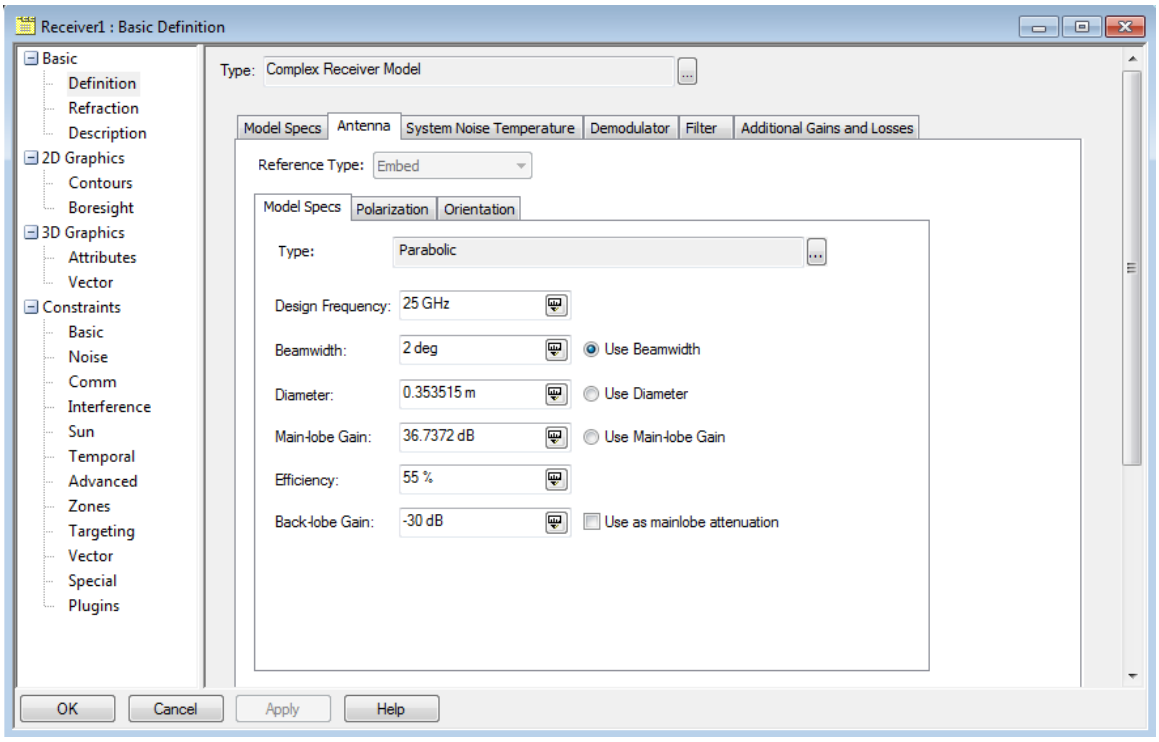

Figure 33. Modeling Three Ka Band Receive Antennas in STK.

b. System Noise and Demodulator

Two other parameters required by STK to be defined in a receiver object are the System Noise Temperature and the Demodulator. The Noise Figure above controls any system noise that might result from temperature fluctuations in the antenna feed assembly/structure. It also controls the noise that could result from energy fluctuations within the antenna's field of view. The Noise Figure variables are configured via the STK Receiver object System Noise Temperature tab. Because the Noise Figure occurs *behind* the "Receiver Gain" measurement (Figure 30), the model needs to ensure that the Noise Figure is the same for each of the three modeled antennas to prevent skewing STK's representation of the measurement. As such, the model uses a constant System Noise Temperature of 290 K. Similarly, in order for STK to create the analysis of the "Receiver Gain", the Receiver objects and the Transmitter objects involved in the

analysis must use the same Demodulator type. This model uses Quadrature Phase-Shift Keying (QPSK) demodulation.

c. Antenna Orientation

Each antenna was pointed (boresight) to emulate Antennas 24, 25, and 34 from Figure 5 (INMARSAT Global Xpress Coverage). In the model, Antenna 1 corresponds to Footprint 25, Antenna 2 corresponds to Footprint 34, and Antenna 3 is Footprint 24. Geographically speaking, the footprints approximately cover the northern section of South America, the southeastern region of Central America, the Caribbean Sea and various Caribbean islands. The footprints are shown in Figure 34.

Figure 34. Graphical Display of Antenna Footprints in STK.

3. Constrain the Area Target

Once the receivers have been modeled, the geographical area that will be used to focus the analysis of the model can be created. The STK Area Target object allows the user to constrain the analysis products to a specific geographical region. In the geolocation method, the interfering source is assumed to be contained in a geographical region bound by the intersection of the fields of view of each antenna. This area was represented in the STK Model by an Area Target object called "Area_Of_Interest", shown in Figure 35. It geographically approximates portions of Colombia, Venezuela, and the Caribbean Sea.

Figure 35. Model of Area of Interest in STK.

4. Configure the Transmitter Model

a. Add a Facility

A Transmitter object is required to complete the initial setup of the geolocation model. STK requires a transmitter object in order to enable communications link analysis with a receiver object (explained in further detail in Part C). For the initial setup of the model, a Facility object was inserted randomly inside the Area of Interest (any terrestrial object can be assigned a Transmitter such as a Facility, Aircraft, Ship, Vehicle, etc.).

Figure 36. Modeling a Facility in STK.

b. Add a Sensor

A Sensor object was attached to the Facility, and an Antenna object was attached to the Sensor. The Sensor object is used to point the Antenna object at the satellite. The Antenna object defines the antenna parameters that the Facility will use to communicate with the satellite. The transmitting antenna was modeled as a 1 meter parabolic reflector

operating at 25 GHz (matches the receiver frequency) and 55% antenna efficiency (η). The resultant main-lobe gain of 45.769 dB is sufficient for completing a communications link with the modeled receive antennas on the satellite. These values are summarized in Figure 37.

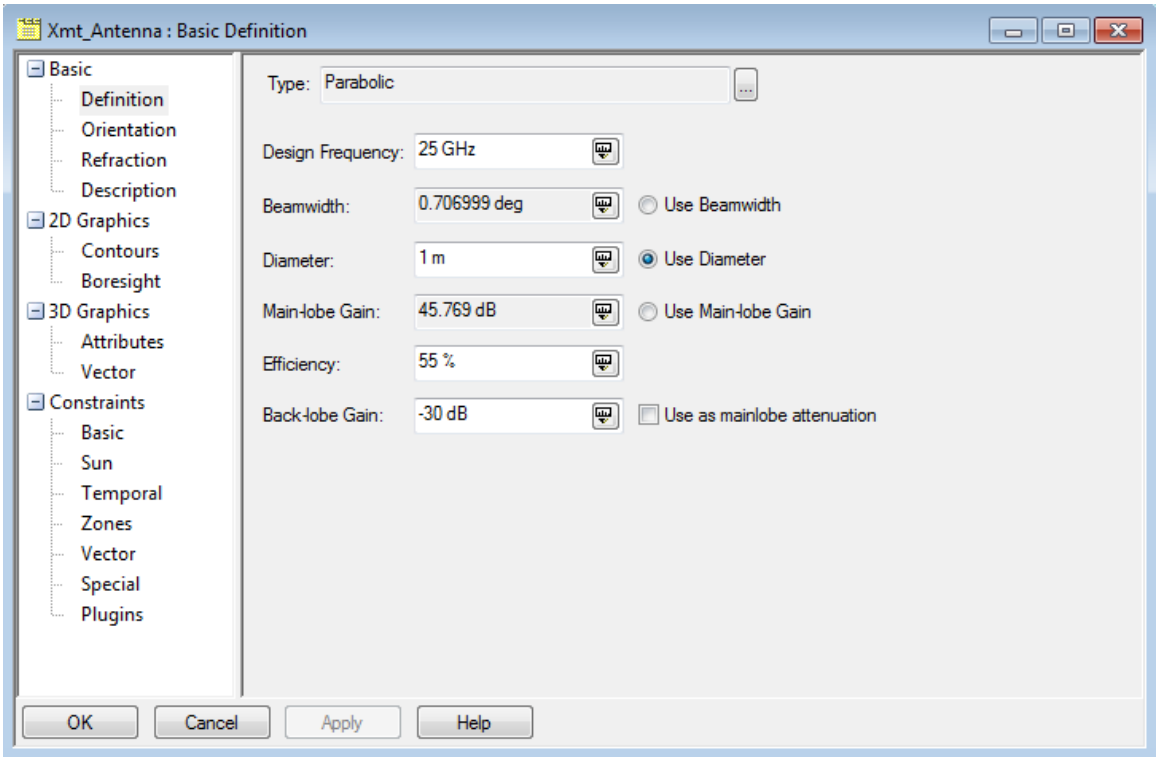

Figure 37. Modeling the Ka Band Transmitter Antenna in STK.

c. Configure the Transmitting Antenna

A Transmitter object is then attached to the Facility. The Transmitter object also operates at 25 GHz, and is linked with the facility's Antenna object described above (see Figure 38). STK allows the user to either embed an antenna inside a receiver/transmitter object or link to a receiver/transmitter. An embedded antenna in STK cannot be targeted at a specific object whereas a linked antenna can, but only if it is attached to a Sensor object. The Receiver object described earlier uses an embedded antenna because the antenna only needs to be pointed toward the Earth to create the associated spot beams. The Transmitter object needs to be able to target the Satellite in order to achieve a

successful communication link. To conclude the Transmitter configuration, it is set to use QPSK modulation to match the Receiver object which was set up to use QPSK demodulation.

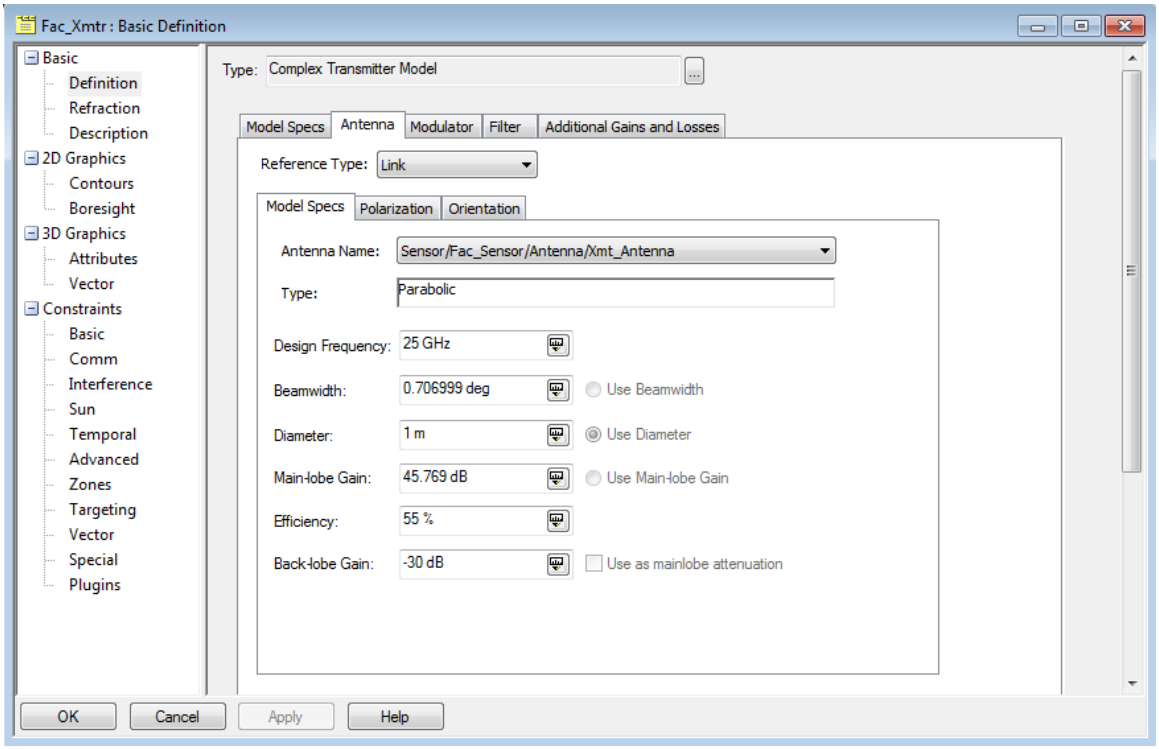

Figure 38. Modeling the Ka Band Transmitter in STK.

C. MANIPULATE STK FUNCTIONALITY

Thus far, the model has been set up with a Transmitting object and a Satellite object containing three Receiver objects all operating at 25 GHz. Each Receiver object models a different spot beam that intersects the surface of Earth, and an area of interest is defined that encompasses the intersection of the three spot beams.

1. Compute Accesses

In order to compute and graphically display the difference contours required for the geolocation technique, the "Receiver Gain" measurements need to be analyzed within the AOI defined by the Area Target object. The first step in progressing toward this

analysis is computing the Access Intervals (or Accesses) between the Receiver objects and the Transmitter object for the defined time interval (24 hours) of the STK scenario.

An Access in STK simply means the times that the two objects are in line of sight of each other. Directing STK to compute the Accesses between the Transmitter and Receivers completes the communication link between the objects and renders the associated link parameters that characterize the link available to the user in a Detailed Link Information report. Figure 39 shows the Access configuration window used to compute Access between the Transmitter and each Receiver.

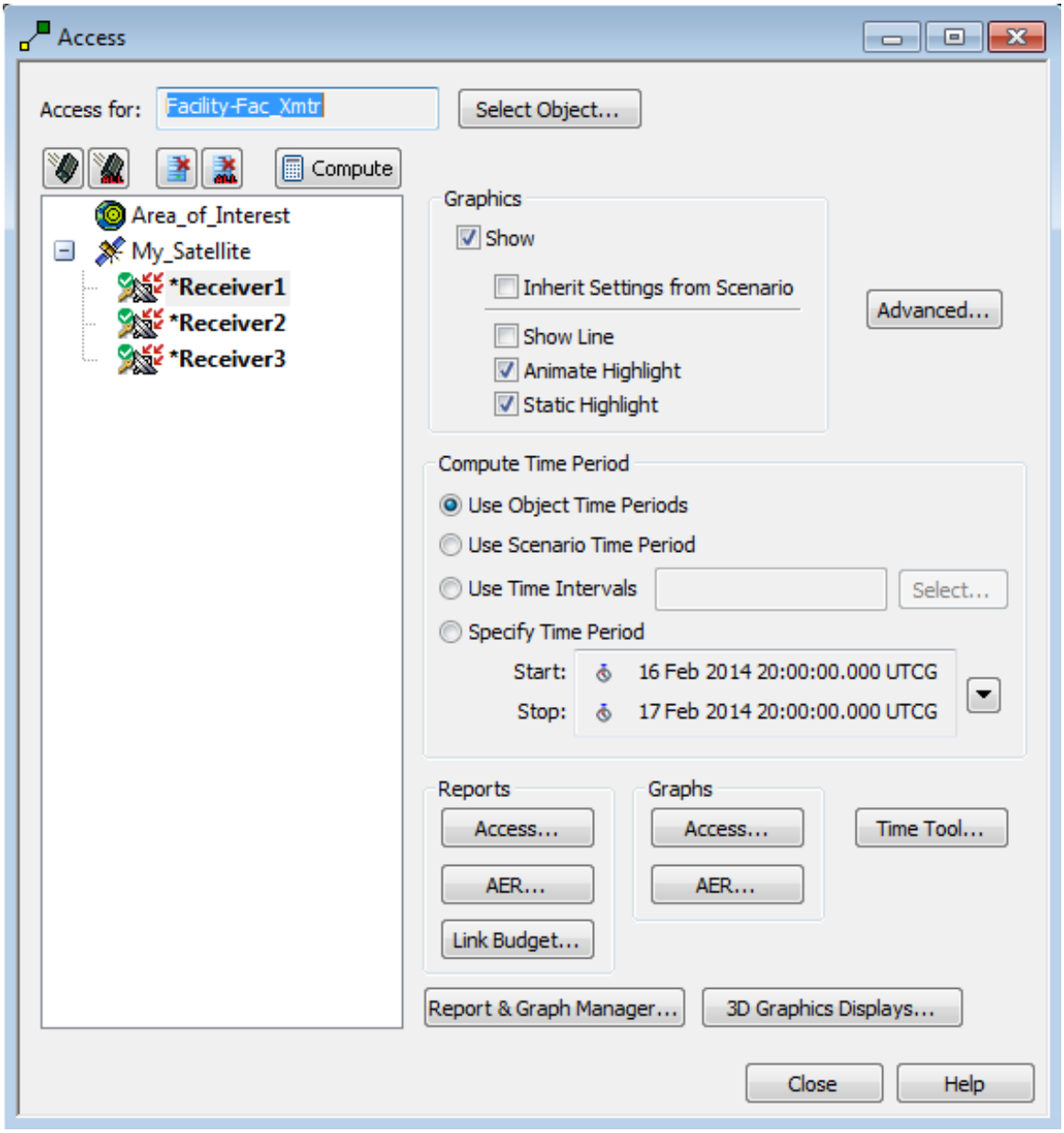

Figure 39. STK Accesses between the Transmitter and Receivers are Computed.

Examples of parameters calculated in the Detailed Link Information report include Transmitter Gain, EIRP, Free Space Loss, and Receiver Gain. Other values are calculated, such as propagation losses, g/T, Eb/No, and BER, but are not used in the model of the geolocation method. Examples of the Link Information report are shown in Figure 40.

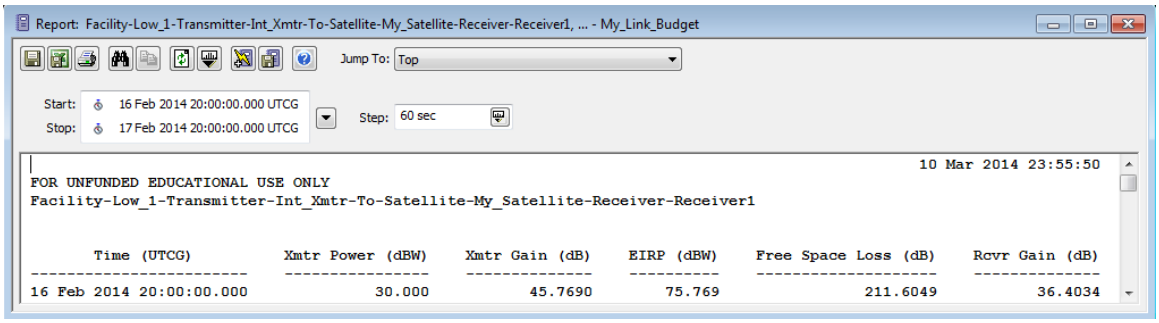

Figure 40. Example of Parameters Calculated in STK Link Budget Report.

Note, since the satellite is geostationary and the Facility object is stationary, the variables mentioned above for the link remain constant over the entire scenario time interval (because the satellite and object would always be stationary with respect to each other). If a mobile object were used for the Accesses (such as a Ship) the variables mentioned above would vary slightly over the scenario time interval.

This is acceptable for the geolocation because the actual values of the "Receiver Gain" measurements are irrelevant. The *differences* between each of these values are needed to create the *difference contours*. In that regard, the only variable in the link budget report that is necessary for the geolocation technique is the "Receiver Gain". At this point in the development of the model, however, the "Receiver Gain" parameter is only available for viewing in the link information report. It cannot yet be accessed for manipulation.

2. STK Analysis Workbench

a. Calculation Tool

One of the most powerful aspects of STK is the degree to which it allows the user to customize and manipulate the data and objects computed by the software. STK offers the Analysis Workbench functionality, which is a menu of tools that gives the user a significant degree of computing options for custom analyses in STK. The Analysis Workbench is subdivided into three main tools. A Time tool that can be used to isolate specific instances or intervals of time, a Vector Geometry tool that can be used to describe an object's location and orientation in space, and a Calculation Tool that allows

the user to generate various time-dependent quantities. The Calculation Tool is the tool that will be used in the model to isolate the "Receiver Gain" measurements and to perform the calculations that produce the difference contours.

b. Scalar Type

STK offers three components of the Calculation Tool: a Scalar type, a Condition type, and a Parameter Set type. The scalar type is relatively self-explanatory. It is essentially a time-varying scalar value or scalar calculation. The condition type allows the user to define a scalar calculation whose value depends on whether the scalar condition has been satisfied in the scenario or not. The parameter set type creates a grouping of scalar calculations. The scalar type is the best choice for accessing the "Receiver Gain" quantity. The other two choices provide functionality beyond the requirements of the geolocation model.

c. Components of the Scalar Type

The Scalar type is offered in a variety of different components. The two elements required for the geolocation model are the Data Element component and the Function (x, y) component. The Data Element component simply allows the user to set a quantity computed in STK equal to a value that can then be accessed by the user. This is the component used in the geolocation model to separate the "Receiver Gain" quantities from the entirety of the link information report. The Function (x, y) component accepts two scalar components and allows the user to apply a power, trigonometric, logarithmic, or exponential function to them. Figure 41 summarizes the Analysis Workbench organization as it is broken down into tools, types, and components. The central branch of the tree describes the associative relationship between the Calculation Tool, Scalar Type, and components used in the model.

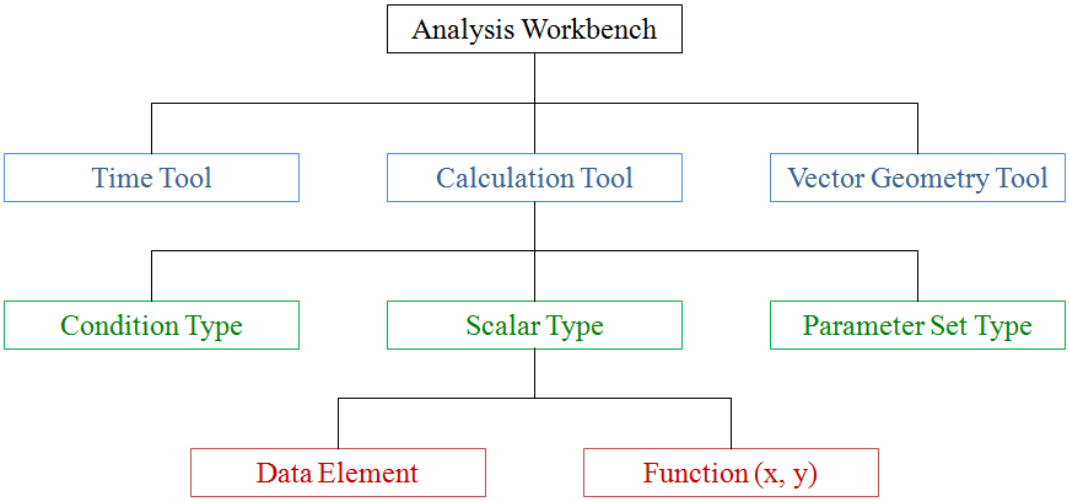

Figure 41. STK Analysis Workbench Organizational Tree.

d. Setup the Equations for Calculation

(1) Create the Data Element Scalars. In the geolocation model, three Data Element scalar calculations are created and set equal to the "Receiver Gain" quantities from each of the three Receiver objects. These scalar calculations are called Gain_Rcvr1, Gain_Rcvr2, and Gain_Rcvr3. The Gain_Rcvr1 scalar is shown in Figure 42. As discussed previously, the "1" (in Figure 42) shows the selection of the Calculation Tool, the "2" shows the use of the Scalar Type, and the "3" shows the created Data Element.

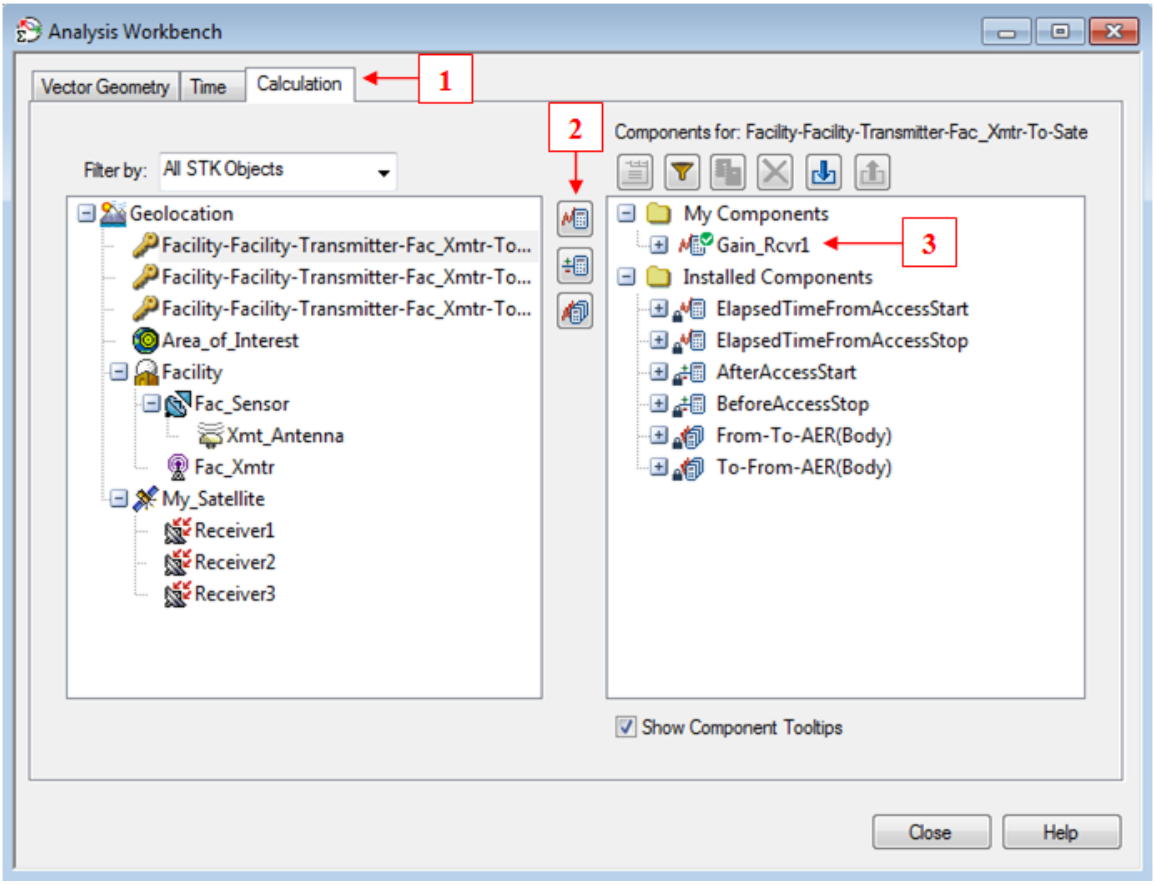

Figure 42. STK Analysis Workbench User Defined Data Element.

(2) Create the Function Scalars. After the three Data Elements are computed, three Function(x, y) components are created and named DeltaGain_1-2, DeltaGain_1-3, and DeltaGain_2-3. This name is a shorthand description for the calculated difference between each of the three scalar calculations. For example, DeltaGain_1-2 represents the difference calculated by taking the Gain_Rcvr1 quantity and subtracting the Gain_Rcvr2 quantity. Figure 43 shows the creation of the DeltaGain_1-2 component. The selected function is a*x + b*y, where *x* is assigned the Gain_Rcvr1 Data Element, y is assigned the Gain_Rcvr2 Data Element, a = 1, and b = -1. The result of these selections is the equation:

$$\text{DeltaGain\_1-2} = \text{Gain\_Rcvr1} - \text{Gain\_Rcvr2} \tag{3.1}$$

Figure 44 shows the three gain difference equations created for the geolocation model.

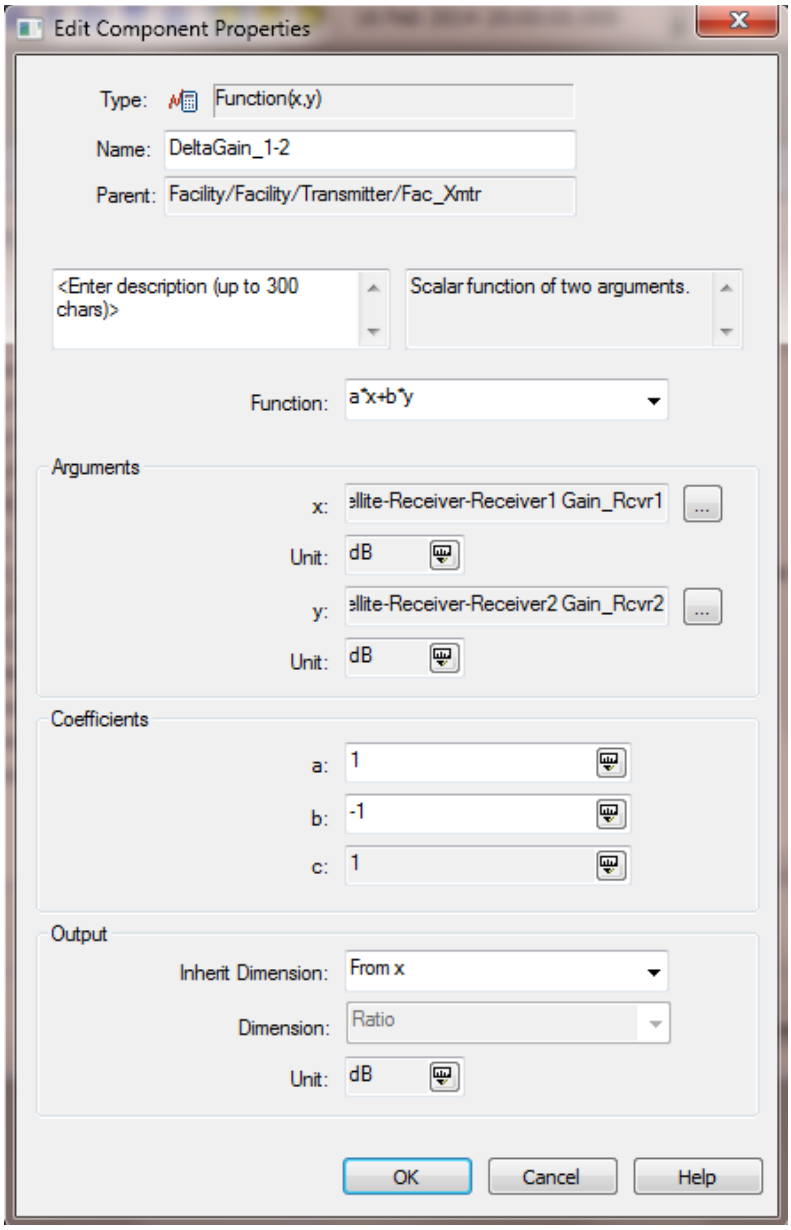

Figure 43. STK Analysis Workbench User Defined Function (x, y) Component.

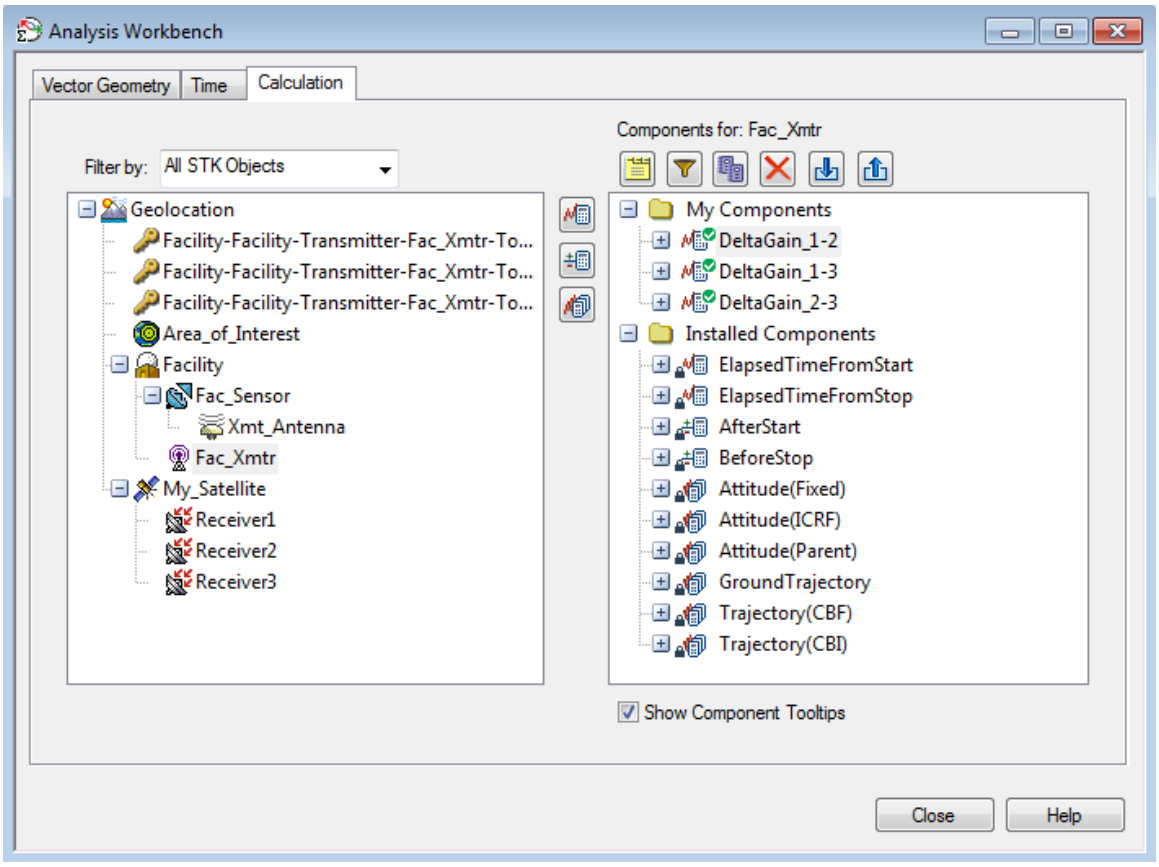

Figure 44. STK Analysis Workbench User Defined Gain Difference Equations.

e. Analysis Workbench Summary

One last point to make regarding the setup of the STK calculations is that each of the scalar components must belong to a Parent object. This concept summarizes the description of this section thus far. In order for these scalar calculations to be available to the user, the Accesses between the Transmitter and the three Receivers had to be computed. When the Accesses were computed, an object representing each possible Transmitter-Receiver relationship was created. The Transmitter to Receiver1 link is one created object, the Transmitter to Receiver2 link is a different object, and the Transmitter to Receiver3 link is also a unique object. Since the Data Element scalar calculation is extracting the "Receiver Gain" quantity for each Receiver based on the computed Accesses, it follows that each of the created objects are the Parent object of the Data Element scalar calculation.

D. THE GRAPHICAL PROCESS

All of the STK calculations in Part C provided the ground work for creating the difference contours using STK. However, the calculations above are applied to the value of the link between the Transmitter and each Receiver at the geographical location of the Transmitter. In order to compute the difference *contours*, the value of the "Receiver Gain" must first be determined for all of the points inside the Area of Interest.

1. Define the Coverage Area

The Coverage Definition object in STK allows the user to conduct analyses on locations inside a designated geographic area. This is different from the Area Target object already described above because the Area Target is a geographic region that is treated as one large object. The user can compute Accesses for the Area Target as a whole but cannot perform detailed analysis on points within the defined Area Target. The Coverage Definition object takes a given region and allows the user to perform operations on subsets of that region.

In the geolocation model, a Coverage Definition object is created and called "CoverageOfAOI" (Coverage of Area of Interest). The Coverage Definition object is assigned the Area_of_Interest Area Target object as the region of consideration. The Coverage Definition object is assigned a granularity of 1 degree, which means it will create a grid of points with approximately 1 degree of latitude/longitude spacing. This is essentially the resolution of the Coverage Definition. Any calculations performed inside the Coverage Definition object will be done at each of these geographic grid points. Figure 45 shows the 136 grid points (each point is represented by a yellow +) created by CoverageOfAOI with 1° resolution.

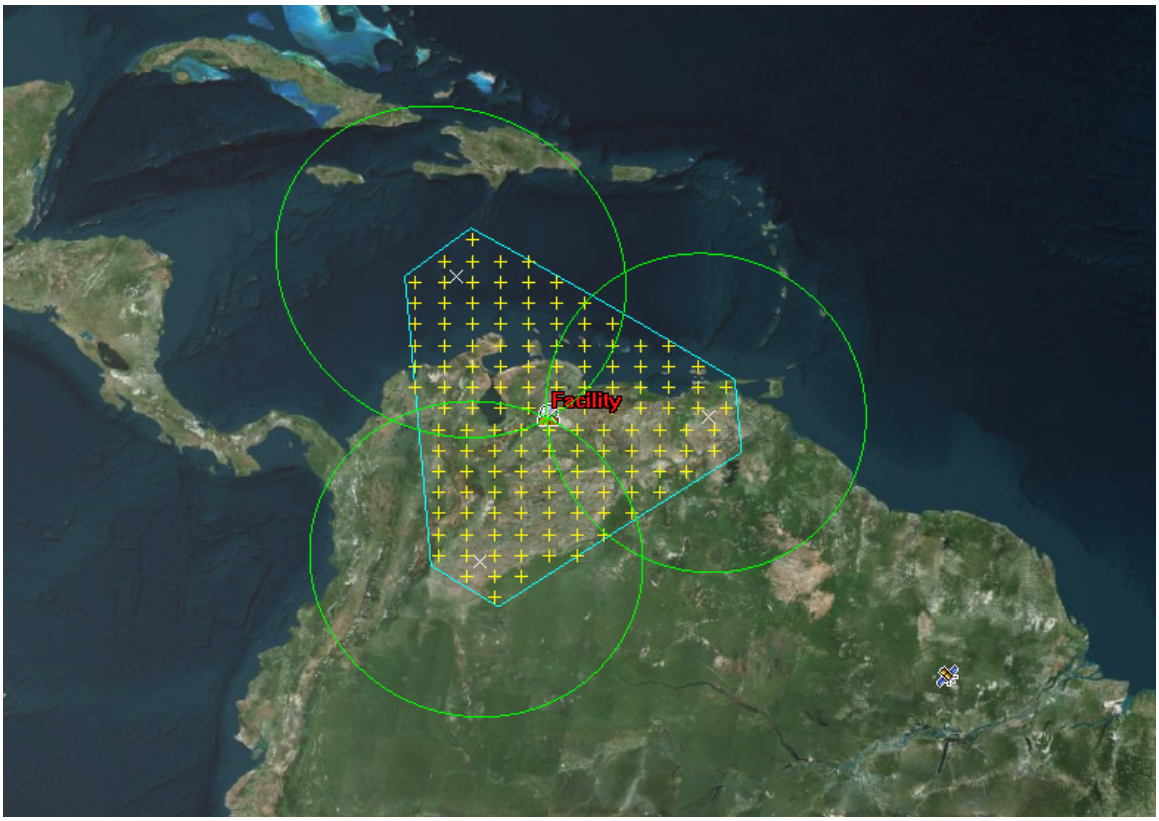

Figure 45. STK Coverage Definition of AOI with 1° Resolution.

2. Constrain the Coverage Area

Next, a constraint is placed on each grid point specifying that the Transmitter object will be used at that grid point (Figure 46). In other words, STK will now calculate the link information as if the Transmitter object were located at each grid point in the Coverage Definition object.

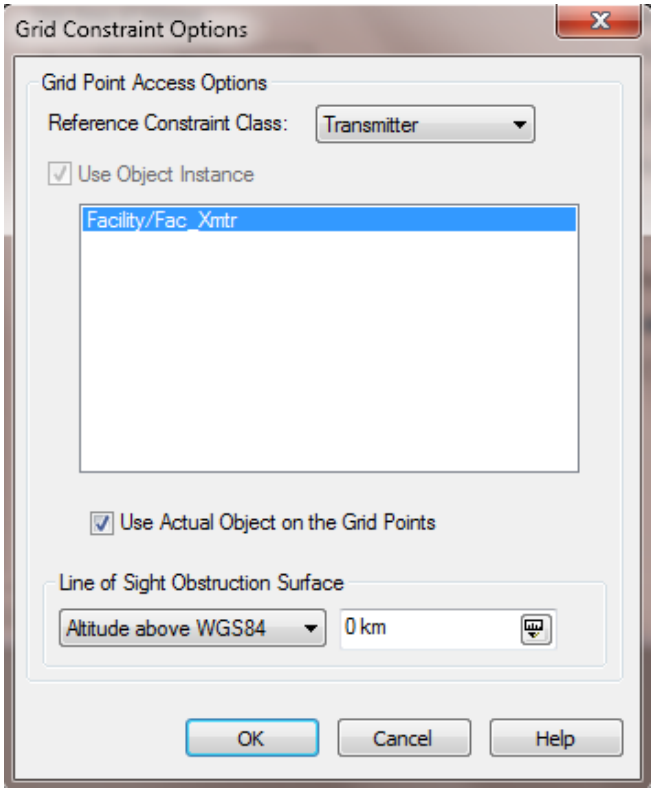

Figure 46. STK Coverage Definition Grid Constraint Options.

3. Assign Assets

Similar to the importance of the grid constraint, Assets must be assigned to the Coverage Definition object. The Assets will be used to calculate the coverage of the grid points inside the Coverage Definition. In the geolocation model, the three Receiver objects are assigned as assets. This is done in Figure 47. In this manner, STK will compute the link information for each Receiver as it accesses each grid point (which has the same properties as the Transmitter). Once these computations are complete, the "Receiver Gain" quantity for each of the three receivers is available at each of the grid data points.

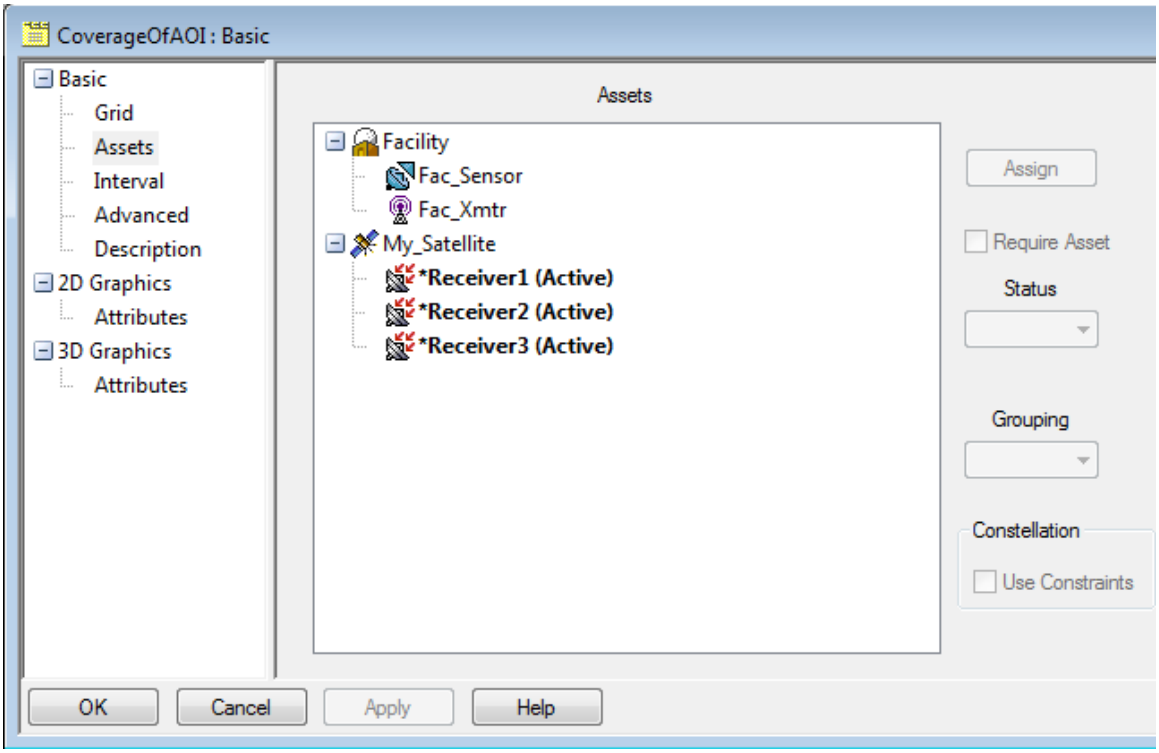

Figure 47. STK Coverage Definition Assigned Assets.

4. Configure Figure of Merit Objects

The last task remaining is the computation of the difference contours for each grid point and their subsequent graphical display in the STK 2D and/or 3D windows. This is accomplished with three Figure of Merit (FOM) objects. The STK FOM object is typically attached to a Coverage Definition and allows the user to specify the method by which the quality of coverage is measured. An FOM object is also a useful object for graphically displaying the quality of coverage that is measured. A few example STK pre-configured FOM options include Access Durations, number of Assets providing coverage, gaps in coverage, dilution of precision, or a scalar calculation.

a. Assign Scalars to FOMs

As described previously, three scalar calculations (DeltaGain_1-2, DeltaGain_1-3, and DeltaGain_2-3) were created for the geolocation model. Each of these scalar

calculations will be assigned to its own FOM object. Once this is complete, all of the actual Accesses described previously must finally be calculated for all of the grid points in the Coverage Definition. This is done in the model with the selection of the "Compute Accesses" command under the Coverage Definition object.

Upon completion of these calculations, all of the values needed to complete a geolocation are complete. This state of readiness of the geolocation model directly parallels the situation described in Chapter II where the antenna gain contours are calculated as soon as a newly launched satellite commences operations.

5. Prepare the Graphics

The graphical display of each difference contour can be controlled inside the associated FOM object. For example, to display the difference contours calculated for DeltaGain_1-2, the user would simply manipulate the 2D and/or 3D graphical display menu inside the DeltaGain_1-2 FOM object. This process is shown in Figure 48, where the DeltaGain_1-2 FOM is configured to display contours ranging from 3 dB to -3 dB, with 1 dB spacing. The colors associated with each contour are assigned in the Level Attributes section. In this example, all of the grid points that produced a delta value between -3 dB and -2.001 dB are plotted in green, all of the points that produced a value between -2 dB and -1.0001 dB are plotted in white, etc.

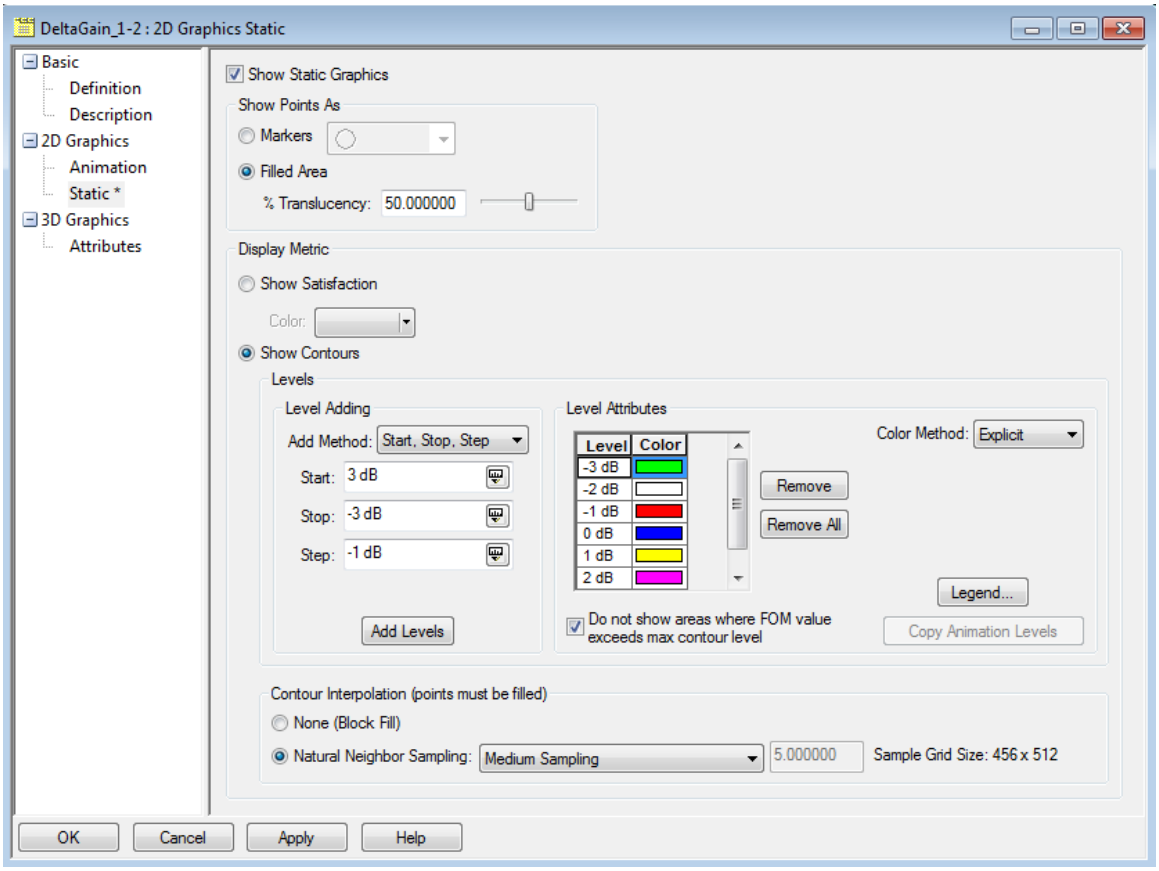

Figure 48. STK FOM Object Manipulated to Display Difference Contours.

The resolution of the Coverage Definition grid point spacing will directly control the accuracy of the computed difference contours. If the granularity is too coarse it could prevent a smooth geometric intersection of difference contours.

E. CHAPTER III CONCLUSION

In conclusion, Chapter III has covered the development and employment of an STK model capable of faithfully testing the new geolocation method. The STK software package has shown to be an invaluable resource for modeling and graphically displaying the geolocation method and subsequent results. Figure 49 provides a summary tree of all of the STK objects used to complete the model.

A limitation of the model that bears emphasis is the fact that, for real world applications, it is not computing the actual observed power measurements at each of the three receive antennas. These values must be measured by the satellite operator (or

satellite manufacturer) and the differences between each value must be manually calculated. Once the gain difference contours are identified, they can be graphically displayed in STK.

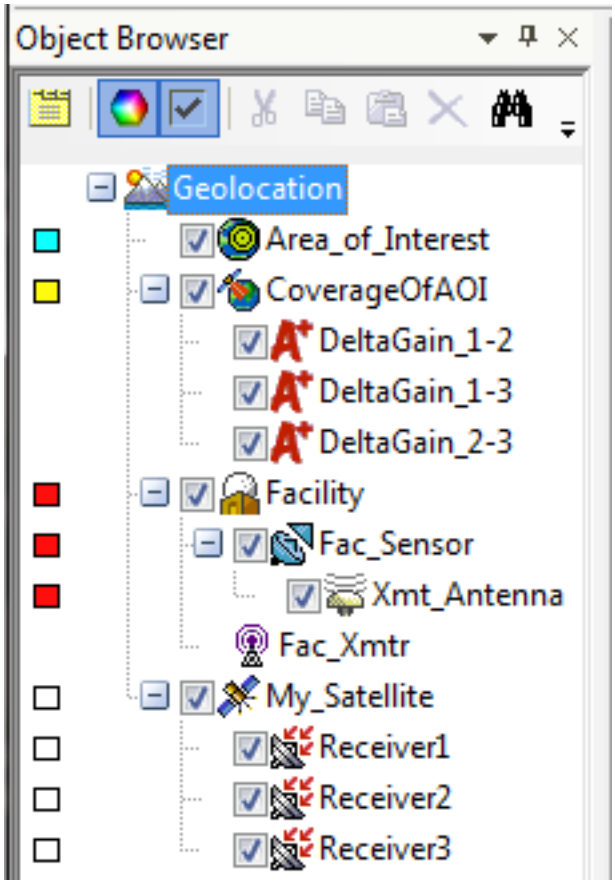

Figure 49. Summary of STK Objects Used to Model the Geolocation Method.

IV. TESTING THE METHOD AND ANALYSIS OF RESULTS

A. CHAPTER IV INTRODUCTION

Now that a high fidelity model has been created, the feasibility of the new geolocation method can be thoroughly explored. Up to this point, the geolocation method has just been a hypothetical means of locating an interfering source. Therefore, the first step in testing is to show that the single satellite, multi-antenna method actually works. The methodology used to prove the validity of the geolocation method is covered in Part B.

Once the method is shown to work, the next step in testing is establishing how well the technique operates under a variety of conditions. To this end, there are two main variables that stand out as requiring investigation: latitude variation and signal strength measurement accuracy.

As seen in the INMARSAT Global Xpress coverage graphic (Figure 5) and explained in Chapter II, the size of the spot beams vary with antenna orientation. If the antenna is oriented straight down from the satellite to the Earth's surface it produces a smaller, more focused antenna gain pattern. The farther the antenna is oriented from nadir, the more elliptical (and larger) the footprint. It is logical to assume that the size of the antenna gain footprint could affect the quality of the resultant geolocation area and therefore needs to be characterized as precisely as possible.

In keeping with the Inmarsat Global Xpress example, four sets of antennas were chosen for testing that approximated four different regions of latitude: a low latitude region, two mid latitude regions, and one high latitude region. The Low Latitude region approximately ranges from 5° to 13° North latitude, the first Mid region covers 16° to 25°, the second Mid region covers 34° to 44°, and the High latitude window is 51° to 71°.

In each latitude region, five interfering emitters were placed pseudo-randomly so as to cover the area of interest at various latitudes inside the AOI, but with approximately equal spacing. This not only allows for testing across different latitudes but also allows for testing how the geolocation method behaves for various locations within the AOI.

Since the satellite is located at SSP 305°, footprints closer to the equator produce the smallest spot beams. Footprints pointing toward higher latitudes produce larger, elliptical fields of view. It is reasonable to hypothesize that a region with more focused spot beams will produce a smaller geolocation area of probability (AOP) compared to a region with larger footprints. So, in the created regions, the low latitude region should produce the smallest AOPs and the high latitude region should produce the largest AOPs.

Similar to the idea that latitude can affect the size of the geolocation area of probability, it is also probable that the accuracy of the signal strength measurement taken at the receive antenna could affect the geolocation AOP. All of the illustrations thus far have assumed a total contour width of 1 dB. This essentially allows for an error tolerance of ±0.5 dB when making the signal strength measurement. It is highly probable that a smaller error tolerance, such as ±0.25 dB, would yield a smaller total geolocation AOP. The accuracy with which signal strength at the receive antenna can be measured will surely vary among different satellite configurations. However, this error tolerance of a given system is likely a parameter known and characterized by the satellite manufacturer and/or satellite operator.

For analysis purposes in Chapter IV, the size of the geolocation AOP generated in each latitude region will be recorded for error tolerances of ±0.5 dB, ±0.25 dB, and ±0.05 dB. These toleranes correspond to difference contour widths of 1 dB, 0.5 dB, and 0.1 dB, respectively. These sample tolerance levels were chosen based upon the assumptions discussed in Chapter II.

These three different contour widths will be referred to extensively throughout this chapter. It is important to understand that when a 1 dB contour (for example) is mentioned in this thesis, the 1 dB corresponds to the line of positions inside the area of interest where the antenna Gx – Gy delta values are within ±0.5 dB of the computed difference in measured signal strengths. The geographic distance on the surface of the Earth that is under the umbrella of a 1 dB contour will vary depending on the location of the AOI on the surface of the earth and the location of the antenna boresights creating the AOI. In this manner, a 1 dB contour for a certain configuration of three antennas at the

equator will be different than the 1 dB contour for a different antenna configuration at a different latitude and longitude.

Chapter IV is organized into five sections. Part B describes the methodology used to prove the validity of the geolocation method. Part C, Part D, and Part E contain analyses of results obtained from testing the geolocation method in the low latitude, mid latitudes, and high latitude regions. For each region, the signal strength was measured at each antenna for each emitter, and then contours of three different error tolerances were plotted to conduct the geolocation. Part F compiles and interprets the results across all latitudes/contour width combinations and offers a summary of final conclusions, questions, and limitations.

B. TESTING THE GEOLOCATION METHOD

To review, the geolocation method can be employed once all of the difference contours have been calculated. In a real world application of the geolocation method, the satellite operator would obtain the actual measurements of the signal strength from the affected satellites, compute the differences, and then simply plot the computed difference contours in STK to geolocate (using the supplied STK Tutorial in the Appendix).

1. Blind Testing

To emulate this process in the model, a *blind* test was conducted between the thesis student and the thesis advisor, whereby the thesis student acted as the satellite operator and the thesis advisor acted as the interfering source. The thesis student created a model STK 10 scenario containing a single satellite with multiple antennas. The satellite was communicating with a ground facility and the gain difference contours for the satellite antennas were calculated. This scenario was then provided to the thesis advisor. This arrangement simulated a satellite with multiple antennas in operation, with antenna gain difference contours already computed. The gain difference contours were not visible to the thesis advisor. The thesis student and thesis advisor conducted two sets of blind tests.

a. Blind Test Set #1

In the first blind test, the thesis advisor randomly inserted four interfering transmitters inside the area of interest and "measured" the corresponding signal strength for each of the receive antennas via the STK Detailed Link Budget report. The thesis advisor provided the signal strength measurements (G_1, G_2, and G_3) and the calculated differences to the thesis student in a Microsoft Excel file. The thesis student was not made aware of the location of the interfering transmitters. The only information provided to the thesis student, summarized in Table 3, was the signal strength measurements and the difference calculations for each receive antenna pair. This portion of the blind arrangement simulates the satellite operator obtaining the signal strength measurements for each receive antenna.

Xmtr	**G_1**	**G_2**	**G_3**	**$G_1 - G_2$**	**$G_1 - G_3$**	**$G_2 - G_3$**
1	32.75	20.00	34.50	12.8	-1.8	-14.5
2	34.00	33.00	33.80	1.0	0.2	-0.8
3	30.75	35.80	31.80	-5.1	-1.1	4.0
4	33.90	34.85	28.50	-1.0	5.4	6.4

Table 3 Blind Run #1 – Simulated Measurements Provided to Thesis Student

The thesis student employed the geolocation method and plotted the received $G_x - G_y$ contours in Table 3 using 0.1 dB contour widths. The best guess geolocation for each simulated interfering transmitter was obtained by recording the latitude and longitude of the center of the area created by the intersecting LOPs. This position was reported to the thesis advisor. The thesis advisor analyzed the reported geolocation positions and found that all were within ~0.25° of the actual position.

A possible issue with this first blind test was the inclusion of the signal strength measurements G_1, G_2, and G_3. Knowing the actual measurements taken at the antennas could theoretically lead to a situation whereby the locations of the transmitters are "reverse engineered" in STK. Since the goal of the blind testing was to definitively prove the geolocation could be completed based on the differences between the signal strength measurements, it was necessary to repeat the blind test with the antenna gain measurements omitted.

b. Blind Test Set #2

In the second blind test, the thesis advisor randomly inserted five interfering transmitters inside the area of interest and "measured" the corresponding signal strength for each of the receive antennas via the STK Detailed Link Budget report. In this blind test, the only information provided to the thesis student were the differential signal strength measurements for each receive antenna pair ($G_x - G_y$). The information provided to the thesis student is summarized in Table 4. The thesis student was not made aware of the location of the interfering transmitters.

Xmtr	**$G_1 - G_2$**	**$G_1 - G_3$**	**$G_2 - G_3$**
1	1.0	0.0	-1.0
2	7.5	7.5	0.0
3	-7.0	-2.0	5.0
4	-14.0	-9.0	5.0
5	3.0	14.0	11.0

Table 4 Blind Run #2 – Only Antenna Gain Differences Provided to Thesis Student

By providing only the gain differences, the possibility of "reverse engineered" results is prevented. This guarantees that the resultant geolocation positions are obtained solely via the new geolocation method. The thesis student plotted the difference contours in the version of the scenario that did not contain the interfering transmitters. The best guess geolocation for each simulated interfering transmitter was obtained by recording the latitude and longitude of the center of the area created by the intersecting LOPs (using 0.1 dB contour widths). These positions were reported to the thesis advisor and are summarized in Table 5.

Xmtr	**Actual Transmitter Position (inserted by Thesis Advisor)**		**Geolocated Transmitter Positions (from Thesis Student)**	
	Lat	**Long**	**Lat**	**Long**
1	8.1	-120.5	8.165	-120.48
2	5.9	-123.5	5.807	-123.56
3	7.0	-116.5	6.954	-116.63
4	8.1	-114.5	8.352	-114.23
5	2.55	-121.5	2.345	-121.47

Table 5 Blind Run #2 – Actual Transmitter Positions Compared to Geolocated Transmitter Positions

2. Initial Conclusion

Based on the results in Table 5, the blind testing methodology appears to validate the new method as a means of geolocating an interfering source. However, this now raises a number of questions about the capabilities and limitations of the method with respect to a number of variables. Specifically, how accurately the method performs

across multiple latitudes and how the accuracy of the method is affected by the precision of the signal strength measurement.

C. LOW LATITUDE TESTING AND ANALYSIS

1. Low Latitude Testing Setup

The STK scenario from Part B was a generic model of a satellite with three antennas. For more extensive testing, an STK scenario modeling sections of the Inmarsat Global Xpress (Figure 5) was used. This was done to provide a potential demonstration of the utility of the method as applied to a real world system. The creation of this model is discussed extensively in Chapter III.

The first round of testing was conducted in a Low Latitude region, ranging from 5.5° to 12.5°. Five STK Facility objects were randomly placed in the AOI of the Low Latitude model. Figure 50 provides a summary of the STK objects used to complete the Low Latitude geolocation model with the five added emitters (Facilities Low_1 through Low_5).

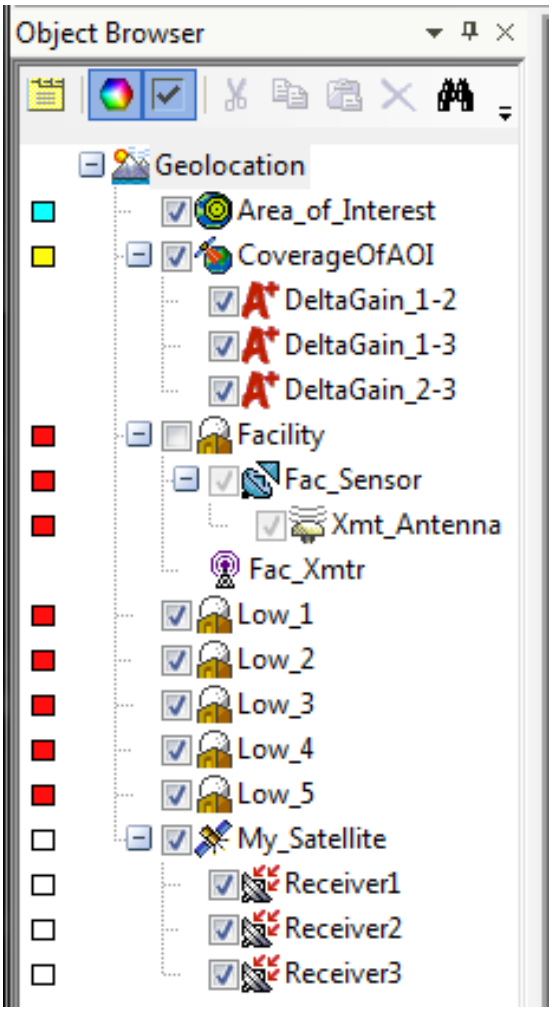

Figure 50. Summary of STK Objects Used to Model the Geolocation Method for Low Latitudes.

Figure 51 shows the 2D display of the antenna boresights, antenna fields of view, corresponding area of interest, and the locations for the five test interfering emitters. Interferers Low_1 and Low_5 are located within close proximity to antenna boresights, Low_2 is positioned toward the edge of the AOI, and Low_3 is in the approximate middle of the AOI. Low_1 and Low_2 occupy the highest latitudes while Low_5 is the lowest.

Figure 51. STK 2D Graphical Display of Single Satellite, Multiple Antenna Geolocation – Low Latitude Model.

The "Receiver Gain" (signal strength measurement) for each of the receive antennas was found by accessing the Detailed Link Budget report for each Interfering Transmitter-Receiver pairing as described in Chapter III. For example, the signal strength measurement for each antenna was found with respect to Low_1. Then, the same measurements were made but with respect to Low_2, then Low_3, etc. The difference contours were then calculated and displayed via the respective FOM objects for each possible contour width (1 dB, 0.5 dB, and 0.1 dB). These values correspond to an error tolerance in the signal strength "measurement" of ±0.5, ±0.25, and ±0.05 dB.

2. Low Latitude Testing Results

Table 6 summarizes the physical location of each emitter, the signal strength measurements at the antennas for each emitter, and the resultant delta contours. Table 7 compiles approximate size of the geolocation area for the three different error tolerance

variables and computes an effective radius for the geolocation area. The effective radius is the radius of a circle with the same area as the computed geolocation area. This offers the reader two distinct avenues for considering the size of the AOPs created in the geolocation method. For example, Interferer #1 was geolocated in area 35 km^2 in size. This is equivalent to the area created by a circle with a radius of approximately 3 km.

Low Latitude - Summary of Results							
Interferer #	Latitude	Signal Strength Measurements (dB)			Difference Contours		
		G1	G2	G3	G1 - G2	G1 - G3	G2 - G3
1	12.5	36.4034	29.0024	30.0930	7.4010	6.3104	-1.0906
2	12	34.5052	34.7167	28.8808	-0.2115	5.6244	5.8359
3	9.5	34.0984	33.3100	33.7715	0.7884	0.3269	-0.4615
4	9	30.8428	36.0609	31.6739	-5.2181	-0.8311	4.3870
5	5.5	28.7129	29.1779	36.5670	-0.4650	-7.8541	-7.3891

Table 6 Summary of Results – Low Latitude Geolocation Model

Low Latitude - Summary of Results							
Interferer #	Latitude	Geolocation Area (km^2)			Approximate Effective Radius (km)		
		1 dB	0.5 dB	0.1 dB	1 dB	0.5 dB	0.1 dB
1	12.5	1894	314	35	25	10	3
2	12	2469	624	40	28	14	4
3	9.5	2687	611	48	29	14	4
4	9	2134	428	12	26	12	2
5	5.5	1778	406	6	24	11	1

Table 7 Summary of Results – Low Latitude Geolocation Model

The average size of the area created using 1dB contour widths is 2,192 km^2, the average size for 0.5 dB contours is 477 km^2, and the average size for 0.1 dB contours is 28 km^2. 1 dB and 0.5 dB contour widths created roughly shaped hexagonal AOPs, while the 0.1 dB contour width created triangular AOPs. To provide an additional frame of reference, 2,192 km^2 is equivalent to 846 square miles, 477 km^2 equals 184 sq mi, and 28 km^2 equals 11 sq mi. Similarly, the average effective radius for the 1 dB, 0.5 dB, and 0.1 dB contours were 26 km (16.2 mi), 12 km (7.5 mi), and 3 km (1.9 mi), respectively.

It is important to note that the geolocation area sizes in Table 7 are not exact calculations. They are the best possible approximation given the irregularly shaped polygons formed by some of the intersecting LOPs. Most of the geolocation areas were comparable to a hexagon in shape, but they were rarely close to a perfect hexagon. To approximate the size of the area, the STK 10 measurement tool was used to measure each of the sides of the AOP. The average of the six sides was computed and then plugged into an online calculator for computing the area of a perfect polygon [19]. The effective radii were computed used the approximated areas of the hexagonal AOPs.

The overall best produced AOP in the Low Latitude group came from Low_5. Interestingly enough, Low_1 and Low_4 were comparable in size to Low_5 and noticeably better than Low_2 and Low_3.

3. Low Latitude Results Graphics

Figure 52 - Figure 61 display the 1 dB geolocation AOPs for the five Low Latitude interfering transmitters.

Figure 52. Low Latitude Model – Geolocation of Interfering Transmitter #1.

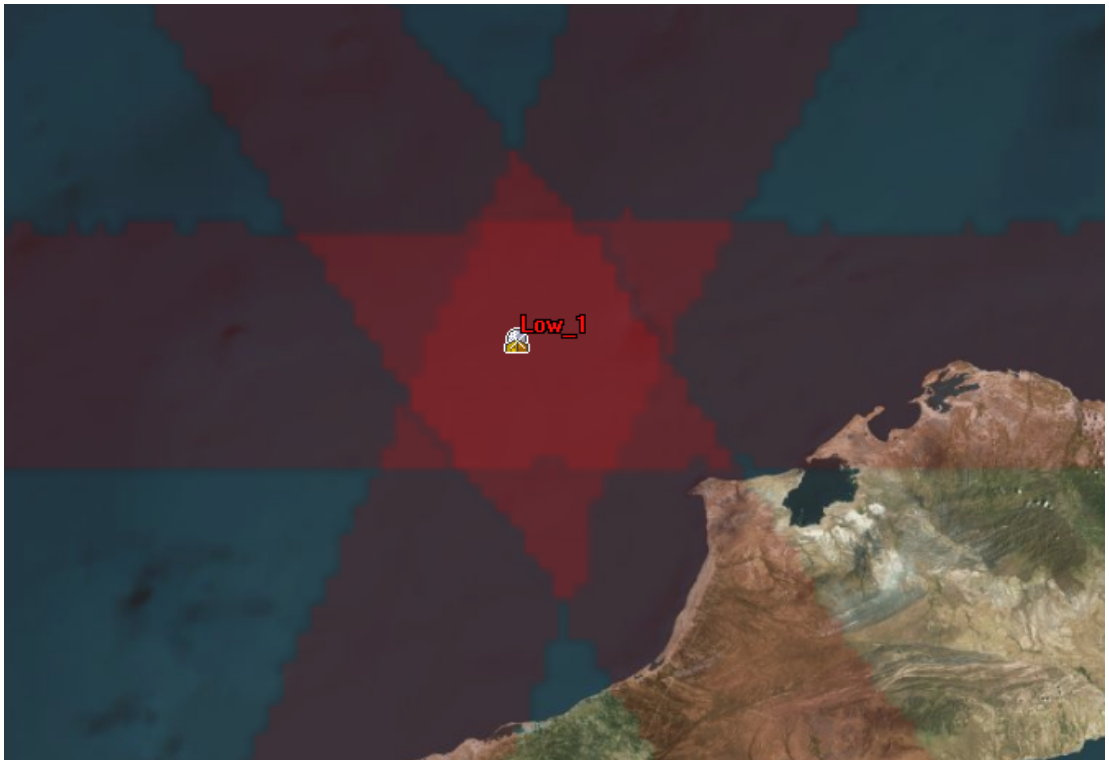

Figure 53. Low Latitude Model – Interferer #1 Geolocation AOP.

Figure 54. Low Latitude Model – Geolocation of Interfering Transmitter #2.

Figure 55. Low Latitude Model – Interferer #2 Geolocation AOP.

Figure 56. Low Latitude Model – Geolocation of Interfering Transmitter #3.

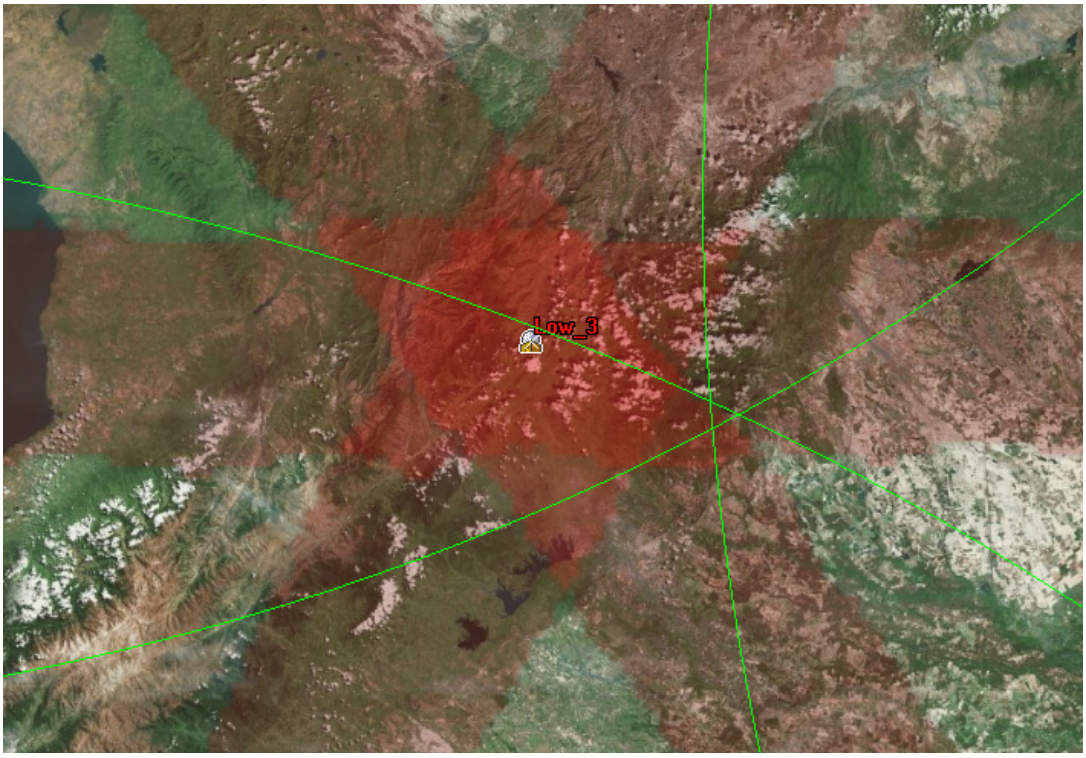

Figure 57. Low Latitude Model – Interferer #3 Geolocation AOP.

Figure 58. Low Latitude Model – Geolocation of Interfering Transmitter #4.

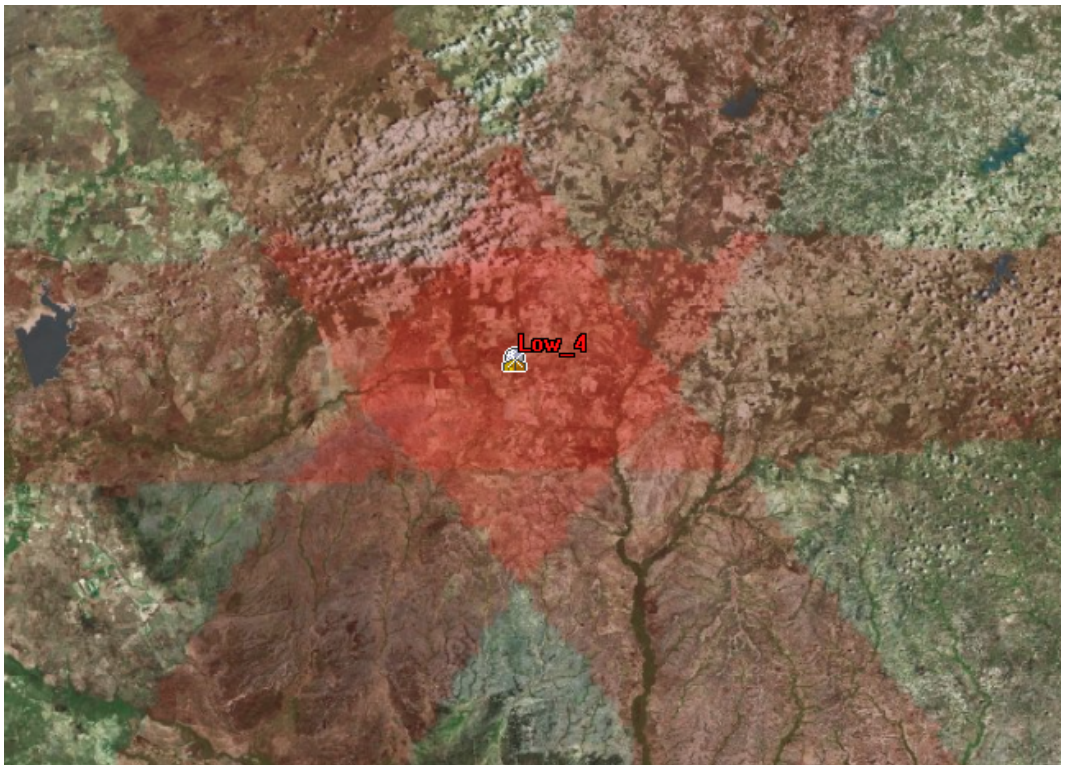

Figure 59. Low Latitude Model – Interferer #4 Geolocation AOP.

Figure 60. Low Latitude Model – Geolocation of Interfering Transmitter #5.

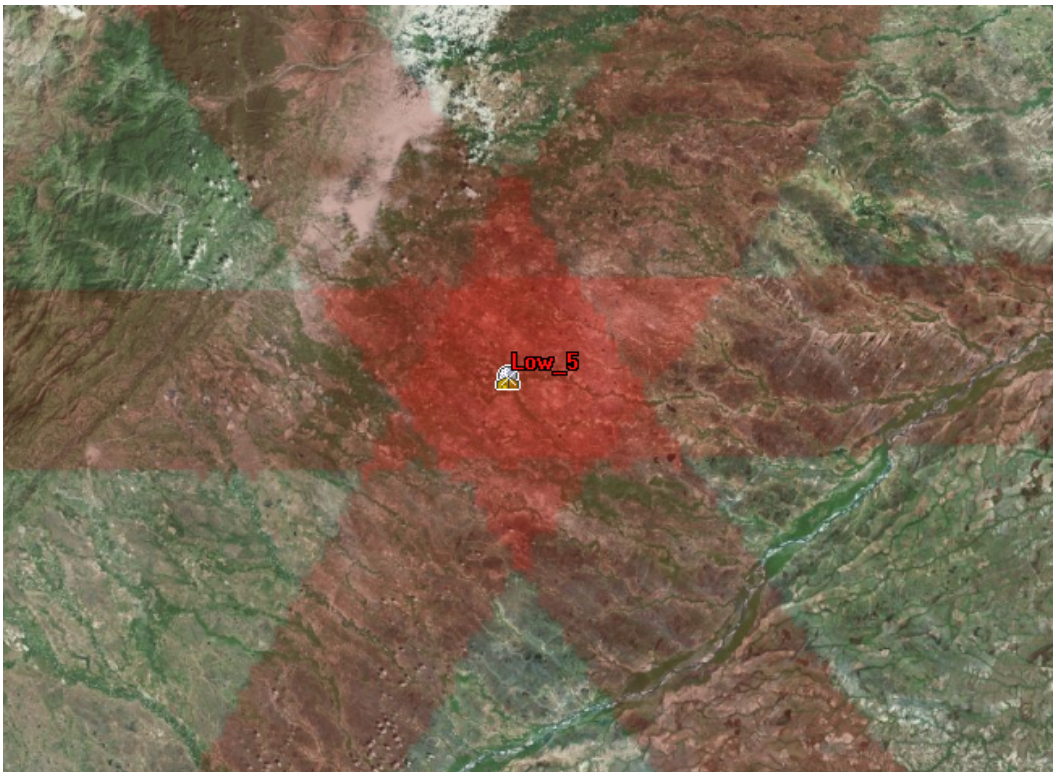

Figure 61. Low Latitude Model – Interferer #5 Geolocation AOP.

D. MID LATITUDE TESTING AND ANALYSIS

The Mid Latitude was broken up into two parts to ensure throrough coverage of all available latitudes. Mid Latitude Part 1 covers 16° to 25° North latitude, and Mid Latitude Part 2 contains 34° to 44°.

1. Mid Latitude Part 1

a. Mid Latitude Part 1 Testing Setup

Figure 62 shows the 2D display of the antenna boresights, antenna fields of view, corresponding area of interest, and the locations for the five test interfering emitters. Interferers Mid_1 and Mid_5 are located within close proximity to antenna boresights, Mid_2 is positioned toward the edge of the AOI, and Mid_3 is in the approximate middle of the AOI. Mid_1 occupies the highest latitude while Mid_5 occupies the lowest.

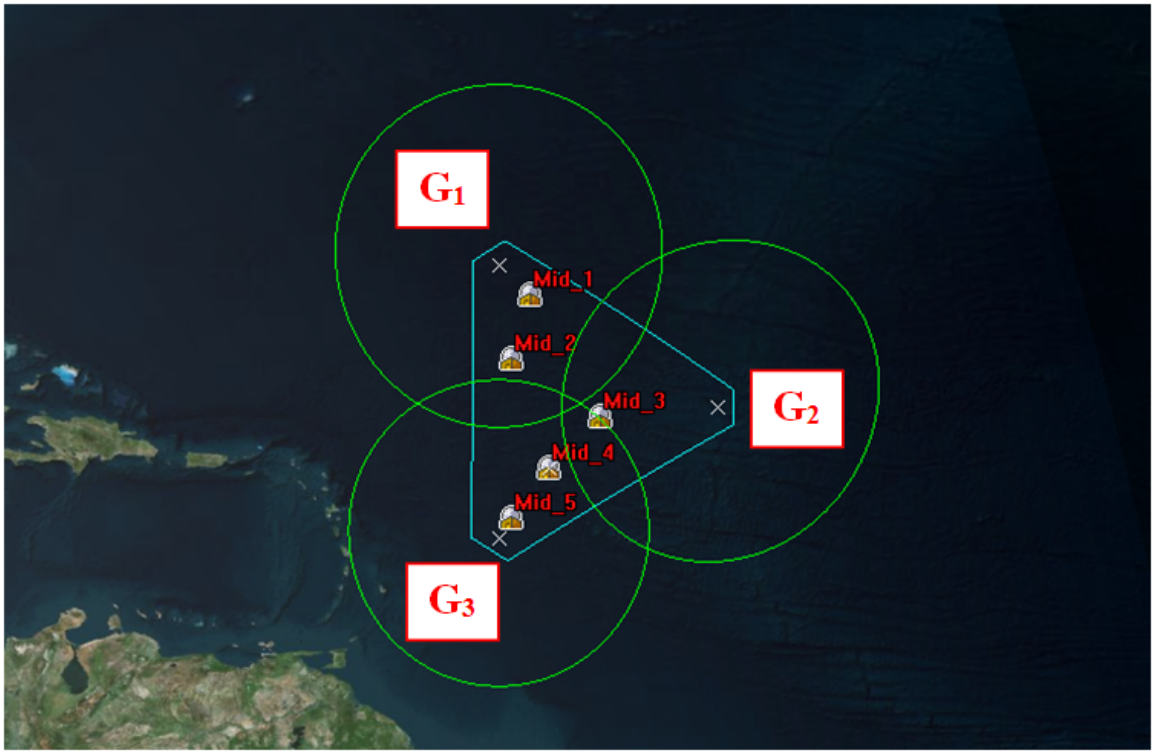

Figure 62. STK 2D Graphical Display of Single Satellite, Multiple Antenna Geolocation – Mid Latitude Model (Part 1).

b. Mid Latitude Part 1 Testing Results

Table 8 summarizes the physical location of each emitter, the signal strength measurements at the antennas for each emitter, and the resultant delta contours. Table 9 compiles approximate size of the geolocation area for the three different error tolerance variables and computes an effective radius for the geolocation area.

Mid Latitude (Part 1) - Summary of Results							
Interferer #	Latitude	Signal Strength Measurements (dB)			Difference Contours		
		G1	G2	G3	G1 - G2	G1 - G3	G2 - G3
1	24.75	36.5360	30.5003	28.8607	6.0357	7.6753	1.6396
2	22.25	35.8021	30.8378	32.7475	4.9643	3.0546	-1.9097
3	20	32.7896	35.1139	33.5901	-2.3243	-0.8005	1.5238
4	18	31.4957	32.8101	35.8142	-1.3144	-4.3185	-3.0041
5	16	28.3390	29.3666	36.6722	-1.0276	-8.3332	-7.3056

Table 8 Summary of Results – Mid Latitude (Part 1) Geolocation Model

Mid Latitude (Part 1) - Summary of Results							
Interferer #	Latitude	Geolocation Area (km^2)			Approximate Effective Radius (km)		
		1 dB	0.5 dB	0.1 dB	1 dB	0.5 dB	0.1 dB
1	24.75	2687	611	44	29	14	4
2	22.25	2159	509	19	26	13	2
3	20	3151	707	16	32	15	2
4	18	2632	558	62	29	13	4
5	16	2060	611	21	26	14	3

Table 9 Summary of Results – Mid Latitude (Part 1) Geolocation Model

The average size of the area created using 1dB widths is 2,538 km^2, the average size for 0.5 dB contours is 599 km^2, and the average size for 0.1 dB contours is 32 km^2. Similar to Table 7, the 1 dB and 0.5 dB contour widths created roughly shaped hexagonal AOPs, while the 0.1 dB contour width created triangular AOPs. To provide an additional frame of reference, 2,538 km^2 is equivalent to 980 sq mi, 599 km^2 equals 231 sq mi, and 32 km^2 equals 12 sq mi. Similarly, the average effective radius for the 1 dB, 0.5 dB, and 0.1 dB contours were 28 km (17.4 mi), 14 km (8.7 mi), and 3 km (1.9 mi), respectively.

The overall best produced AOP (0.1 dB contour) in the Mid Latitude (Part 1) group came from Mid_3 but Mid_2 and Mid_5 were extremely close in size. This is intriguing because Mid_3 had the largest AOP for both 1 dB and 0.5 dB width. Mid_5 had the smallest 1 dB AOP and Mid_2 had the smallest 0.5 dB AOP. Mid_1 and Mid_5 are the closest to antenna boresights; Mid_1 was neither the smallest nor the largest in any of the three categories and Mid_5 was only smallest for 1 dB contours.

c. Mid Latitude Part 1 Results Graphics

Figure 63 - Figure 72 show the 1 dB geolocation AOPs for the five Mid Latitude (Part 1) interfering transmitters.

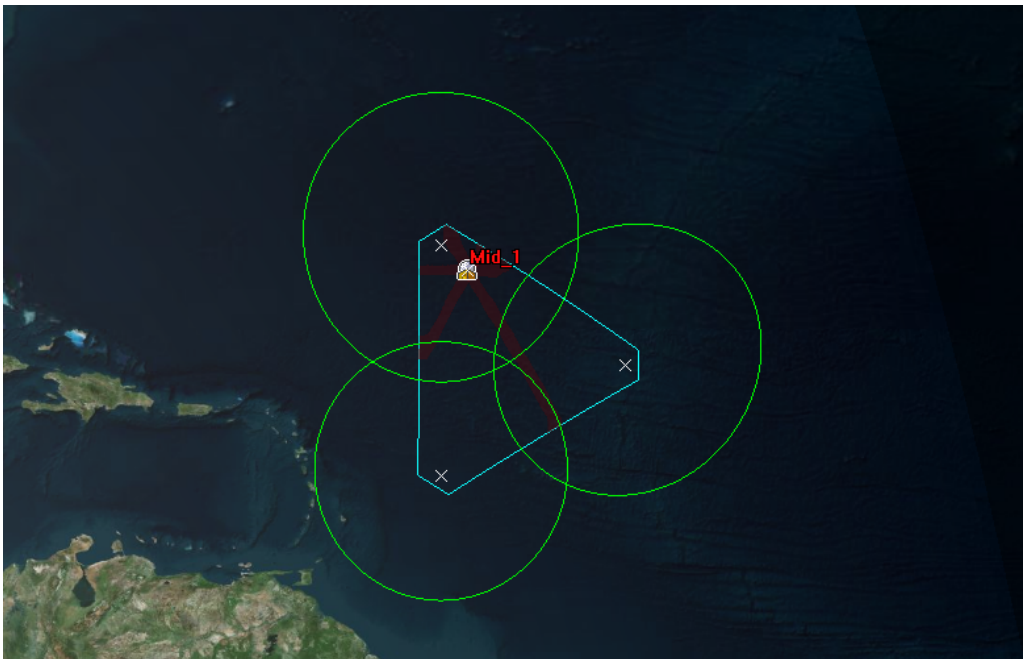

Figure 63. Mid Latitude (Part 1) Model – Geolocation of Interfering Transmitter #1.

Figure 64. Mid Latitude (Part 1) Model – Interferer #1 Geolocation AOP.

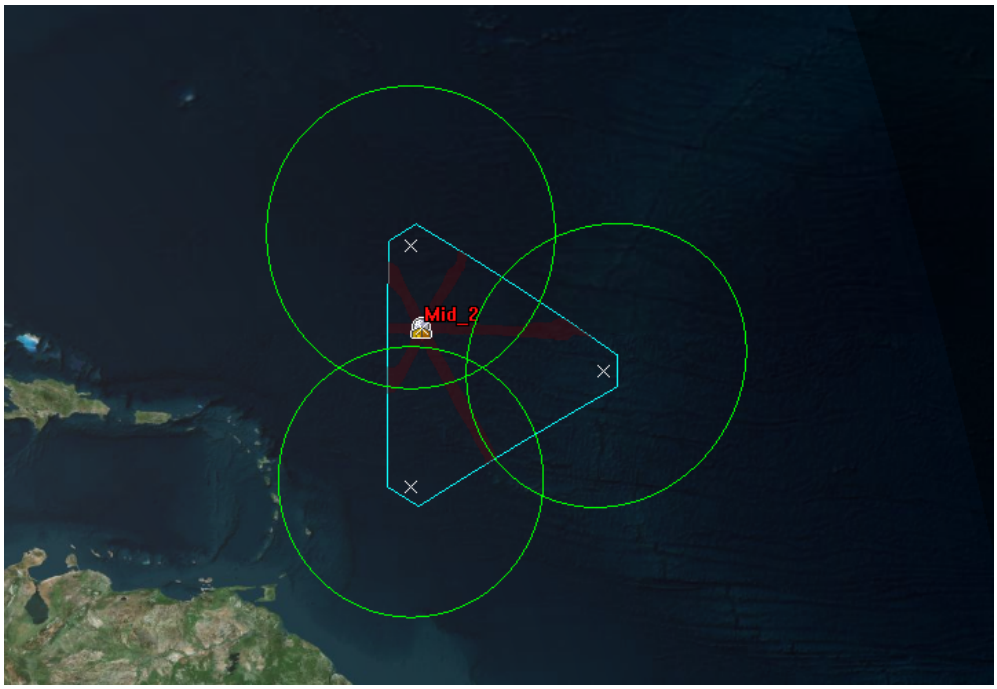

Figure 65. Mid Latitude (Part 1) Model – Geolocation of Interfering Transmitter #2.

Figure 66. Mid Latitude (Part 1) Model – Interferer #2 Geolocation AOP.

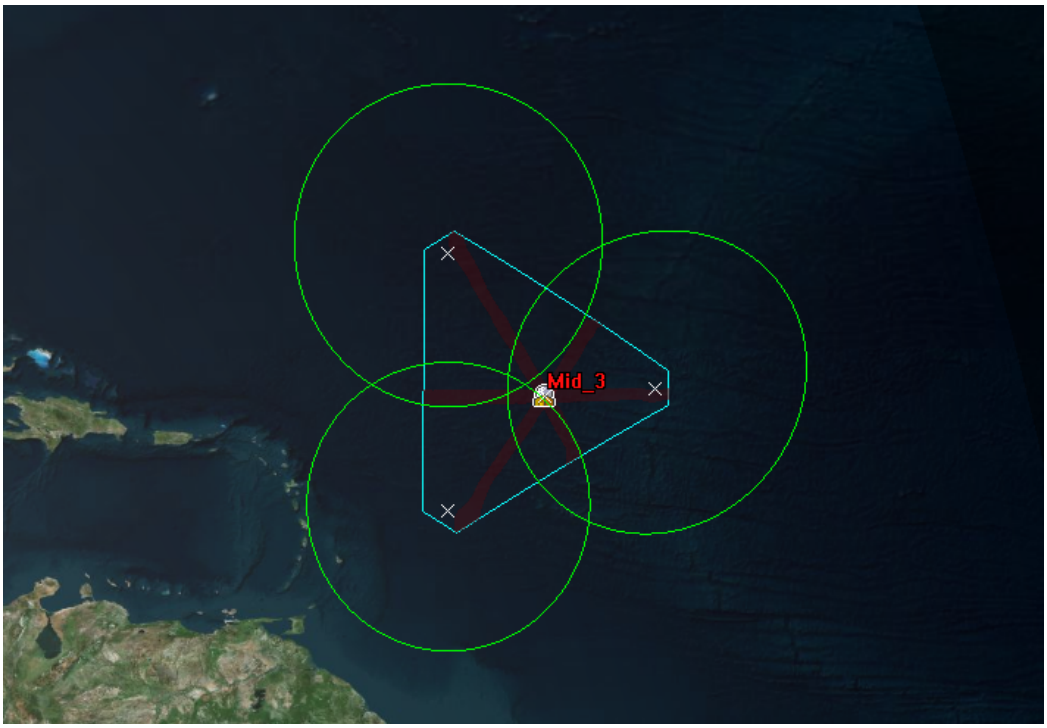

Figure 67. Mid Latitude (Part 1) Model – Geolocation of Interfering Transmitter #3.

Figure 68. Mid Latitude (Part 1) Model – Interferer #3 Geolocation AOP.

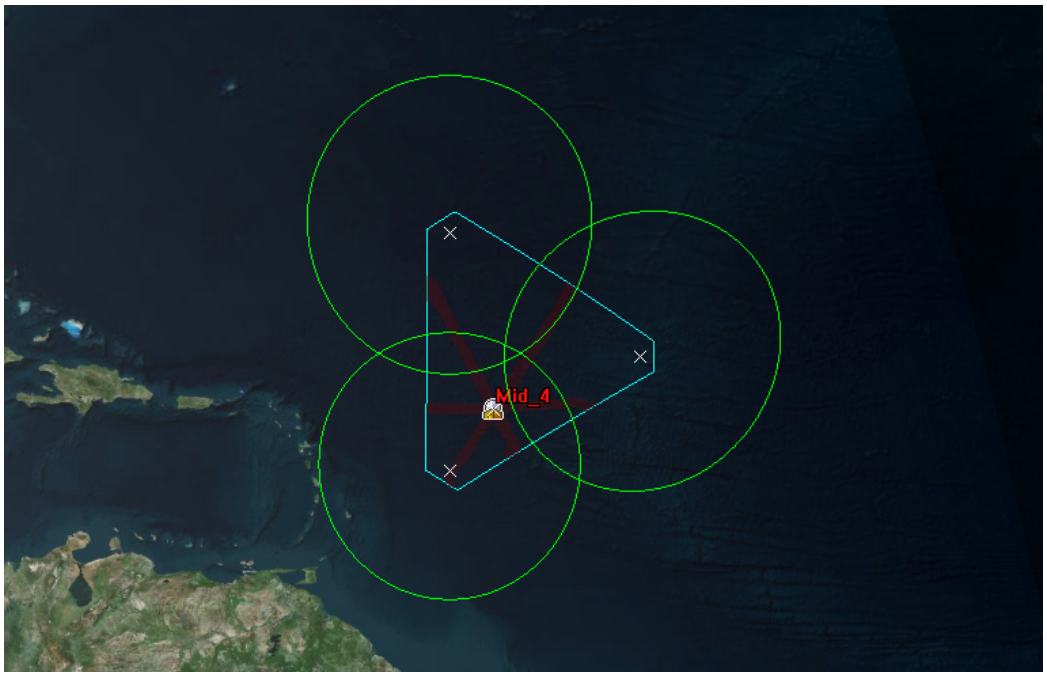

Figure 69. Mid Latitude (Part 1) Model – Geolocation of Interfering Transmitter #4.

Figure 70. Mid Latitude (Part 1) Model – Interferer #4 Geolocation AOP.

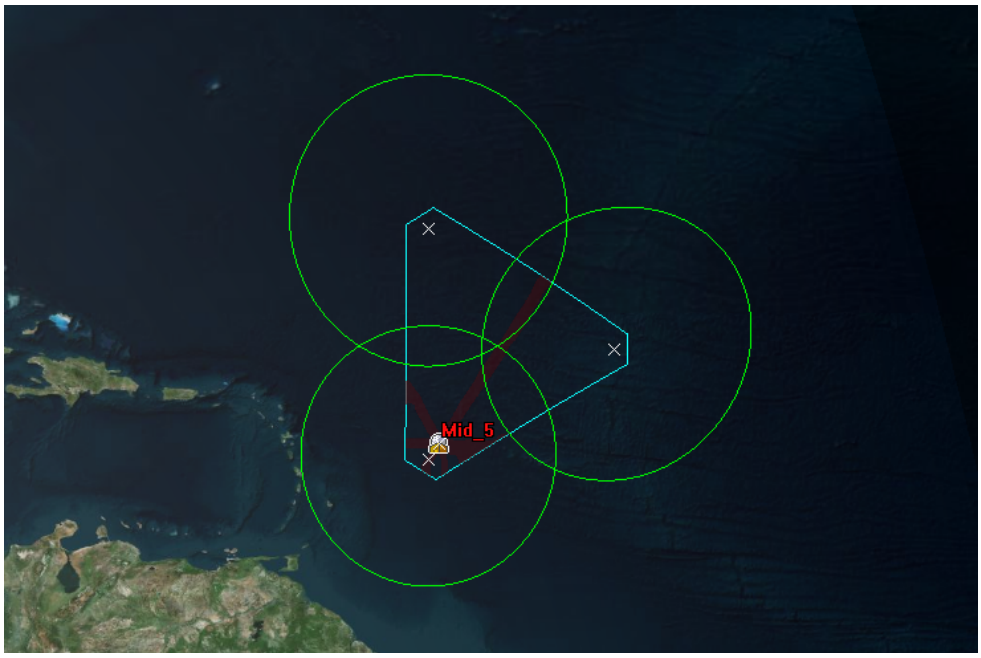

Figure 71. Mid Latitude (Part 1) Model – Geolocation of Interfering Transmitter #5.

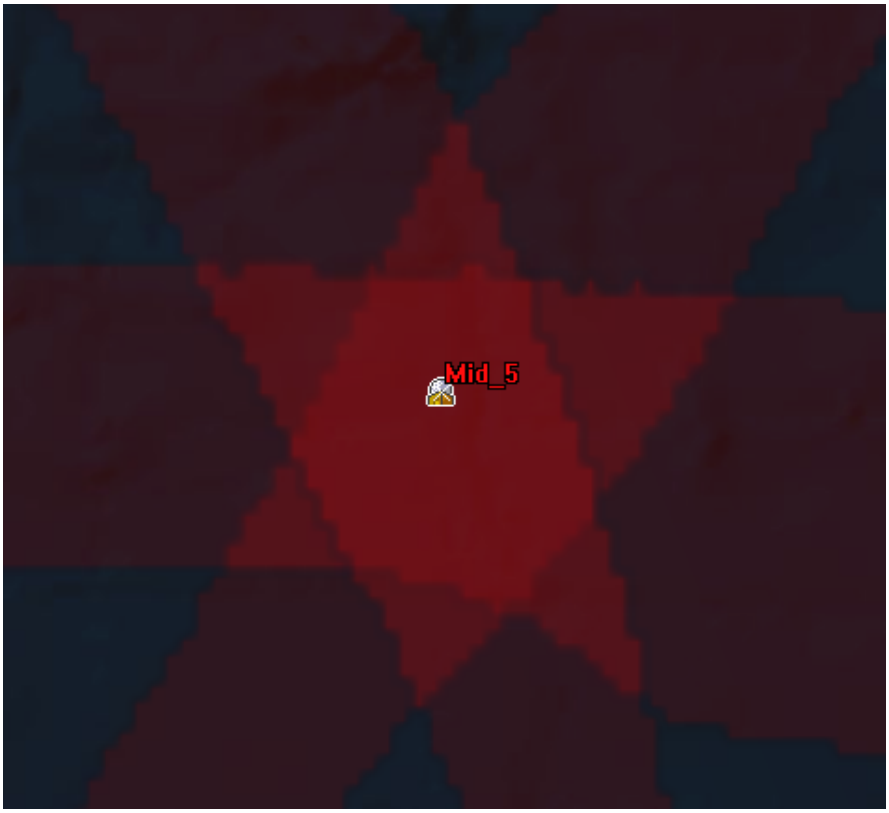

Figure 72. Mid Latitude (Part 1) Model – Interferer #5 Geolocation AOP.

2. Mid Latitude Part 2

a. Mid Latitude Part 2 Testing Setup

Figure 73 shows the 2D display of the antenna boresights, antenna fields of view, corresponding area of interest, and the locations for the five test interfering emitters. Interferers Mid_1, Mid_2, and Mid_5 are located within close proximity to antenna boresights while Mid_3 and Mid_4 are in the approximate middle of the AOI. Mid_2 occupies the highest latitude while Mid_5 occupies the lowest.

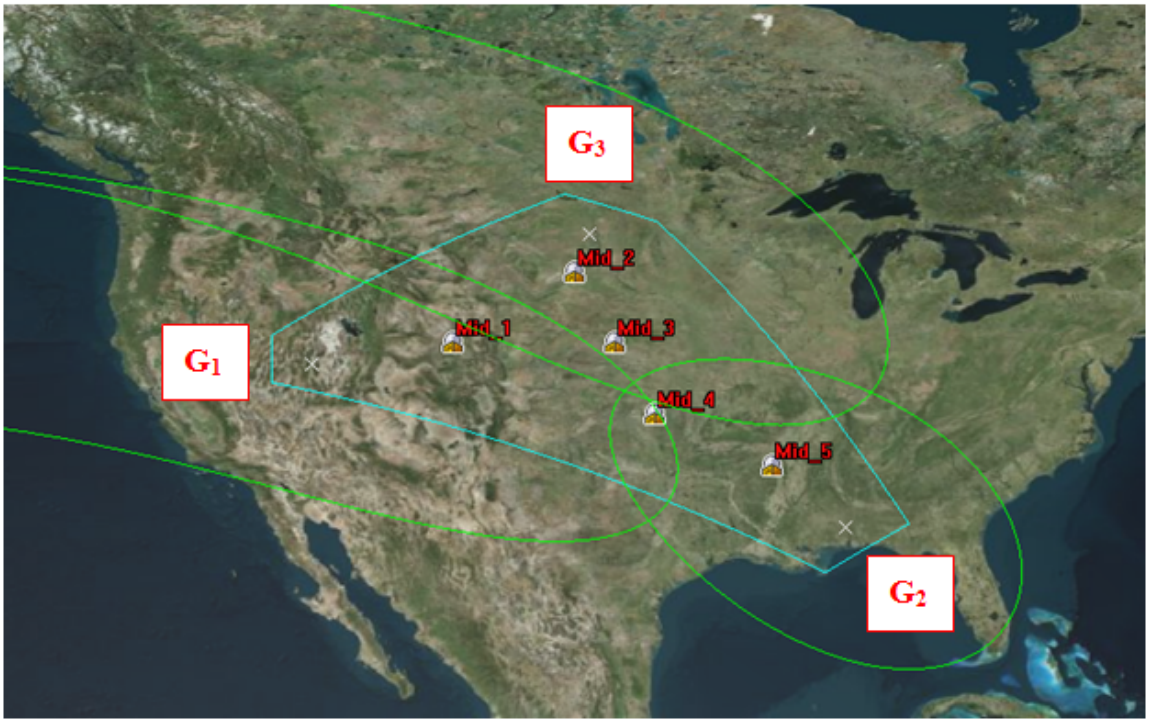

Figure 73. STK 2D Graphical Display of Single Satellite, Multiple Antenna Geolocation – Mid Latitude Model (Part 2).

b. Mid Latitude Part 2 Testing Results

Table 10 summarizes the physical location of each emitter, the signal strength measurements at the antennas for each emitter, and the resultant delta contours. Table 11 compiles approximate size of the geolocation area for the three different error tolerance variables and computes an effective radius for the geolocation area.

Mid Latitude (Part 2) - Summary of Results							
Interferer #	Latitude	Signal Strength Measurements (dB)			Difference Contours		
		G1	G2	G3	G1 - G2	G1 - G3	G2 - G3
1	40	35.9060	29.9394	32.6911	5.9666	3.2149	-2.7517
2	44	30.5613	29.7865	36.4859	0.7748	-5.9246	-6.6994
3	40	32.9142	32.6312	35.4054	0.2830	-2.4912	-2.7742
4	37	33.7937	34.4594	33.2156	-0.6657	0.5781	1.2438
5	34	30.1785	36.2023	31.9310	-6.0238	-1.7525	4.2713

Table 10 Summary of Results – Mid Latitude (Part 2) Geolocation Model

Mid Latitude (Part 2) - Summary of Results							
Interferer #	Latitude	Geolocation Area (km^2)			Approximate Effective Radius (km)		
		1 dB	0.5 dB	0.1 dB	1 dB	0.5 dB	0.1 dB
1	40	9772	2085	40	56	26	4
2	44	9560	1825	41	55	24	4
3	40	8943	1989	65	53	25	5
4	37	7071	1475	49	47	22	4
5	34	5145	1127	28	40	19	3

Table 11 Summary of Results – Mid Latitude (Part 2) Geolocation Model

The average size of the area created using 1dB widths is 8,098 km^2 (3,127 sq mi), the average size for 0.5 dB contours is 1,700 km^2 (656 sq mi), and the average size for 0.1 dB contours is 45 km^2 (17 sq mi). The average effective radius for the 1 dB, 0.5 dB, and 0.1 dB contours were 50 km (31.1 mi), 23 km (14.3 mi), and 4 km (2.5 mi), respectively.

Similar to Table 7 and Table 9, the 1 dB and 0.5 dB contour widths created roughly shaped hexagonal AOPs, while the 0.1 dB contour width created triangular AOPs. However, it is interesting to note that the hexagonal AOPs produced at this latitude appear to be "stretched" across the longitudinal width of the AOI. In the Low and Mid (Part 1) latitudes, the intersection of the antenna FOVs created a roughly symmetrically shaped AOI. In Mid Latitude (Part 2), the footprints of Antennas 1 and 3 exhibit a more elliptical intersection with the surface of the Earth, which creates an AOI that is similarly skewed in the direction of the major axis of the elliptical footprints. The end result as an AOI that appears stretched in parallel across lines of latitude.

The overall best produced AOP for each contour width in the Mid Latitude (Part 2) group came from Mid_5. For the 0.1 dB width, Mid_1, Mid_2 and Mid_4 were all similar in size, but obviously greater than Mid_5 and less than Mid_3, which produced the largest 0.1 dB AOP. Mid_1 and Mid_2 had the largest AOP for 1 dB; Mid_3 was noticeably higher than Mid_4, which was noticeably higher than Mid_5. Mid_1, Mid_2, and Mid_3 had significantly worse (but approximately similar) 0.5 dB width AOPs than Mid_4 and Mid_5.

c. Mid Latitude Part 2 Results Graphics

Figure 74 - Figure 83 show the 1 dB geolocation AOPs for the five Mid Latitude (Part 2) interfering transmitters.

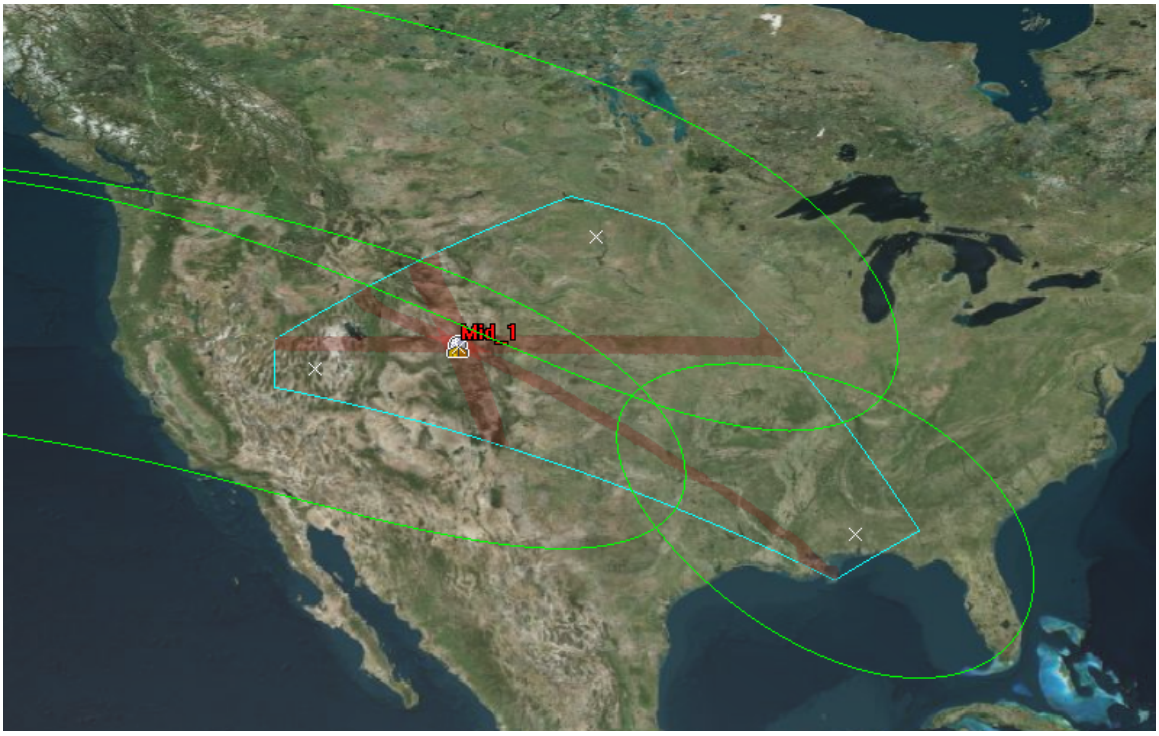

Figure 74. Mid Latitude (Part 2) Model – Geolocation of Interfering Transmitter #1.

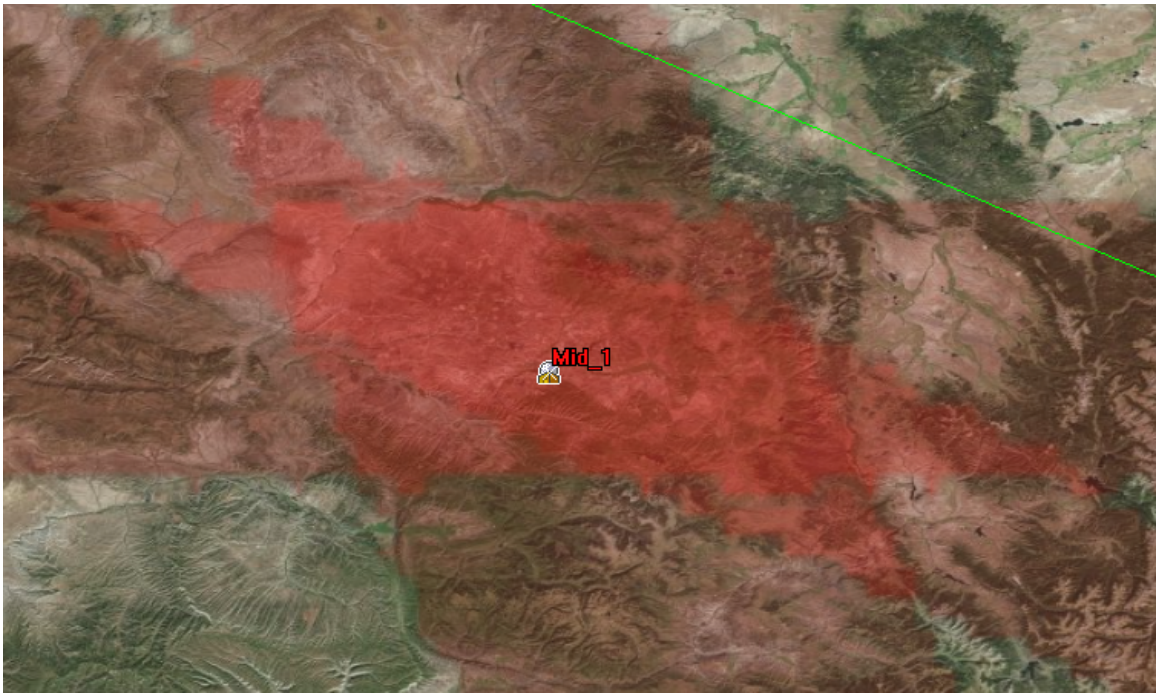

Figure 75. Mid Latitude (Part 2) Model – Interferer #1 Geolocation AOP.

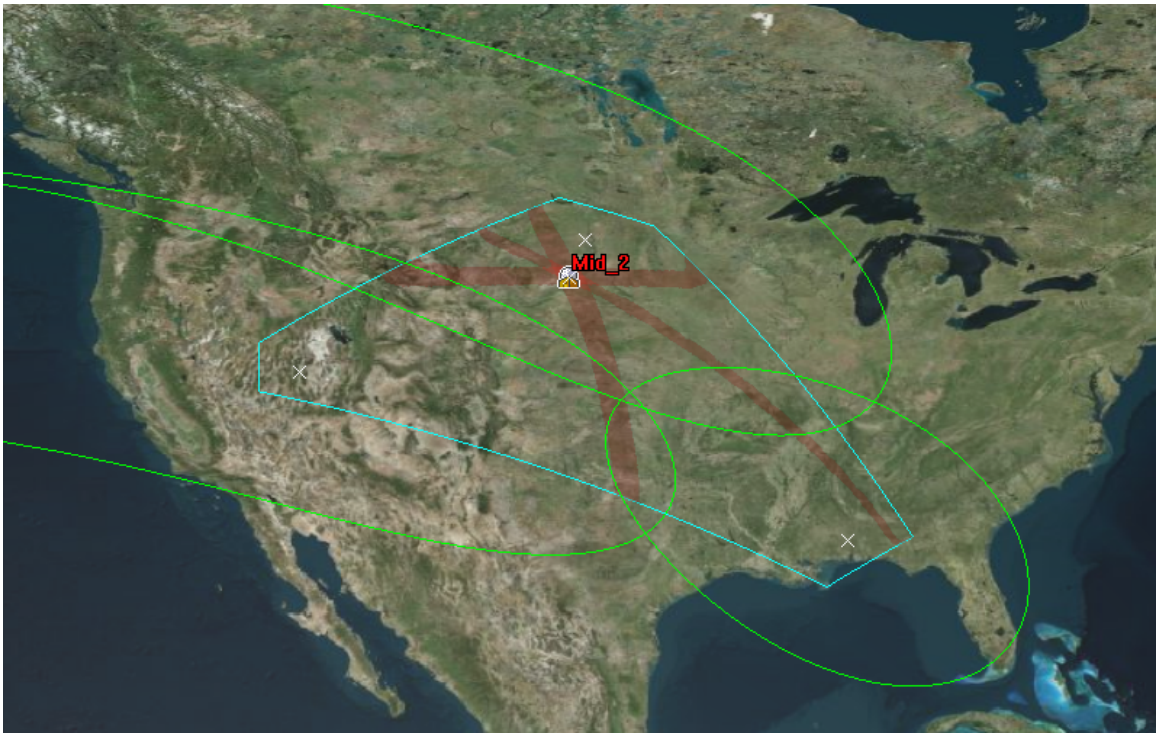

Figure 76. Mid Latitude (Part 2) Model – Geolocation of Interfering Transmitter #2.

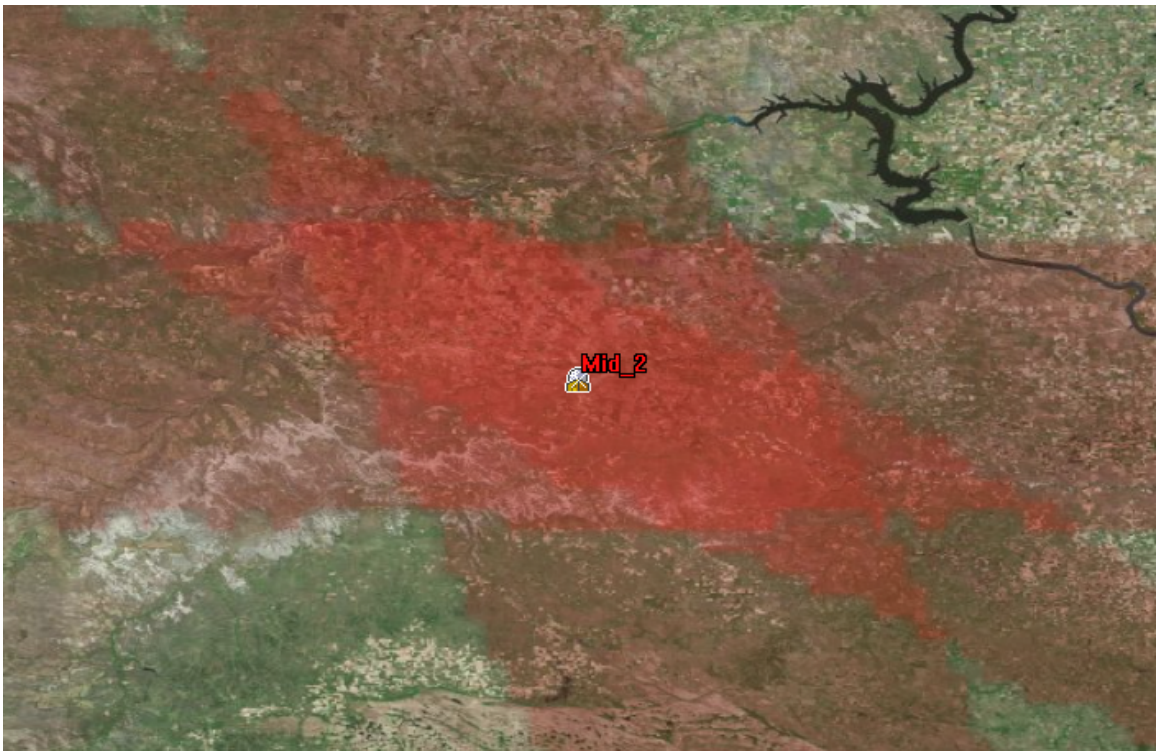

Figure 77. Mid Latitude (Part 2) Model – Interferer #2 Geolocation AOP.

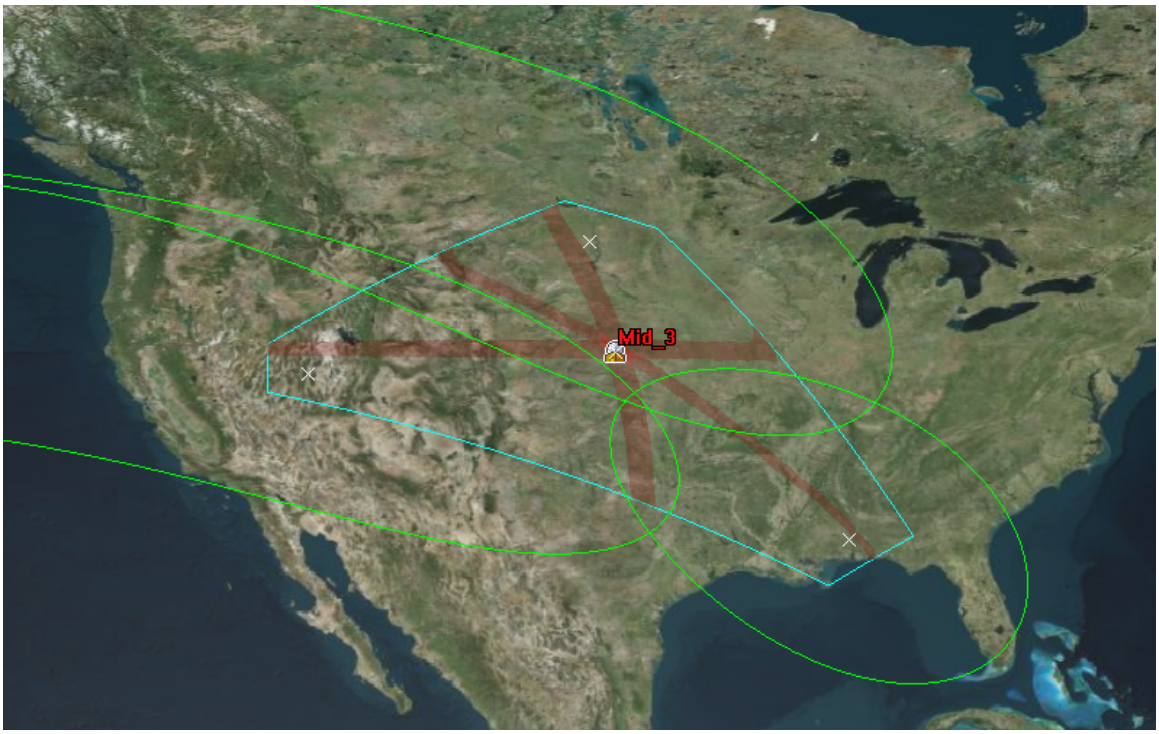

Figure 78. Mid Latitude (Part 2) Model – Geolocation of Interfering Transmitter #3.

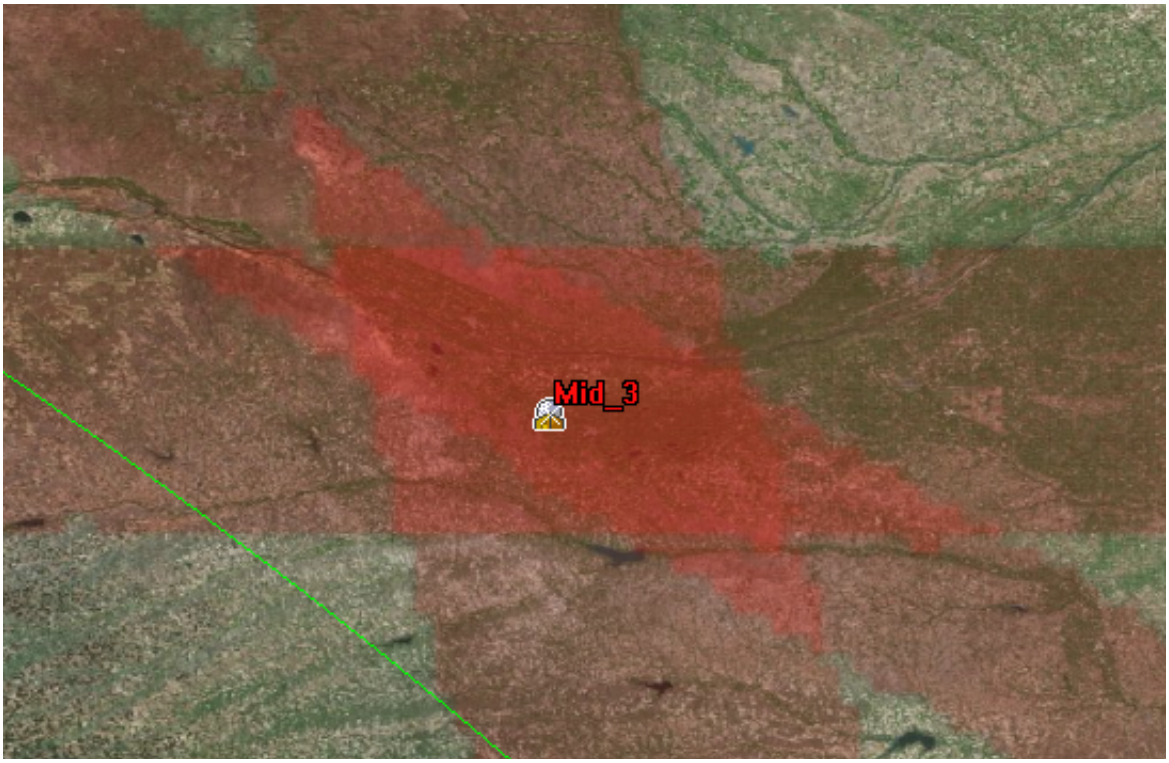

Figure 79. Mid Latitude (Part 2) Model – Interferer #3 Geolocation AOP.

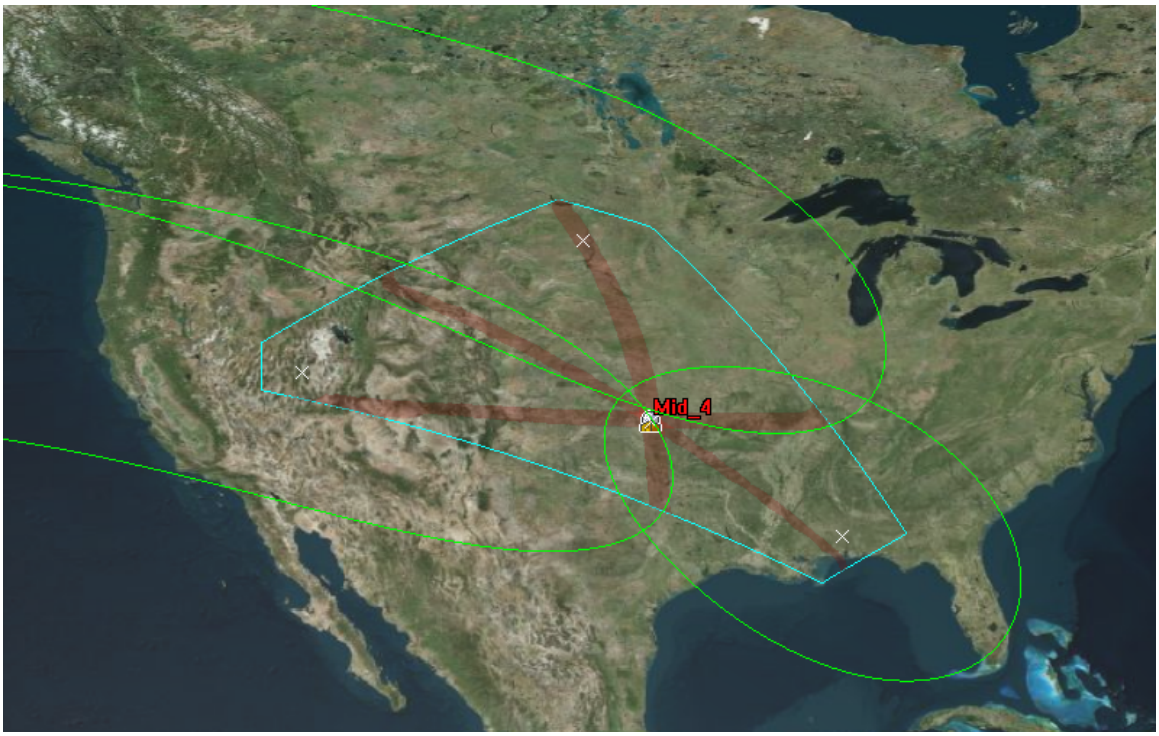

Figure 80. Mid Latitude (Part 2) Model – Geolocation of Interfering Transmitter #4.

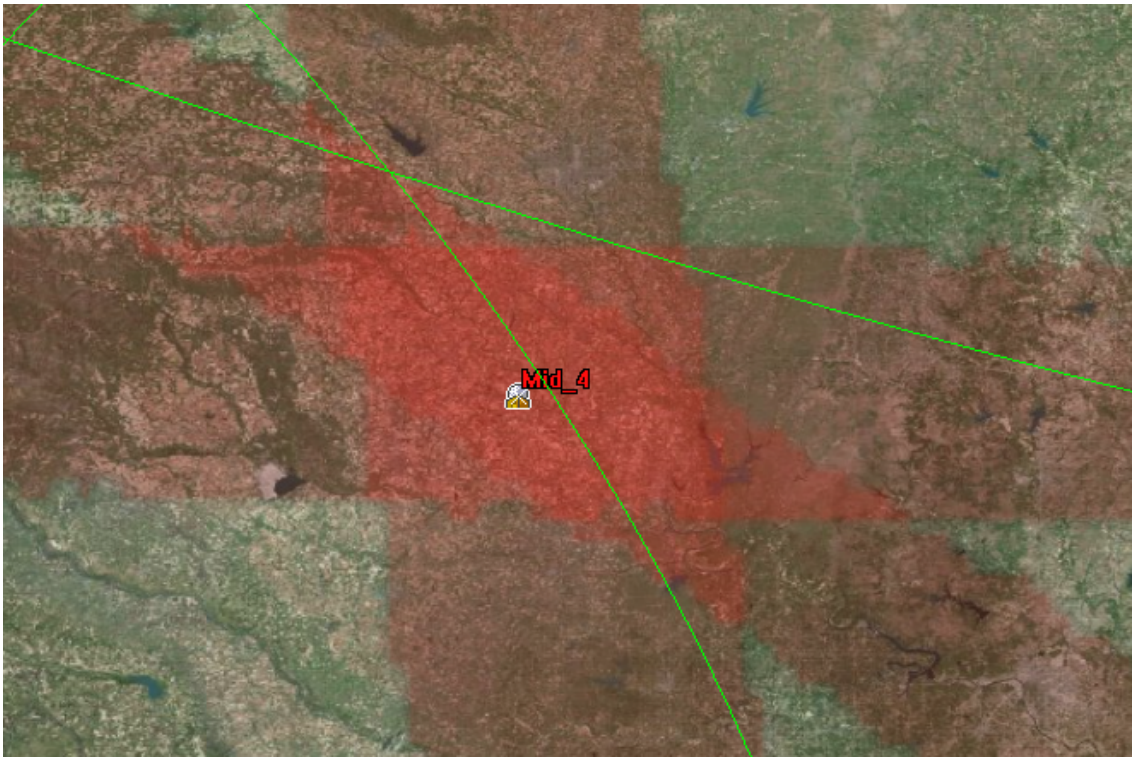

Figure 81. Mid Latitude (Part 2) Model – Interferer #4 Geolocation AOP.

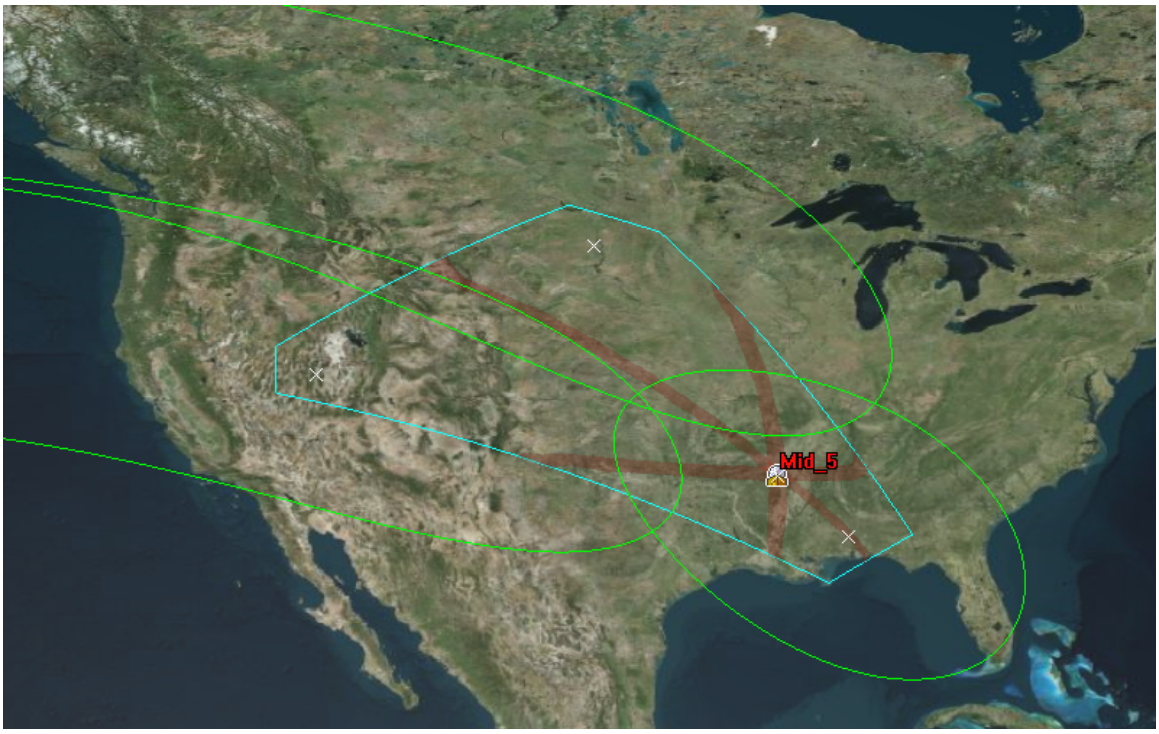

Figure 82. Mid Latitude (Part 2) Model – Geolocation of Interfering Transmitter #5.

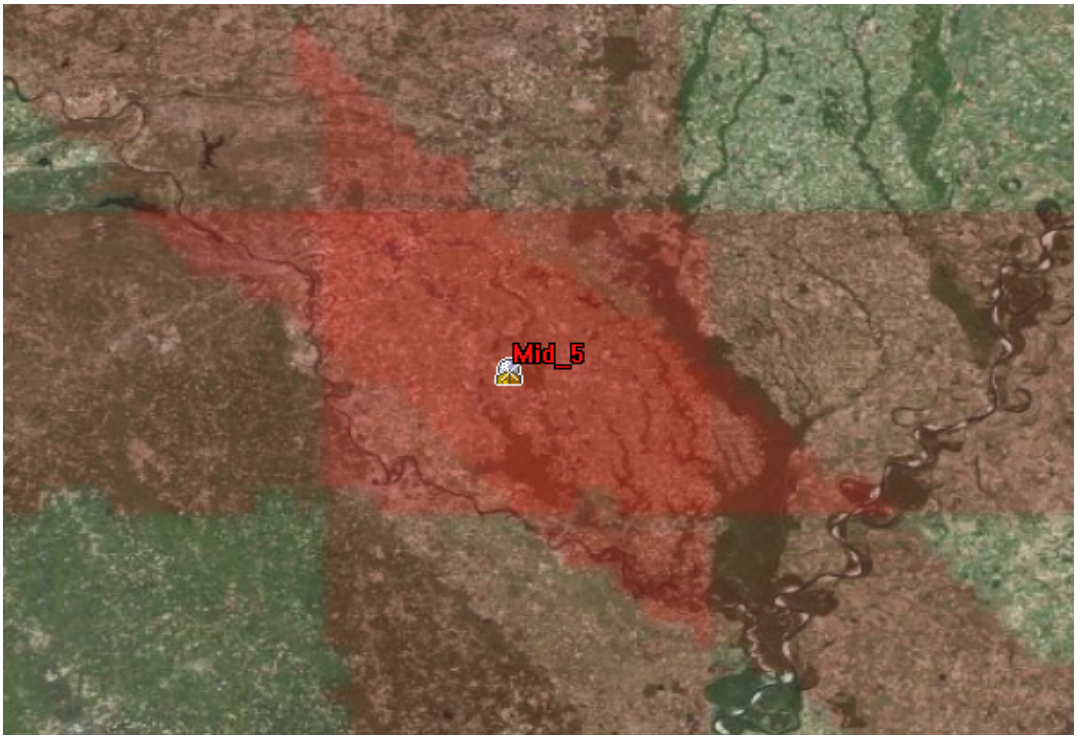

Figure 83. Mid Latitude (Part 2) Model – Interferer #5 Geolocation AOP.

E. HIGH LATITUDE TESTING AND ANALYSIS

1. High Latitude Testing Setup

Figure 84 shows the 2D display of the antenna boresights, antenna fields of view, corresponding area of interest, and the locations for the five test interfering emitters. Interferers High_1 and High_2 are located at the highest overall latitudes. High_3 is in the approximate center of the AOI while High_4 and High_5 are in the lowest latitudes of the group. High_1, High_4, and High_5 are located in close proximity to antenna boresights.

Also of note is the manner in which the AOI is stretched in the high latitude region. As was seen in the Mid Latitude (Part 2) region, elliptical antenna footprints alter the geometry of the AOI. Contrary to the shape created in the Mid Latitude (Part 2) region, which was created by multiple antennas with elliptical footprints parallel to lines of latitude, the High Latitude AOI is heavily influenced by two antennas intersecting the Earth parallel to lines of longitude.

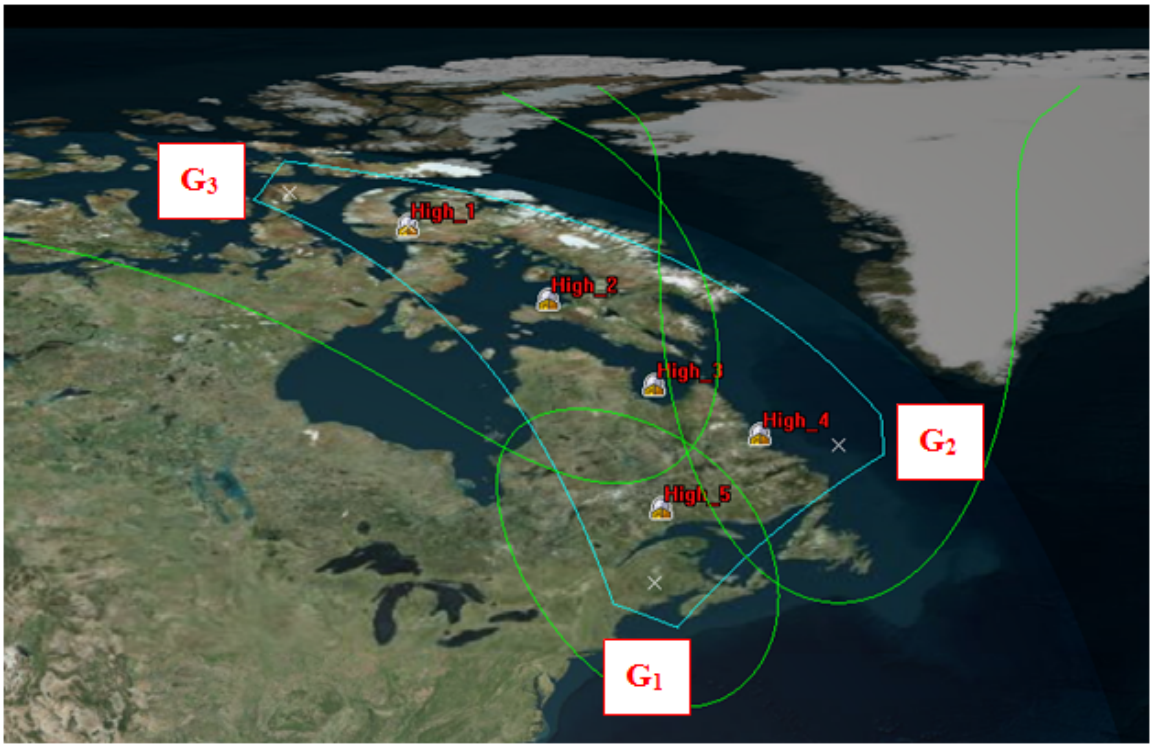

Figure 84. STK 2D Graphical Display of Single Satellite, Multiple Antenna Geolocation – High Latitude Model.

2. High Latitude Testing Results

Table 12 summarizes the physical location of each emitter, the signal strength measurements at the antennas for each emitter, and the resultant delta contours. Table 13 compiles approximate size of the geolocation area for the three different error tolerance variables and computes an effective radius for the geolocation area.

High Latitude - Summary of Results							
Interferer #	Latitude	Signal Strength Measurements (dB)			Difference Contours		
		G1	G2	G3	G1 - G2	G1 - G3	G2 - G3
1	71.25	28.2543	27.6611	36.6976	0.5932	-8.4433	-9.0365
2	66	30.0399	30.2455	36.4186	-0.2056	-6.3787	-6.1731
3	60	32.1439	33.1976	35.2295	-1.0537	-3.0856	-2.0319
4	56.5	30.8841	36.0202	31.5318	-5.1361	-0.6477	4.4884
5	51.25	35.9340	31.0206	32.5205	4.9134	3.4135	-1.4999

Table 12 Summary of Results – High Latitude Geolocation Model

High Latitude - Summary of Results							
Interferer #	Latitude	Geolocation Area (km^2)			Approximate Effective Radius (km)		
		1 dB	0.5 dB	0.1 dB	1 dB	0.5 dB	0.1 dB
1	71.25	54625	2520	66	132	28	5
2	66	18114	4297	115	76	37	6
3	60	11088	1280	40	59	20	4
4	56.5	7251	1559	50	48	22	4
5	51.25	6670	1182	41	46	19	4

Table 13 Summary of Results – High Latitude Geolocation Model

The average size of the area created using 1dB widths is 19,550 km^2 (7,548 sq mi), the average size for 0.5 dB contours is 2,168 km^2 (837 sq mi), and the average size for 0.1 dB contours is 62 km^2 (24 sq mi). The average effective radius for the 1 dB, 0.5 dB, and 0.1 dB contours were 72 km (44.7 mi), 25 km (15.5 mi), and 4 km (2.5 mi), respectively.

The AOPs created by the intersection of the various contour LOPs in the High Latitude region were more irregularly shaped than the AOPs from other regions. The 1 dB contour widths still attempted to make hexagons, but the High_1 was skewed into an approximate parallelogram. High_2 created a recognizable but distorted hexagonal AOP; High_3, High_4, High_5 AOPs were obviously hexagonal and slightly stretched.

High_5, located at the lowest overall latitude of the group, enjoyed the smallest AOP across all three contour widths. High_1 in the 1 dB width category produced the largest AOP by far. This AOP was so large it severely increased the average geolocation area size for the 1 dB width contours. The uncharacteristically large AOP in High_1 can be attributed to abnormally thick $G_1 - G_3$ LOPs. This particular contour pairing is thicker because the resulting deltas are approximately parallel to lines of latitude. Since the overall AOI is skewed parallel to lines of *longitude* it encompasses more overall lines of latitude with respect to the satellite located in a geostationary orbit. As seen in Figure 85 and Figure 86, this phenomenon is most amplified at the highest latitudes, where the contour widths are approximately 300% wider than the contour widths in the lowest latitudes of the High Latitude region. Figure 85 shows the High Latitude region in 2D while Figure 86 shows the same region in 3D.

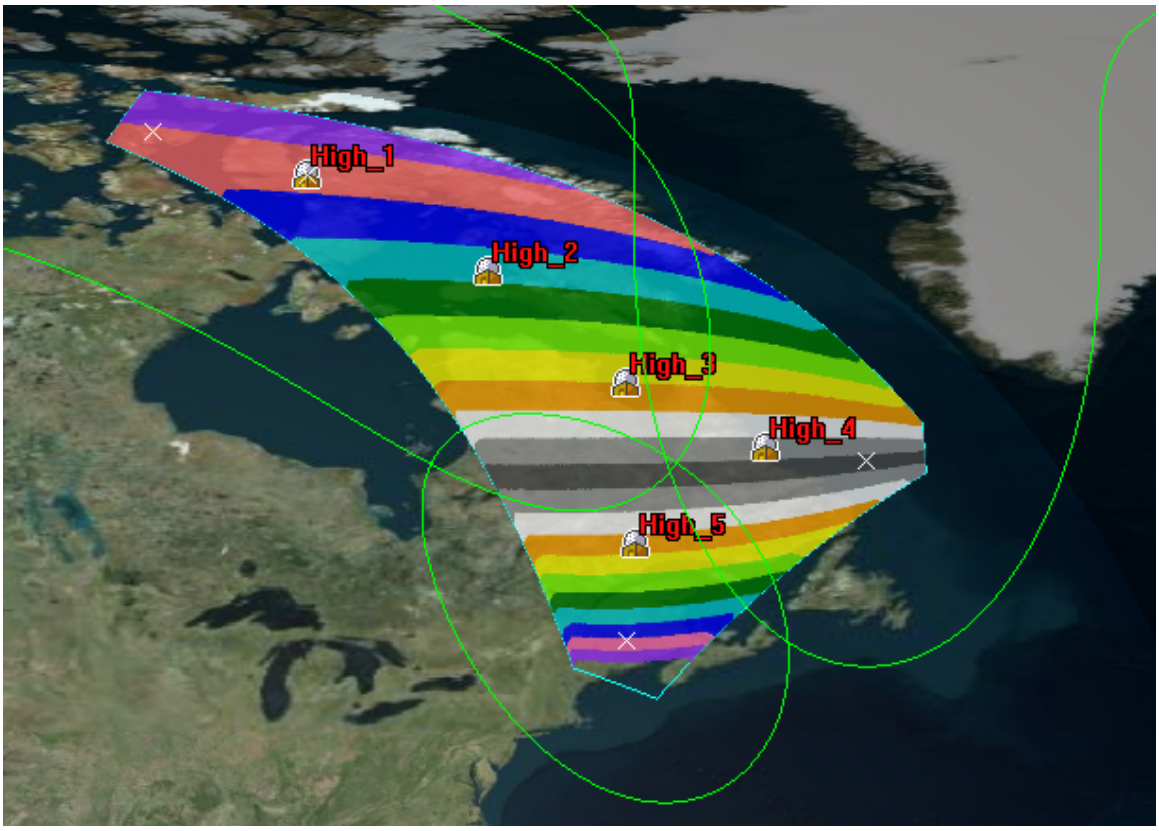

Figure 85. High Latitude 2D Model – Contour Width Deltas at Higher Latitudes.

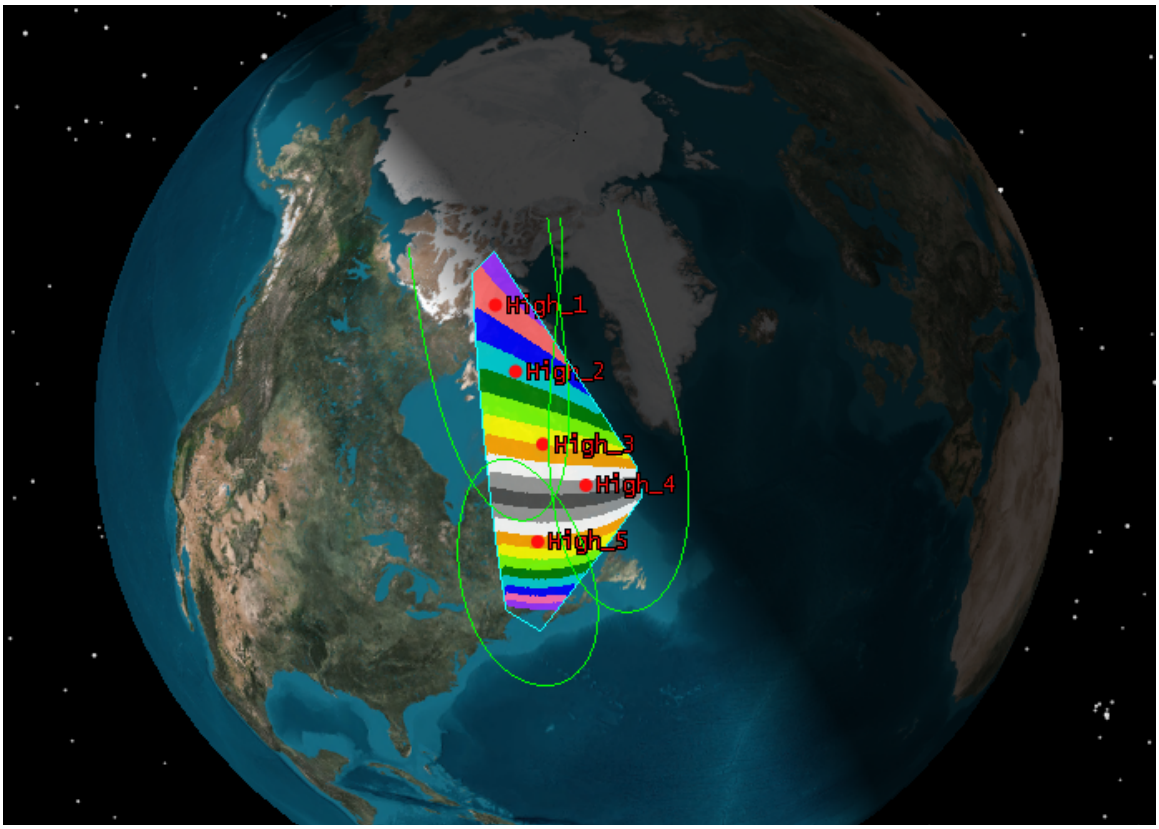

Figure 86. High Latitude 3D Model – Contour Width Deltas at Higher Latitudes.

3. High Latitude Results Graphics

Figure 87 - Figure 96 show the 1 dB geolocation AOPs for the five High Latitude interfering transmitters. Figure 87 - Figure 90 specifically show the consequence of the increased width of the $G_1 - G_3$ contour lines on the overall geolocation AOP area.

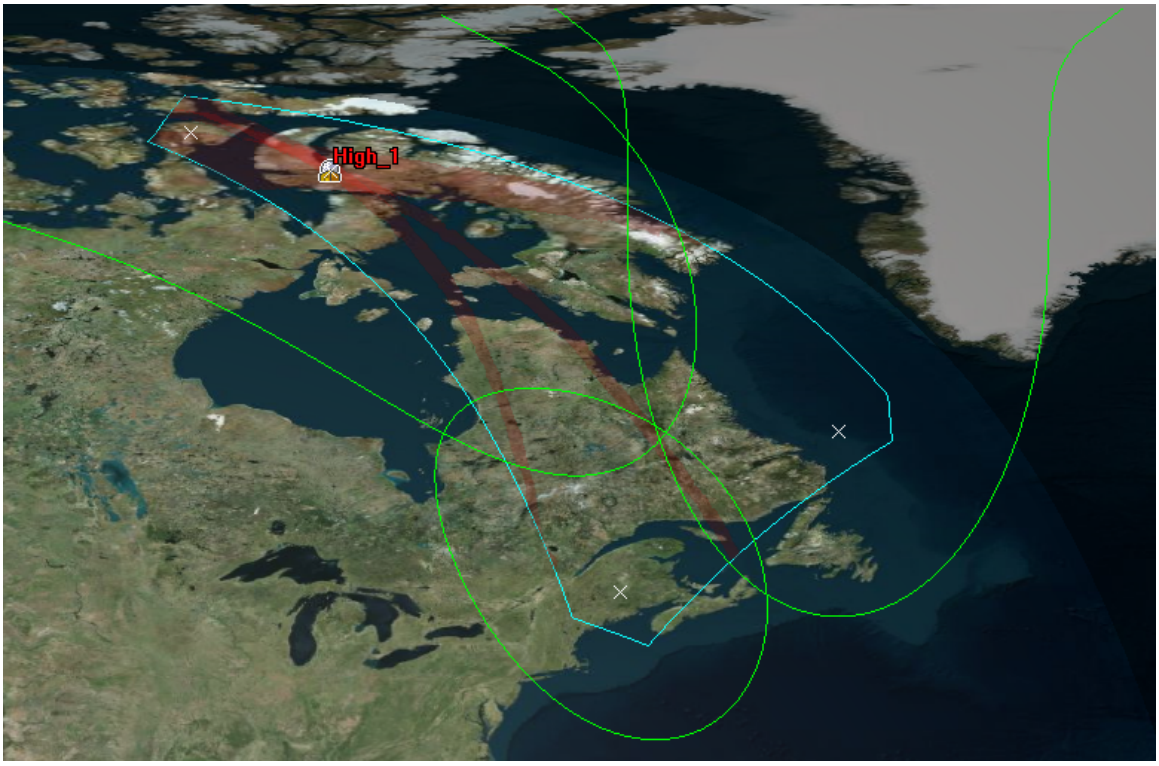

Figure 87. High Latitude Model – Geolocation of Interfering Transmitter #1.

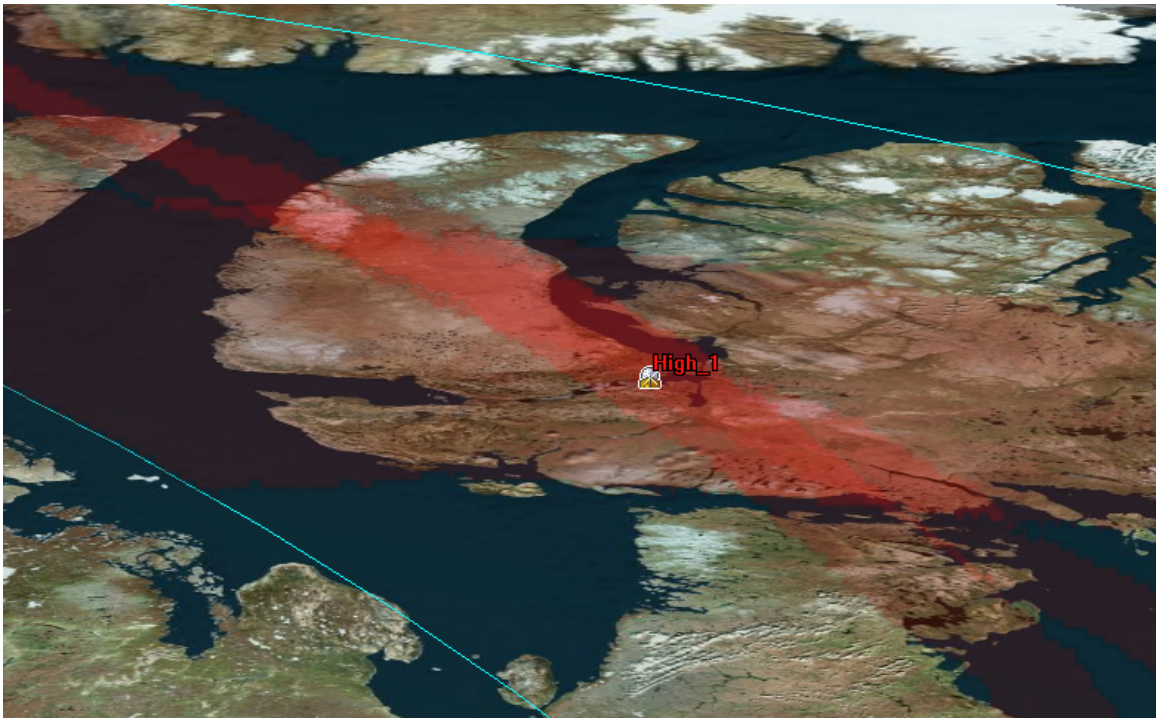

Figure 88. High Latitude Model – Interferer #1 Geolocation AOP.

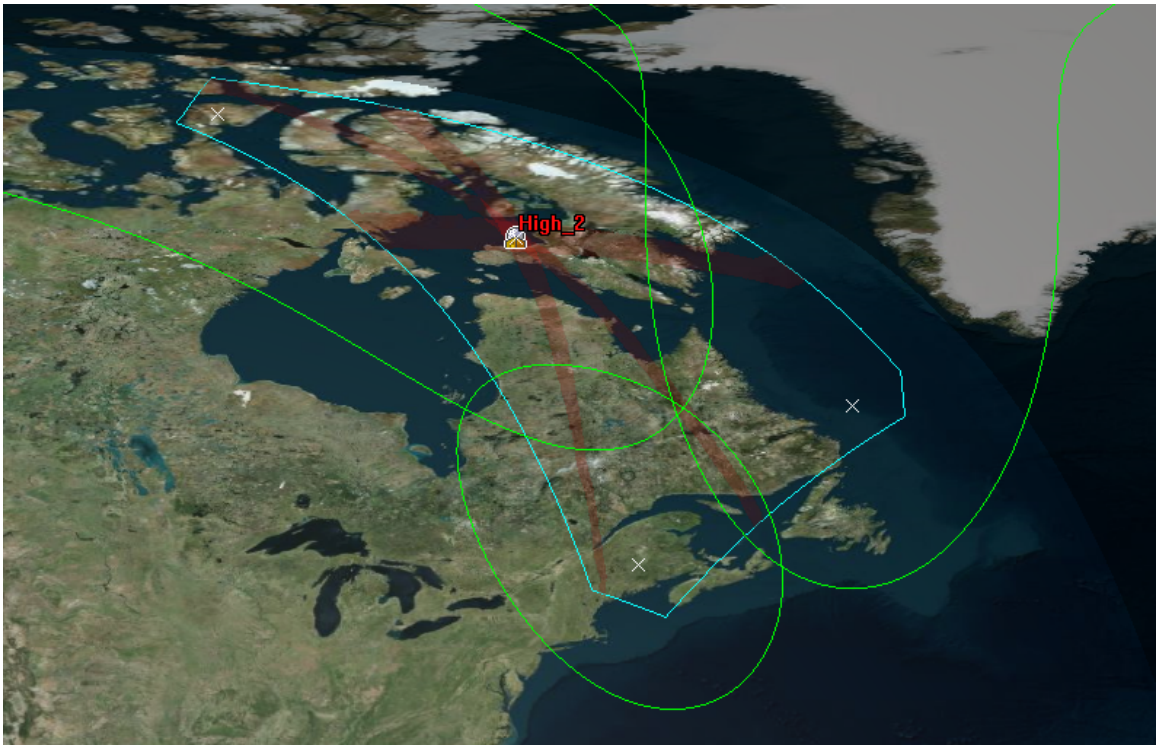

Figure 89. High Latitude Model – Geolocation of Interfering Transmitter #2.

Figure 90. High Latitude Model – Interferer #2 Geolocation AOP.

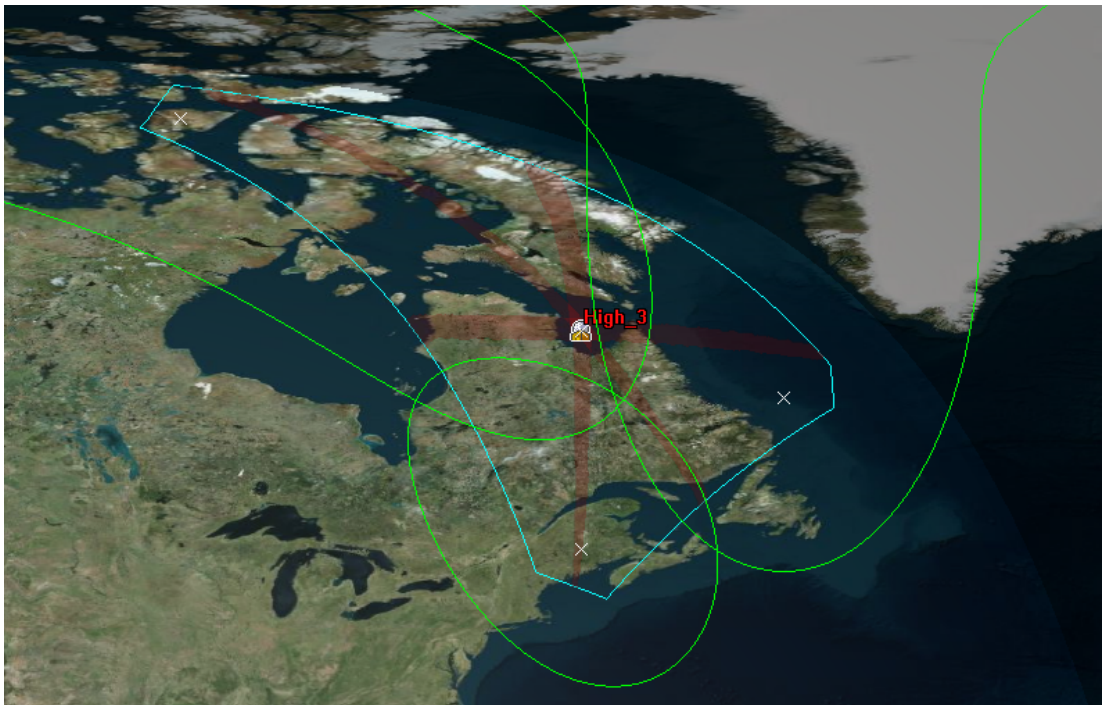

Figure 91. High Latitude Model – Geolocation of Interfering Transmitter #3.

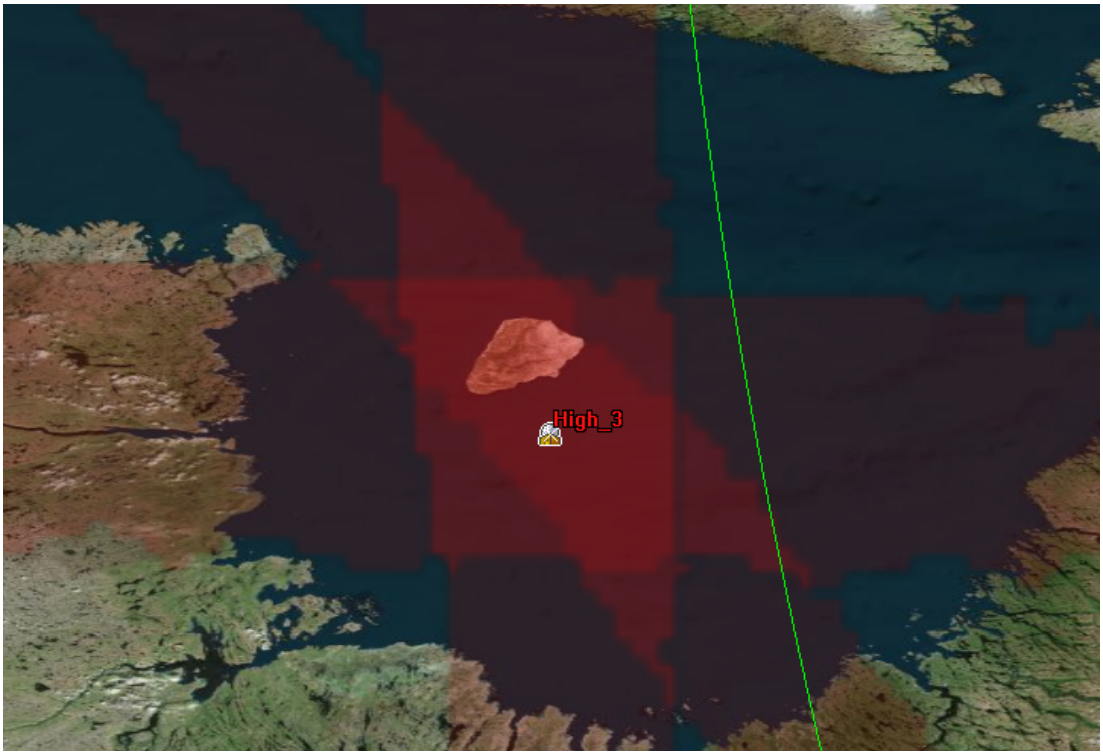

Figure 92. High Latitude Model – Interferer #3 Geolocation AOP.

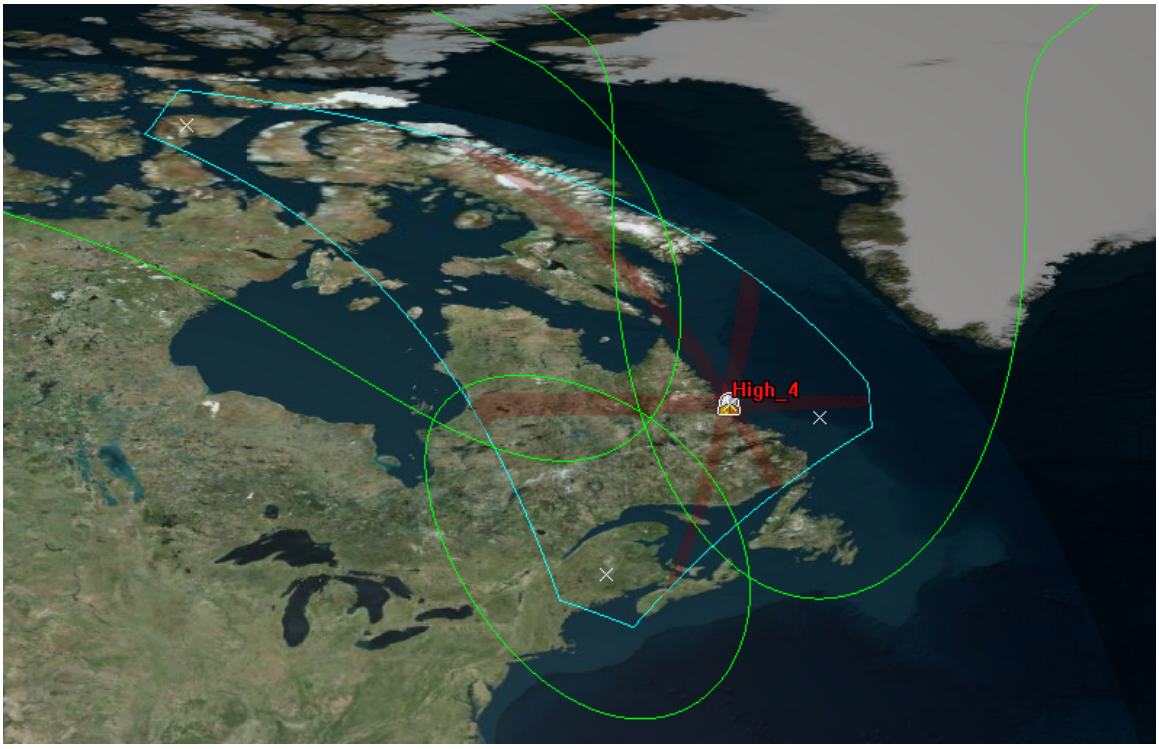

Figure 93. High Latitude Model – Geolocation of Interfering Transmitter #4.

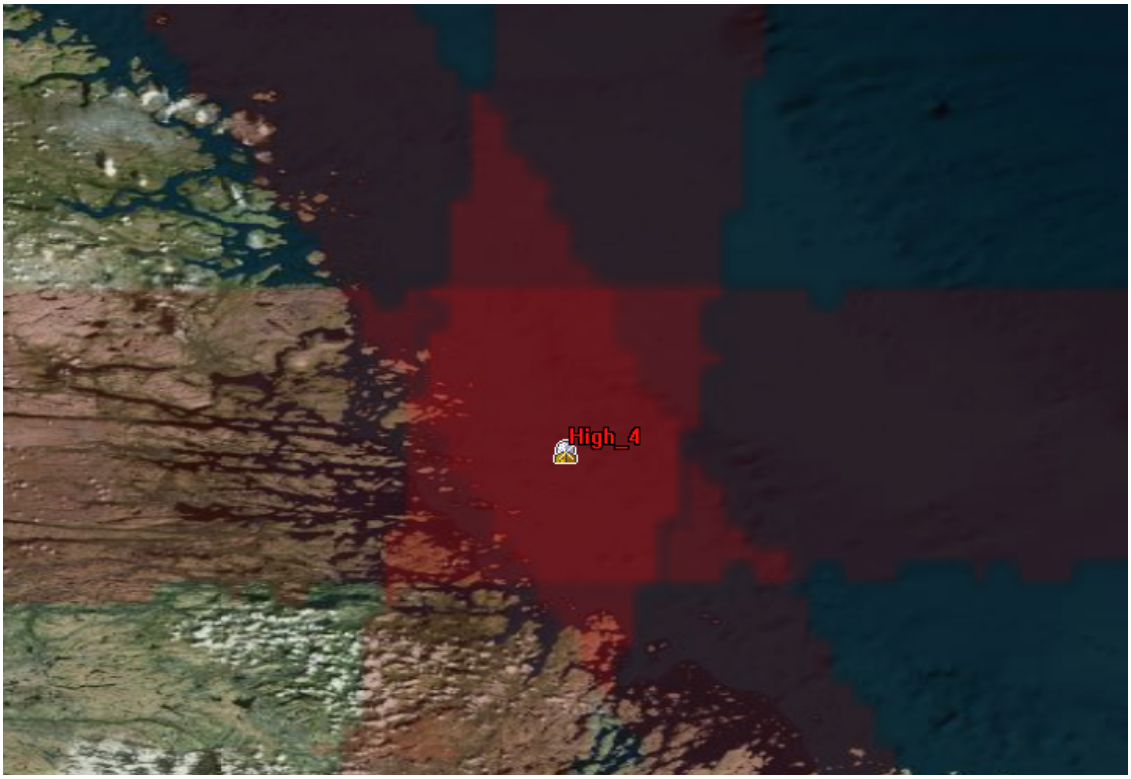

Figure 94. High Latitude Model – Interferer #4 Geolocation AOP.

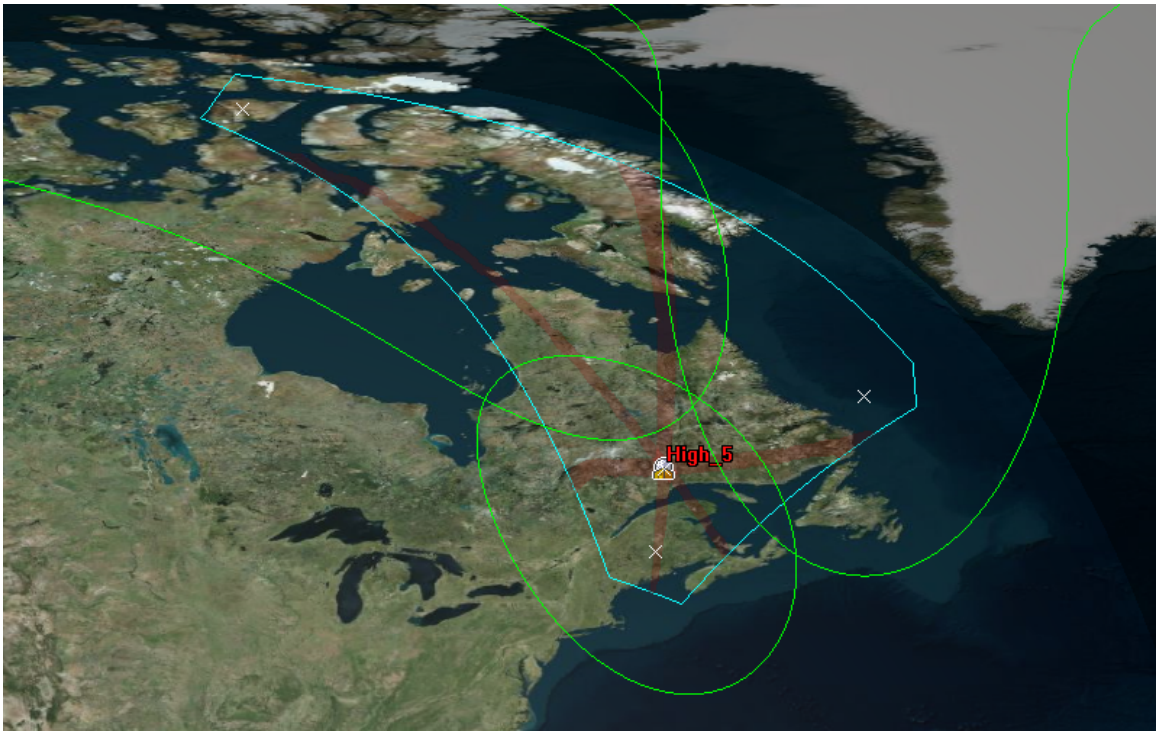

Figure 95. High Latitude Model – Geolocation of Interfering Transmitter #5.

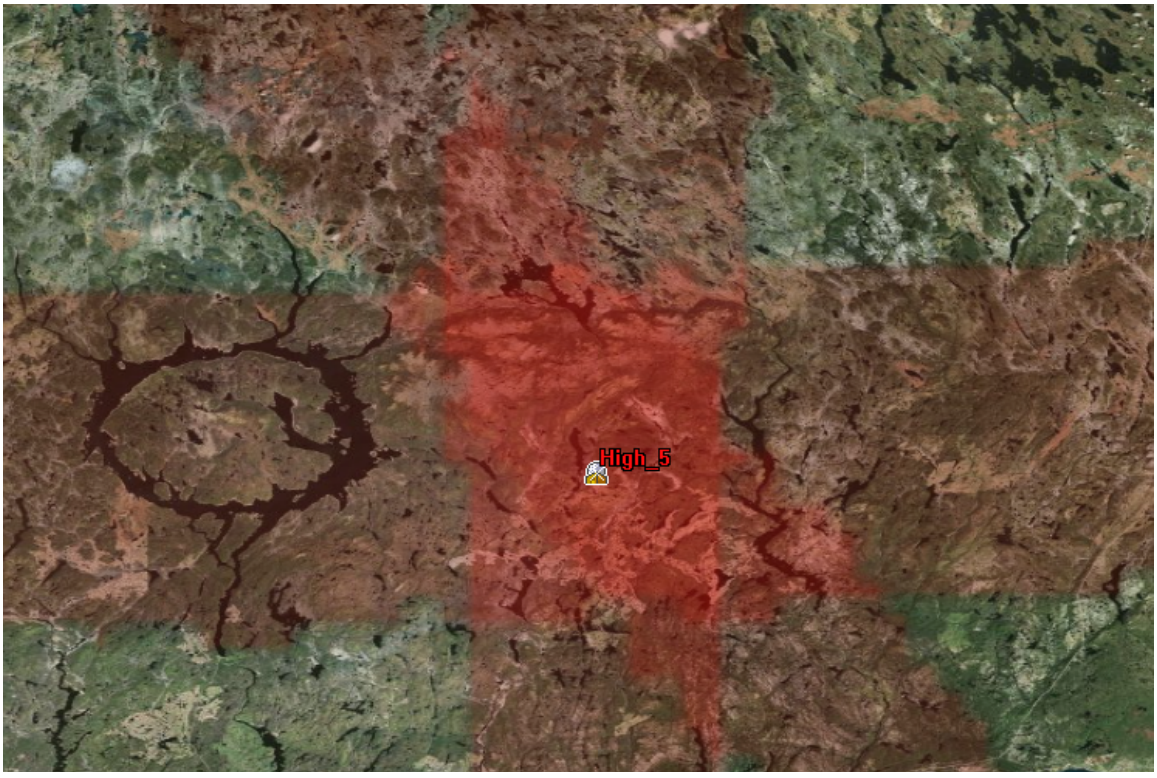

Figure 96. High Latitude Model – Interferer #5 Geolocation AOP.

F. CHAPTER IV CONCLUSIONS

First and foremost, it has been shown that the technique presented in this thesis provides a viable means for geolocating an interfering source from a single satellite with multiple antennas. From there, the size of the area resulting from the geolocation method that contains the interfering transmitter needs to be characterized. The two main variables identified at the beginning of Chapter IV for testing the performance of the geolocation model were latitude variation and signal strength measurement accuracy. It was hypothesized that regions of lower latitude would produce smaller AOPs than regions of higher latitude due to the fact that the lower latitudes contained more focused antenna footprints. It was also hypothesized that increased error tolerance in the measurement of the signal strength would lead to an increase in the size of the final geolocation area of probability.

After reviewing all of the data points created for each combination of latitude region and contour width, a number of conclusions can be reached but also, a number of questions are still left to be answered.

1. Compilations

Table 14 and Table 15 include a summary of the average geolocation area sizes and effective radius sizes for the tested combinations of latitude and error tolerance of the signal strength measurement.

Latitude Region	Average Geolocation Area (km^2)		
	1 dB	0.5 dB	0.1 dB
Low	2,192	477	28
Mid 1	2,538	599	32
Mid 2	8,098	1,700	45
High	19,550	2,168	62

Table 14 Average Geolocation Area Size Compared Across Multiple Latitude Regions and Contour Widths

Latitude Region	Average Geolocation Effective Radius (km)		
	1 dB	0.5 dB	0.1 dB
Low	26	12	3
Mid 1	28	14	3
Mid 2	50	23	4
High	72	25	4

Table 15 Average Geolocation Effective Radius Compared Across Multiple Latitude Regions and Contour Widths

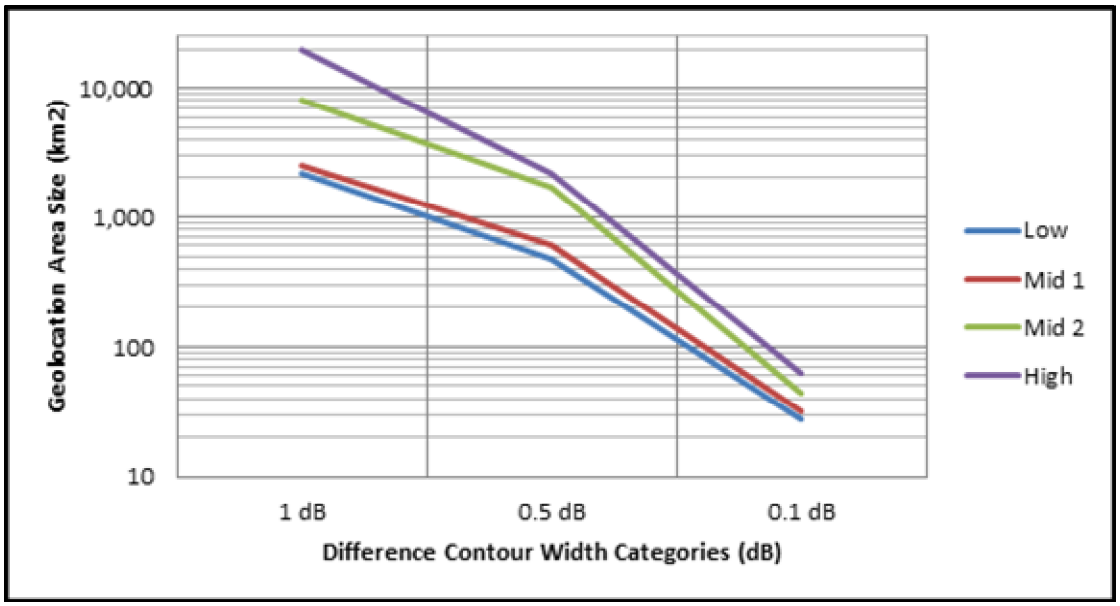

Figure 97. Graphical Representation of Area Size versus Contour Width over Four Regions of Latitude.

Figure 97 is a graphical representation of the results summarized in Table 14 and Figure 98 is a graphical representation of the results summarized in Table 15.

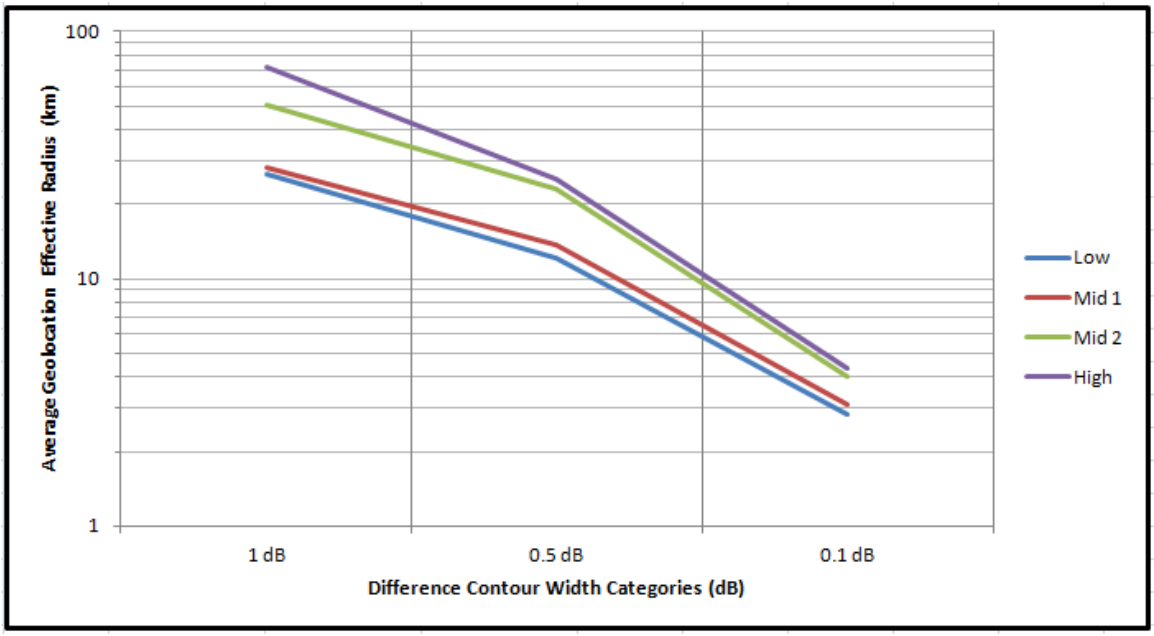

Figure 98. Graphical Representation of Effective Radius versus Contour Width over Four Regions of Latitude.

Table 16 provides a compilation of the percent increase in geolocation AOP size as latitude of the AOI increases. With regard to the error tolerance of the signal strength measurement, the average size of the geolocation AOP for a 1 dB total contour width is 8,095 km^2. The average size of the geolocation AOP for a 0.5 dB contour width is 1,236 km^2 and the average AOP size for a 0.1 dB contour is 42 km^2. In other words, the size of a 1 dB AOP is 555% greater than a 0.5 dB; a 0.5 dB AOP is 2,850% greater than a 0.1 dB AOP, and a 1 dB AOP is 19,219% greater than a 0.1 dB AOP.

This increase in geolocation AOP size was also seen with increases in latitude. The size of the 1 dB geolocation AOP for the Mid Latitude (Part 1) region is 16% larger than the Low Latitude region. The Mid Latitude (Part 2) geolocation AOP is 219% larger than the Mid Latitude (Part 1) AOP. The High Latitude AOP is 141% larger than the Mid Latitude (Part 2) AOP, 670% larger than the Mid Latitude (Part 1) AOP, and 792% larger than the Low Latitude AOP.

The rate of change of geolocation AOP size seen for 1 dB contour widths is echoed for the 0.5 dB contour width, albeit to a lesser degree. In the 0.5 dB region, moving from Low Latitude to Mid Latitude (Part 1) sees an increase in AOP size of 26%,

Mid Latitude (Part 1) to Mid Latitude (Part 2) is an increase of 184%, and Mid Latitude (Part 2) to High Latitude is only a 27% increase. The High Latitude AOP is 262% larger than the Mid Latitude (Part 1) and 355% larger than the Low Latitude AOP. In both of these cases, the rate of change between the two lower latitude regions and the rate of change between the two upper latitude regions is relatively small but the rate of change from a low latitude to a much higher latitude is quite significant.

The geolocation AOPs for 0.1 dB contours appears to be more directly proportional rather than exponentially proportional. Here, going from Low to Mid (Part 1) is a 15% increase in size, Mid (Part 1) to Mid (Part 2) is a 38% increase, and Mid (Part 2) to High is a 40% increase. Mid (Part 1) to High is a 93% increase, and Low to High is an increase of 121%.

Latitude Progression	% Change in Average Geolocation Area (km^2)		
	1 dB	0.5 dB	0.1 dB
Low to Mid 1	16	26	15
Mid 1 to Mid 2	219	184	38
Mid 2 to High	141	27	40
Mid 1 to High	670	262	93
Low to High	792	355	121

Table 16 Percent Increase in Average Geolocation AOP with Increased Latitude

2. Conclusions

a. Geolocation AOP Size versus Contour Width

The figures and tables in Section 1 above clearly show that the size of the geolocation area is proportional to the accuracy of the signal strength measurement. The disparity between the possible sizes of the resultant geolocation AOP increases as the error of the signal strength measurement increases. The range in sizes for the 1 dB

contour width was larger than the range for the 0.5 dB contour, which was then in turn larger than the range of sizes for the 0.1 dB contour width.

An interesting observation of note is that, for the 1 db and 0.5 dB contour widths, the emitter was located with a noticeable bias toward the approximate center of the AOP. This bias was not quantified because the exact center of the AOP is difficult to determine. However, the existence of this bias suggests that, while considering error tolerances is necessary to provide the most inclusive AOP, accurate signal strength measurements will generally produce a much better solution than suggested by the size of the AOP.

b. Geolocation AOP Size versus Latitude

Also, in most cases, the size of the geolocation AOP is proportional to the latitude of the AOI. The AOP is smaller in lower regions of latitude. This occurred both between varying regions of latitude, but also in some cases inside a specified region of latitude. The variations in the size of the geolocation AOP appear to be a direct result of the size of the spot beam as it intersects the curvature of the Earth. From the perspective of the geostationary satellite, the farther the AOI is from the equator, the more elliptical the footprint of the antennas. A larger footprint encompasses a greater number of lines of latitude in the AOI which then results in larger contour widths forming the geolocation AOP.

Therefore, it is reasonable to conclude that the smallest geolocation areas will be produced by the most precise measurement of the signal strength in areas of interest at or near the equator. The largest geolocation areas will occur for imprecise signal strength measurements and areas of interest in the vicinity of the highest possible latitudes within view of the satellite. And finally, generally speaking, the size of the geolocation area increases significantly with increased latitude.

c. Conclusions Apply Symmetrically About the Equator

All of the latitudes discussed to this point have focused on the Northern Hemisphere. It should be said however, that the same conclusions apply to the Southern Hemisphere. Since the satellite is in a geostationary orbit, antenna orientations in the

north that are exactly mirrored in the south should produce identically shaped footprints that are mirror images of the footprints in the north (assuming that Earth is exactly symmetrical about the Equator—the difference in behavior of the model due to differences in the shape of the Earth close to each pole is not covered further in this thesis).

For example, an antenna pointed 1° true north would produce the exact same footprint as an antenna pointed 1° true south. In this manner, the sizes of the footprints for each line of northern latitude are mirrored at the same lines of latitude south of the Equator. As such, all of the conclusions drawn in this section for AOPs created in the Northern Hemisphere can be extended to the application of the geolocation method in the Southern Hemisphere.

3. Questions

a. Emitter Location in AOI

One question left unanswered is the nature of the size of the AOP with respect to the location of the AOP inside the AOI. The AOI is defined by the intersection of the fields of view of three receive antennas so it is possible that the interfering transmitter can be located anywhere inside the AOI, including on the hypothetical border of two potential areas of interest. There did not seem to be any correlation between the size of the AOP and the proximity of the AOP to an antenna boresight. Similarly, there did not seem to be a correlation between the size of the AOP and the proximity of the AOP to a neighboring AOI. For some combinations of contour width and latitude, an AOP close to an antenna boresight was the most accurate and in other situations, an AOP on the border of the AOI or in the middle of the AOI was smaller.

b. High Latitudes

An interesting observation surfaces when considering the overall highest latitude data point. The geolocation area produced by the highest latitude transmitter (High_1) in the High Latitude group was significantly larger than any of the areas produced by other transmitters. The end result was that it had a considerable impact on the computation for

the *average* area size for the group. The average of the other four interfering transmitters in the High Latitude group at 1 dB contour width is approximately 4,276 km^2. This is a difference of almost 50%! The savings in area size can be attributed to the fact that a large portion of the High Latitude AOI is located in the vicinity of 60° N latitude. It has been argued in Section 2 that increased latitude, especially into regions skewed by the overlap of highly elliptical footprints, significantly increases the size of the resultant geolocation area. Is the large geolocation AOP from (High_1) indicative of an exponential relationship between AOP size and High latitude or is it an outlier that results from the particular AOI configuration in this test group?

c. Geometry of Intersecting LOPs

Along those same lines is the uncertainty surrounding how the geometry of the intersecting LOPs that produce the geolocation area interact with the latitude of the AOP. It was asserted in Section 2 that increased latitude results in increased size of the geolocation AOP. However, three interferers in the Mid Latitude (Part 2) group produced geolocation areas from 1 dB contours that were larger than two interferers from the High Latitude group. The transmitters in questions from the Mid Latitude (Part 2) group are Mid_1, Mid_2, and Mid_3. Mid_1 and Mid_3 are located at 40° latitude and Mid_2 is located at 44° latitude. High_4 and High_5, located at 56.5° and 51.25° respectively produced 1 dB contour AOPs that were smaller than the AOPs generated by Mid_1, Mid_2, and Mid_3.

This is most likely due to the geometry of the interfering transmitters inside the AOI. As the AOI is skewed by highly elliptical footprints, increased uncertainty is introduced into the geolocation AOPs created in these skewed regions of the AOI. Mid_1, Mid_2, and Mid_3 are located in the stretched areas of their AOI; Mid_1 and Mid_2 more so than Mid_3. In contrast, High_4 and High_5 are positioned in the less distorted area of the High Latitude AOI. These geolocation AOPs have the advantage of thinner contours intersecting to create the final geolocation area. The exact effect of less than ideal geolocation geometry versus latitude is not clearly revealed in this study.

d. Outliers

Another important area of discussion is with regard to a curious observation in the 0.1 dB contour width group of data points. In 5 of the 20 data points for this contour width, the predicted geolocation AOP did not actually contain the interfering transmitter. This occurred for emitters Mid_2 and Mid_5 in the Mid Latitude (Part 1) group, emitters Mid_1 and Mid_3 in the Mid Latitude (Part 2) region, and for emitter High_5 in the High Latitude group. The average distance of the actual emitter from the edge of the geolocation AOP (all triangular shaped) was 7 km, with the closest at 5 km and the farthest at 11 km. 100% of the 1 dB contour widths and 100% of the 0.5 dB contour widths were located inside the predicted geolocation AOPs. However, for the 0.1 dB contour width, only 75% of the emitters were located inside the predicted area. This fact explains why this thesis has continuously referred to the geolocation area as an area of *probability*.

The reason(s) these five emitters were not located inside the predicted AOP is unknown, but can be possibly attributed to a number of different factors (or a combination of some or all factors). It is possible that, while STK reports Receiver Gain within ± 0.0001 dB, the actual accuracy of the measurement within STK is more like ± 0.05 dB. If this measurement is not as accurate as believed, it would explain why some of the 0.1 dB solutions did not contain the interfering emitter. The AOPs generated in Chapter IV should always include the interfering transmitter if the Receiver Gain measurements in STK are accurate. The different sized AOPs were created to show how erroneous measurements could lead to error in determining the exact location of the interfering transmitter. For the outliers in the 0.1 dB contour width group, it is possible that a limit has been reached and STK cannot produce a more accurate model.

Another possible explanation is that three of the five offending emitters are located in close proximity to an antenna boresight. Whether this could be a potential influencing factor or not was alluded to at the beginning of this section. One of the five was located almost on the border between two potential areas of interest. Mid_3 from the Mid Latitude (Part 2) group was located relatively centrally to that AOI, although still in a stretched section. It is possible that the locations could have added error to the method.

Other possible explanations include some unknown behavior of the STK software, a bug in the capability of the graphics card to display the 0.1 dB contours or of course, and/or user error.

(1) Mitigating Outliers. In each case, a potential mitigating factor could be the use of neighboring antennas to create a different AOI, which will then have a different associated geometry. This solution could provide enough additional information to resolve the issue.

If a neighboring antenna is not available, an interesting observation can be seen with some quick math. Adding the average distance of error from the five emitters to the overall average AOP of the 0.1 dB contour width increases the average area size for the 0.1 dB contour group from 42 km^2 to 163 km^2. This would be extremely conservative because 75% of the emitters were already located inside the AOP. However, by this conservative logic, an average 0.1 dB contour width measurement that produces an average 163 km^2 area will contain the interfering emitter 100% of the time.

4. A Limitation

The last analysis item left to discuss in this study is the limitation on the applicability of the geolocation method to all latitudes. The geolocation model can only be performed up to latitudes with the field of view of a geostationary satellite. Figure 99 is a good example of this limitation. In this graphic, the satellite is shown as a white node (overlaying South America) and the satellite orbit is shown in white. The three antenna footprints from the High Latitude region are visible toward the surface of the Earth. In High Latitude region, the antenna fields of view are cut off at approximately 80° N latitude. In other words, the antennas simply cannot “see” latitudes above 80° N.

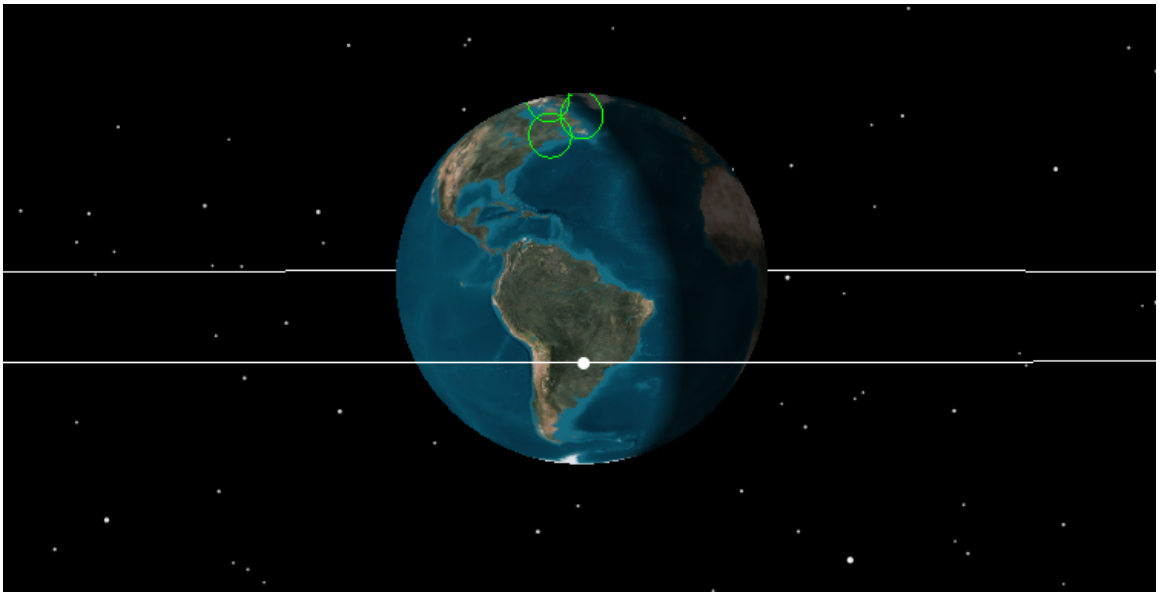

Figure 99. High Latitude Limitation Shown via 3D Model.

Additionally, the highest antenna boresight in Figure 99 is located at 74° N. Since the geolocation method assumes the source of interference is located inside the FOV (i.e. boresight) of all three antennas, it follows that the maximum latitude supported by this geolocation method is 74° N. It is theoretically possible to create an AOI such that the most northern antenna boresights are located at 80° N. This would theoretically provide geolocation availability up to that latitude. But, a point to remember is that the size of the geolocation area created at this latitude may be exponentially large, as it is a full 9° further north than the High_1 emitter from the High Latitude test region.

V. CONCLUSIONS, APPLICATIONS, AND FUTURE WORK

Chapter V is the final chapter of this thesis, and is organized into three parts. Part A summarizes the conclusions derived from all of the research conducted in this thesis. Part B discusses possible applications of the geolocation method. Part V.C details recommended avenues of future research with regard to the geolocation method.

A. THESIS CONCLUSIONS

Myriad arguments have been made throughout this thesis. Chapter I introduced the concept of satellite communications, RF interference, and current methods for locating that interference. Accounting for the current paradigm shift in satellite communications systems from single antenna large area coverage designs to multiple spot beams configurations, it is evident that the way geolocation is currently conducted needs to be reconsidered. Algorithms and techniques that require multiple satellites for the successful geolocation of interference will no longer be available as those satellites reach end of life.

1. The New Geolocation Method Works

As shown in Chapter II and Chapter IV, the method introduced in this thesis can be used to geolocate a source of RF interference. Any communications satellite that can create a multiple spot beam antenna pattern can exploit areas of overlapping antenna gain to employ this geolocation method with some degree of success. The geolocation method offers a number of advantages beyond the fact that it can be conducted from a single satellite. If the antenna gain difference contours for a given satellite are computed in advance of the satellite being put into operation, the geolocation method can be completed in real time once interference is detected. An interfering source can be geolocated passively so as not to alert an interfering transmitter and without a significant amount of equipment/cost added to the satellite design.

2. The Geolocation Method Can Be Modeled

Systems Tool Kit software provides an excellent test bed for modeling the geolocation method due to its uniquely tailored design for use in space technology applications. The geolocation method can also be modeled using a number of different software packages, such as MATLAB or Microsoft Excel. A tutorial for modeling the geolocation method is included in the Appendix.

3. The Quality of the Geolocation Method Can Vary

The quality of the AOP produced by the geolocation method is very much dependent upon the quality of the parameters required for its completion. Two specific parameters tested in this thesis were the performance of the method for different accuracies of signal strength measurement and for different areas of interest created at various latitudes. It was found in Chapter IV that the size of the geolocation AOP decreased with increased accuracy of the signal strength measurement. Similarly, any additional sources of error in the communications system, such as knowledge of the satellite's position and antenna boresight location, induce additional potential for error in the final geolocation AOP. Also, the size of the geolocation AOP increased with increased latitude (but is symmetrical about the Equator).

B. APPLICATIONS OF THE GEOLOCATION METHOD

1. Satellite Systems

Any satellite that can create the spot beam geometry described in Chapter II of this thesis can use this method to geolocate a source of interference. Four specific examples include INMARSAT Global Xpress satellites, WGS satellites, ViaSat, and Mobile User Objective System (MUOS) satellites.

a. INMARSAT Global Xpress

The communications system modeled throughout this thesis was the INMARSAT Global Xpress System. This system is a planned constellation of four satellites designed to provide high speed, global Ka band coverage by the end of 2014. The first satellite of this constellation was launched on 8 December 2013 and had completed all required

platform and payload testing at the time of this thesis' publication [20]. Each INMARSAT Global Xpress spacecraft can provide up to 89 fixed spot beams with 72 beams simultaneously active at one time.

b. WGS

Another platform that could make use of this geolocation technique is Wideband Global SATCOM (WGS). The WGS system is the DoD's highest capacity satellite communications system with six spacecraft currently on orbit [21]. Each WGS spacecraft can provide 19 coverage areas, including 10 Ka-band independently steerable antennas.

c. ViaSat

ViaSat is a company whose specific mission is to produce "innovative and other digital communication products that enable fast, secure, and efficient communications to any location" [22]. Within that concept, ViaSat-1 was launched on October 19, 2011 and began operational service in January 16, 2012 [23]. ViaSat-1 employs 72 Ka-band spot beams (56 active at any given time) [24].

d. MUOS

MUOS satellites offer a unique application of the geolocation method because they operate in the UHF region of the RF spectrum (as opposed to Ka band). There are currently two MUOS satellites in operation, each offering 16 wideband code division multiple access (WCDMA) spot beams. These beams are slightly larger than the Ka beams discussed in previous satellite applications but are still applicable for use with the geolocation method [25].

2. An Excellent First Step

Once an interfering transmitter has been geolocated, there are a number of courses of action available to the satellite operator. These actions could range anywhere from a tactical strike (in military applications) to a number of passive solutions such as changing the antenna orientation (more on this in Section V.B.3) or simply pursuing diplomatic

solutions. Some of these actions may be highly dependent on the size of the geolocation AOP, while others may not. For example, none of the AOPs produced in Chapter IV are obviously accurate enough to specifically identify the interfering source.

However, the geolocation method should not be discarded if it does not immediately result in an AOP small enough for certain application as it can still provide valuable information. Further analysis of the geolocation AOP itself might serve to reduce the AOP and therefore assist in identifying the interfering source. This applies to both intentional and unintentional interference. Knowledge of whether a system is seeing intentional or unintentional interference in and of itself is useful information.

For instance, if the resultant AOP covers regions over both land and water, this may help to refine the AOP. If the AOP is entirely over water then it is likely that the source of interference is a ship inside the AOP. If the AOP is partially in a politically friendly region and partially in an unfriendly region, it may be more likely that the interference is coming from the unfriendly region. This concept also applies when the geolocation method is used in concert with other potential sources of intelligence. If the geolocation AOP includes known broadcast entities, perhaps they are the source of intentional/unintentional interference.

3. Neutralize an Interfering Transmitter

While the geolocation method may not be able to identify the exact source of interference, it is certainly good enough to mitigate it. The effects of the interfering transmitter can be reduced or eliminated by placing it in the null of the receiving antenna. As discussed in Chapter II, a null is an area where the antenna will produce a significantly reduced amount of gain to the signal it is meant to amplify. A null is bad place to be for a user attempting to connect to its associated satellite. But this effect can be applied in reverse to benefit the satellite operator and negate the effects of an interfering transmitter.

For example, Figure 100 shows an example AOP created using the geolocation method from this thesis, superimposed with the gain contours of the antenna affected by the interference. The interfering transmitter, Low_1, is located approximately within the

28-30 dB band of the antenna footprint. The AOP produced in the geolocation of Low_1 (assuming 1 dB contour width) has an effective radius of 25 km (and therefore has a maximum diameter of 50 km).

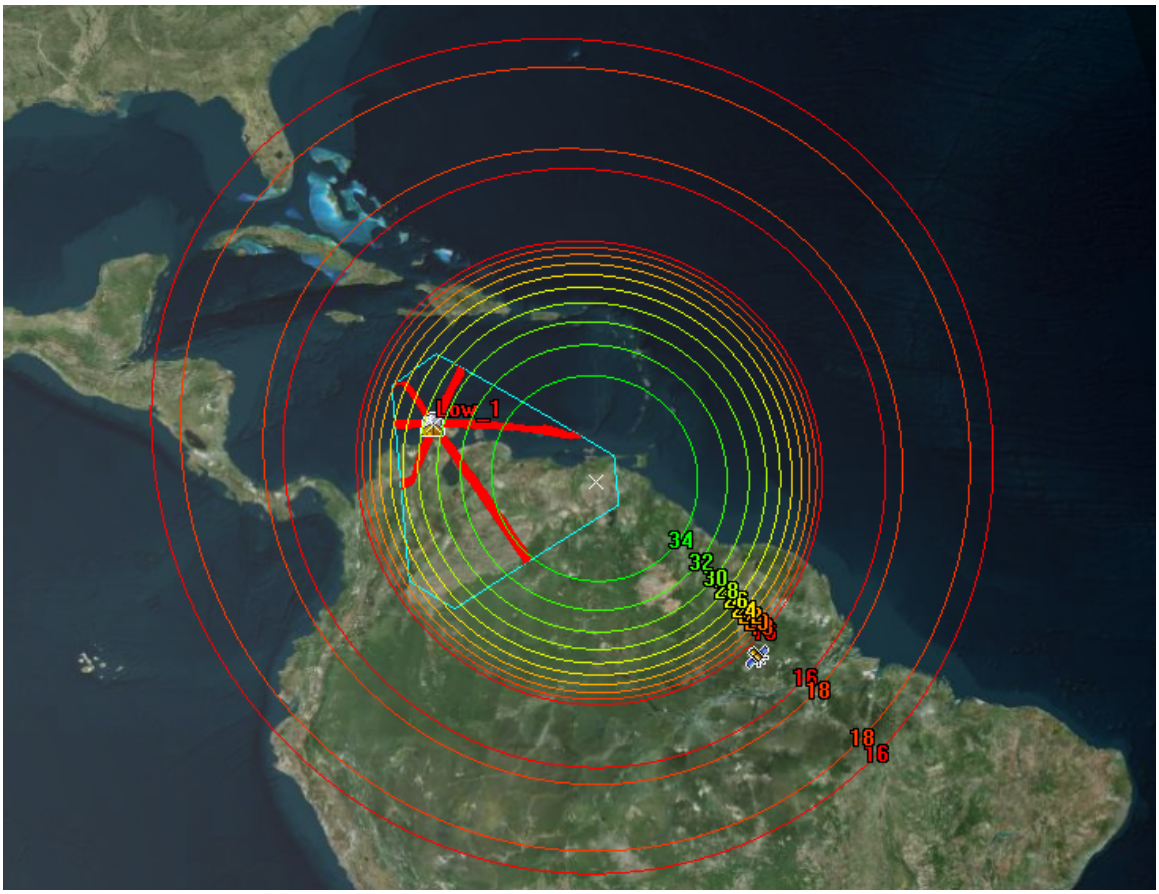

Figure 100. Interfering Transmitter Located Inside Antenna Footprint.

Not far from the interfering transmitter, the gain from the antenna rapidly falls below 16 dB, shown by red contour lines in Figure 100, then comes back above 18 dB (dark orange lines) before once again falling below 16 dB. The width of this null is approximately 440 km.

Figure 101 shows how a satellite operator can slightly change the antenna orientation to use the antenna null to minimize the effects of the interfering transmitter. Shifting the antenna boresight approximately 500 km to the east places the source of interference in the lowest area of antenna gain without significantly impacting the overall

region of service. To minimize the impact on the user, the orientation can be changed in any direction that is advantageous to the user while still placing the inteference inside the antenna null.

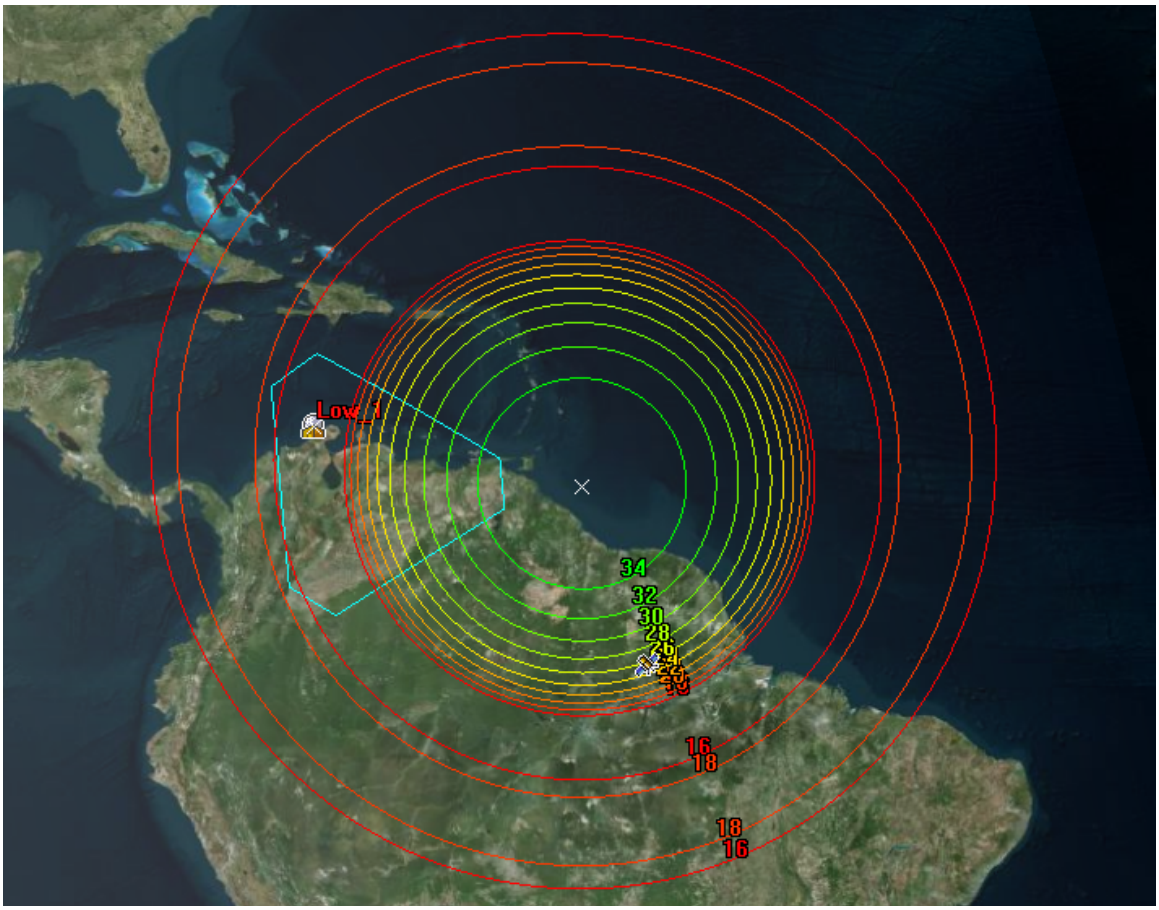

Figure 101. Interfering Transmitter Placed in Antenna Null.

C. RECOMMENDATIONS

In wrapping up the research for this thesis, there are a number of areas that can be explored in future research. The first and most obvious recommendation is testing the geolocation method with an operational satellite. This would help provide a better understanding of the questions regarding real world applications of the geolocation method. Working with satellite designers on a real world test bed would provide a better characterization of both the availability and the accuracy of the signal strength

measurement. The results of such an analysis could either show that the contour widths used in Chapter IV were conservative or optimistic. If the accuracy of the signal strength measurement is found to be better than assumed, the accuracy of the geolocation method could improve greatly. This would both alter the potential benefits of and increase the available applications of the geolocation method.

Also, based on the positive results seen in this thesis, it is recommended that any communications satellite not currently able to accurately measure the signal strength received at each antenna install a means to do so. The applicability of this recommendation will likely vary for different spacecraft and is an idea that requires further research. For example, it is not likely the addition of this capability would involve a significant amount of hardware, software, or overall cost if it were included early in the design process of a satellite. For satellites already on orbit however, it is not clear whether this recommendation can realistically be implemented. Perhaps a software upgrade could provide access to the signal strength measurement for some satellite designs.

Another recommendation is for more extensive testing of the behavior of the method over different latitudes and AOI geometries. This testing could provide a better understanding of the applicability of the method in certain scenarios. It could also identify whether certain configurations of adjacent antennas offer more accurate geolocation AOPs than other configurations and answer questions surrounding the size of the geolocation AOP with respect to an interfering emitter's location inside the AOI.

Finally, it is recommended that further research be conducted into the applications of the geolocation method. This research could identify additional applications that might benefit from the ideas presented in this thesis.

THIS PAGE INTENTIONALLY LEFT BLANK

APPENDIX. SINGLE SATELLITE, MULTIPLE ANTENNA GEOLOCATION OF INTERFERENCE TUTORIAL (STK 10)

The purpose of this Appendix is to provide the reader with a basic yet meticulous, step-by-step tutorial for setting up a generic model of the single satellite, multiple antenna interference geolocation method. This tutorial walks the reader through inserting a satellite, configuring that satellite to operate with multiple antennas, defining an area of interest, creating a transmitting object to create the communications link, setting up STK to perform the requisite calculations, and configuring STK to display the difference contours needed to complete the geolocation of an interfering source.

A comprehensive explanation of all of the STK objects used in this tutorial can be found in Chapter III. Questions, comments, or issues with this tutorial should be directed to either the thesis student or the thesis advisor.

A. Create the Scenario

1. Open STK 10 and click the *Create a Scenario* button.
2. Enter the following in the *New Scenario Wizard* dialog box:

Option	Value
Name	Geolocation_of_Interference
Description	Tutorial to demonstrate geolocation of an interfering source from a single satellite with multiple antennas.
Location	C:\Users\<user>\Documents\STK 10
Start	Change the analysis period if required; otherwise, just use the default period of 24 hours.
Stop	

3. When you finish, click OK.
4. After the scenario loads, click *Save* ( ).
5. Verify the scenario name and location, then click *Save*.

B. Model the Satellite

1. Select *Insert STK Objects* ( ) if the window is not already open.
2. Select *Satellite* in the *Scenario Objects* section.
3. Select *Orbit Wizard* in the *Select a Method* section.
4. Select *Insert…*
5. Enter the following in the Orbit Wizard dialog box:

Option	Value
Type	Geosynchronous
Satellite Name	My_Satellite
Subsatellite Point	240 deg
Inclination	0 deg
Color	White

6. Click OK.

C. Configure the Satellite Receiver Model

1. Select *Insert STK Objects* ( ) if the window is not already open.
2. Select *Receiver* in the *Attached Objects* section.
3. Select *Insert Default* in the *Select A Method* section.
4. Select *Insert…*
5. Select *My_Satellite* from the *Select Object* popup window.
6. Click OK.
7. Close the *Insert STK Objects* tool.
8. Double click on "Receiver1" to open its Properties page.
    a. In the *Receiver1 : Basic Definition* window, verify the *Model Specs* tab is active and enter the following:

Option	Value
Type	Complex Receiver Model
Auto Track	Not Checked
Frequency	25 GHz

        i. Click on the *Antenna Tab.*
            1. On the *Antenna Tab -> Model Specs Tab*, enter the following:

Option	Value
Type	Parabolic
Design Frequency	25 GHz
Use Beamwidth	Checked
Beamwidth	2 deg
Efficiency	55%
Back-lobe Gain	-30 dB

            2. On the *Antenna Tab -> Orientation Tab*, enter the following:

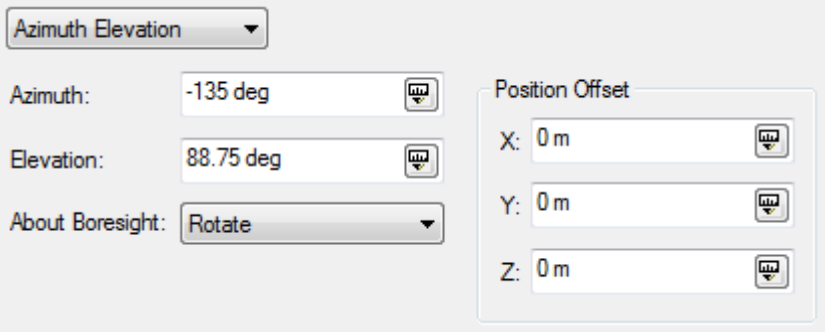

ii. Click on the *System Noise Temperature* tab and verify that *Constant* is selected with a value of 290K.
iii. Click on the *Demodulator* tab:
1. De-select *Auto-select Demodulator*.
2. Select the (…) next to *Name* and choose QPSK.

b. Click *Apply*.
c. In the *Receiver1 : 2D Graphics Contours* window:
i. Verify that *Show* and *Show Contour Graphics* are both checked.
ii. Verify that *Type* is set to Antenna Gain.
iii. Verify that *Relative to Maximum* is checked.
iv. Select *Add Method* Explicit.
v. Enter -3 into the *Level* box and click *Add Level*.
vi. Select *Color Method* Explicit.
vii. Double click on the color box that appears in the *Level Attributes* box and change the color to green.
viii. Verify that *Set azimuth and elevation resolution together* is not checked.
ix. Enter 1 deg into the *Azimuth Resolution* box.
x. Enter 0.1 deg into the *Elevation Resolution* box.
d. In the *Receiver1 : 2D Graphics Boresight* window:
i. Verify that *Show Boresight Graphics* is checked.
ii. Set the *Color* to White.
iii. Set the *Marker Style* to X.
iv. Click OK.

9. Save your progress.
10. Select “Receiver1” by clicking on it once with the left mouse button.
11. Press “CTRL + C”.
12. Select “My_Satellite” by clicking on it once with the left mouse button.
13. Press “CTRL + V” two times.
14. This action should have copied “Receiver1” and pasted two more Receiver objects attached to “My_Satellite”.
15. Select “Receiver11” by clicking on it once with the left mouse button.
16. Press F2 and rename it “Receiver2”.
17. Select “Receiver12” by clicking on it once with the left mouse button.
18. Press F2 and rename it “Receiver3”.

19. Double click on “Receiver2” to open its Properties page.
    a. Verify the values for “Receiver2” are the same as those used to define “Receiver1” with one exception (they should be the same since we copied the object but it does not hurt to double check):
        i. On the *Receiver2 : Basic Definition -> Antenna Tab -> Orientation Tab*, change *Azimuth* and *Elevation* to:

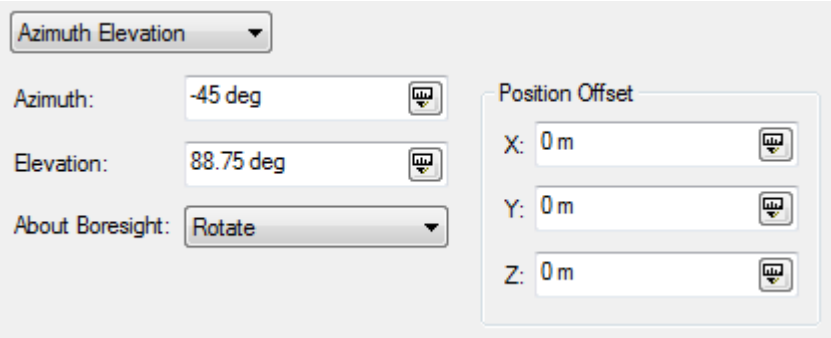

        ii. Click OK.
20. Double click on “Receiver3” to open its Properties page.
    a. Verify the values for “Receiver3” are the same as those used to define “Receiver1” and “Receiver2” with one exception:
        i. On the *Receiver3 : Basic Definition -> Antenna Tab -> Orientation Tab*, change *Azimuth* and *Elevation* to:

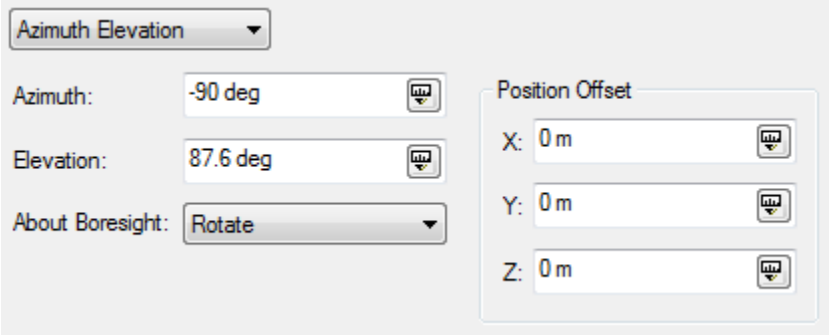

        ii. Click OK.
21. Save your progress.
22. The 2D Graphics Window should look like this (you may have to zoom in):

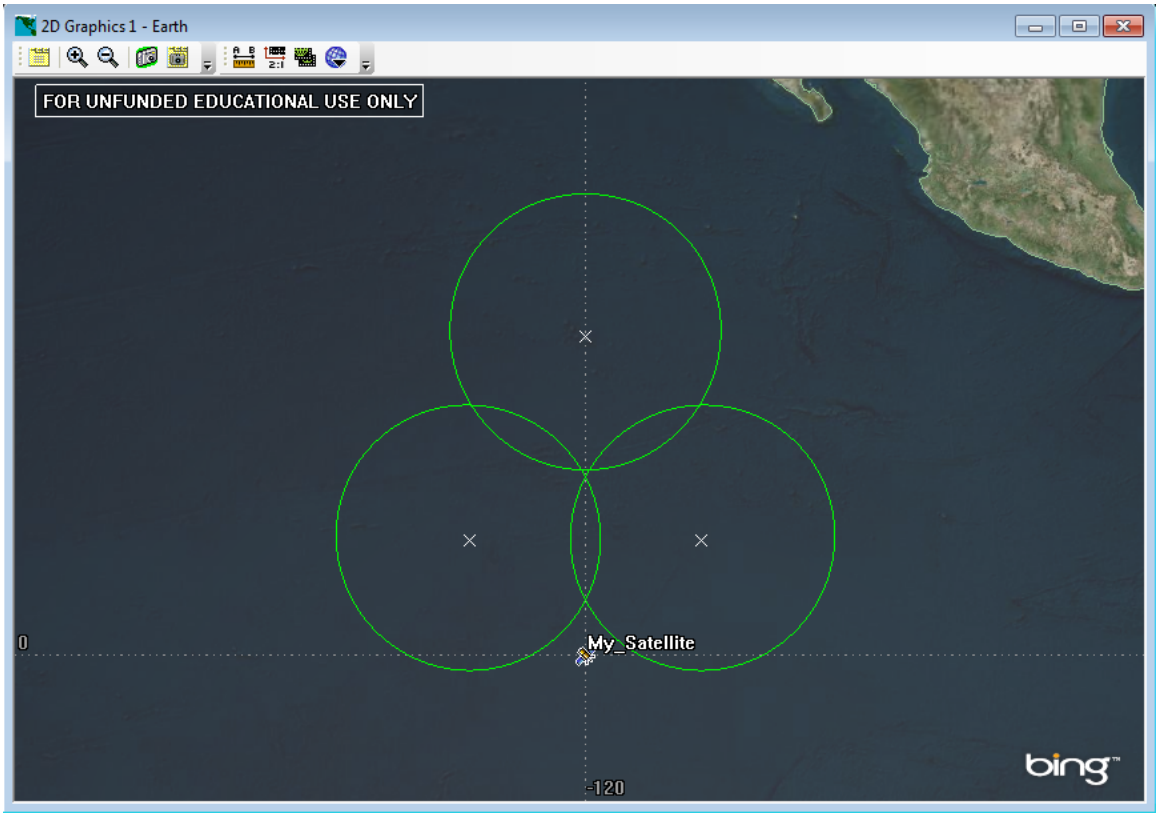

D. Create an Area Target

1. Select *Insert STK Objects* ( ) if the window is not already open.
2. Select *Area Target* in the *Scenario Objects* section.
3. Select *Insert Default* in the *Select A Method* section.
4. Select *Insert…*
5. Close the *Insert STK Objects* tool.
6. There should now be a new Area Target object in the Object Browser window entitled “AreaTarget1”.
7. Select “AreaTarget1” with a single click of the left mouse button.
8. Press F2 and rename it “Area_of_Interest”.
9. Double click on the color box to the left of “Area_of_Interest” and change the color to Cyan.
10. Double click on the “Area_of_Interest” object to bring up its Properties page.
11. In the *Area_of_Interest : Basic Boundary* window, select *Add* four times and enter the following coordinates:

Latitude	Longitude
15 deg	-126 deg
4 deg	-126 deg
4 deg	-114 deg
15 deg	-114 deg

12. Click OK.
13. The 2D Graphics Window should look like this:

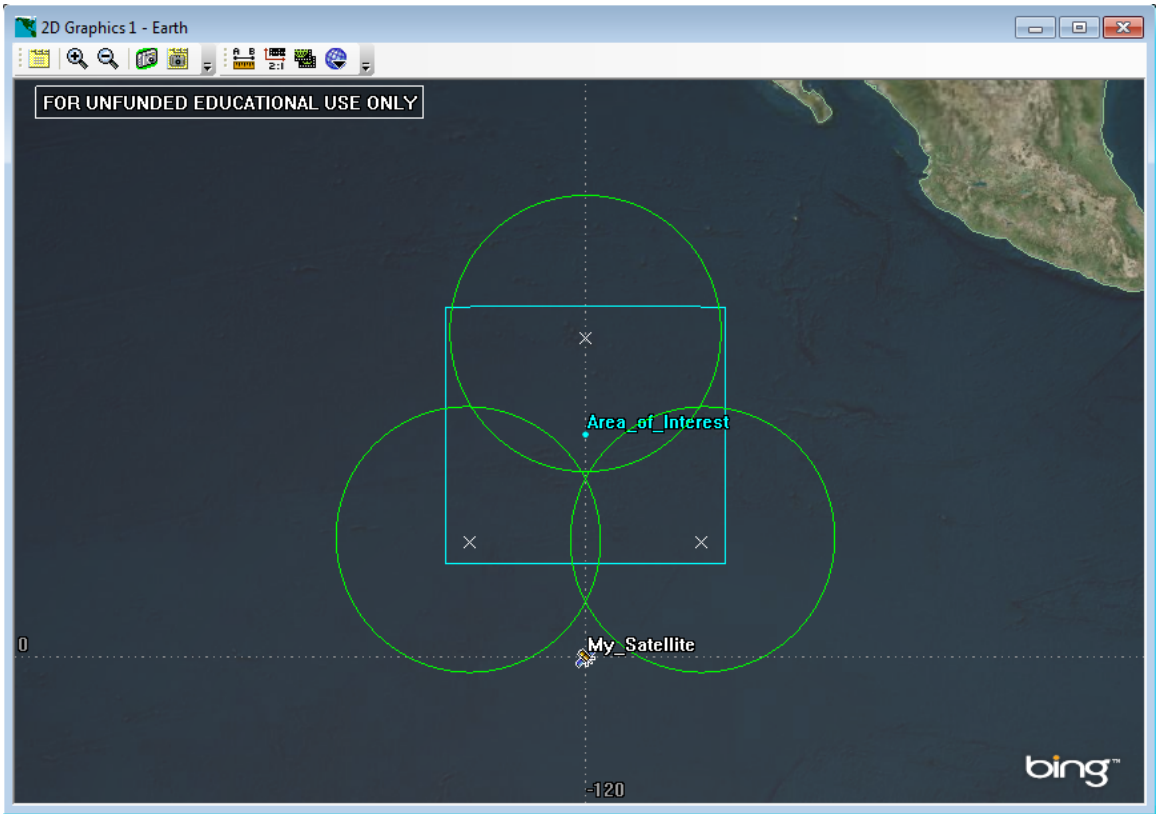

14. Double click “Area_of_Interest” to open its properties page.
    a. Select the *Area_of_Interest : 2D Graphics Attributes* page.
        i. De-select *Inherit from Scenario*.
        ii. De-select *Show Label*.
        iii. De-Select *Show Centroid*.
        iv. Click OK.
15. Double click “My_Satellite” to open its properties page.
    a. Select the *My_Satellite : 2D Graphics Attributes* page.
    b. De-select *Inherit from Scenario*.
    c. De-select *Show Label*.
    d. Click OK.
16. Save your progress.

E. Model a Transmitter

In this tutorial, this transmitter plays two separate roles: (1) first, it acts as the transmitter required by STK to close the communication link, which then allows STK to

calculate link budget parameters (i.e. Rcvr Gain) and (2) it also represents an interfering transmitter used by the tutorial to verify accurate setup at the conclusion of the tutorial.

1. Select *Insert STK Objects* ( ) if the window is not already open.
2. Select *Facility* in the *Scenario Objects* section.
3. Select *Insert Default* in the *Select A Method* section.
4. Select *Insert…*
5. Close the *Insert STK Objects* tool.
6. Select "Facility1" with a single click of the left mouse button.
7. Press F2 and rename it "Interferer".
8. Double click on the color box to the left of "Interferer" and change the color to Red.
9. Double click on the "Interferer" object to bring up its Properties page.
    a. In the *Interferer : Basic Position* window:
        i. Set *Latitude* to 10 deg.
        ii. Set *Longitude* to 239 deg.
        iii. Click OK.
10. Select *Insert STK Objects* ( ) if the window is not already open.
11. Select *Sensor* in the *Attached Objects* section.
12. Select *Insert Default* in the *Select A Method* section.
13. Select *Insert…*
14. Select *Interferer* from the *Select Object* popup window.
15. Click OK.
16. Still in the *Insert STK Objects* window, select *Antenna* in the *Attached Objects* section.
17. Select *Insert Default* in the *Select A Method* section.
18. Select *Insert…*
19. Select *Sensor1* from the *Select Object* popup window.
20. Click OK.
21. Still in the *Insert STK Objects* window, select *Transmitter* in the *Attached Objects* section.
22. Select *Insert Default* in the *Select A Method* section.
23. Select *Insert…*
24. Select *Interferer* from the *Select Object* popup window.
25. Click OK.
26. Close the *Insert STK Objects* tool.
27. Save your progress.
28. Change the colors associated with the facility objects to Red.
29. Rename "Sensor1" to "Int_Sensor".
30. Double click on "Int_Sensor" to open its Properties page.
    a. In the *Int_Sensor : Basic Definition* window,
        i. Verify *Sensor Type* is Simple Conic.
        ii. Enter 0.1 deg into the *Cone Half Angle* box.
    b. In the *Int_Sensor : Pointing* window,

i. Change *Pointing Type* to Targeted.
ii. Select *My_Satellite* from the *Available Targets* and click the right arrow to move it to the *Assigned Targets* window.
iii. Click OK.

31. Rename "Antenna2" to "Int_Antenna".
32. Double click on "Int_Antenna" to open its Properties page.
    a. In the *Int_Antenna : Basic Definition* window, enter the following:

Option	**Value**
Type	Parabolic
Design Frequency	25 GHz
Use Diameter	Checked
Diameter	1 m
Efficiency	55%
Back-lobe Gain	-30 dB

    b. Click OK.
33. Rename "Transmitter1" to "Int_Xmtr".
34. Double click on "Int_Xmtr" to open its Properties page.
    a. In the *Int_Xmtr : Basic Definition* window, enter the following:

Option	**Value**
Model Specs Tab:	
Type	Complex Transmitter Model
Frequency	25 GHz
Antenna Tab:	
Reference Type	Link
Antenna Name	Verify it is "Sensor/Int_Sensor/Antenna/Int_Antenna"
Modulator Tab:	
Name	QPSK

    b. Click OK.
35. Your *Object Browser* window should look like this:

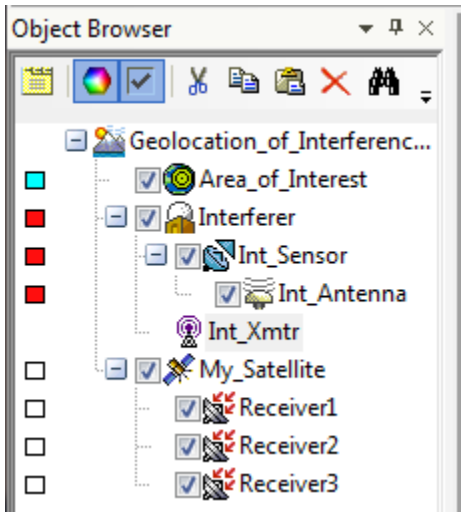

36. Click on the *Access* icon ( ).
    a. Click on *Select Object* and select Int_Xmtr.
    b. Hold CTRL and left click to select Receiver1, Receiver2, and Receiver3 (you may have to click the + button to the left of "My_Satellite" to expand its object tree).
    c. Verify *Inherit Settings from Scenario* is de-selected.
    d. Verify *Show Line* is de-selected.
    e. Click *Compute.*
    f. Click *Close*.
37. Save your progress.

F. Create a Coverage Definition

1. In the *Object Browser* window, left click to highlight "Geolocation_of_Interference".
2. Select Insert from the STK toolbar and select *Default Object*.
3. Select *Coverage Definition* from the menu.
4. Click *Insert*.
5. Rename the "Coverage Definition" object to "CoverageOfAOI".
6. Change the object color to Yellow.
7. Double click on "CoverageOfAOI" to open its Properties page.
    a. In the *CoverageOfAOI : Basic Grid* window:
        i. Change *Grid Area of Interest Type* to Custom Regions.
        ii. Click on the *Select Regions* button and move "Area_of_Interest" into the *Selected Regions* area of the window.
        iii. Click OK.
        iv. Change *Grid Definition Point Granularity* to 1 deg.
        v. Click the *Grid Constraint Options* button.
            1. Change the *Reference Constraint Class* to Transmitter.
            2. Highlight *Interferer/Int_Xmtr.*
            3. Check *Use Actual Object on the Grid Points.*
            4. Click OK.

b. In the *Coverage Definition : Basic Assets* window:
    i. Highlight "Receiver1", "Receiver2", and "Receiver3".
    ii. Click on the *Assign* button.
c. In the *CoverageOfAOI : 2D Graphics Attributes* window:
    i. Verify the *Show* box is checked.
    ii. Verify *Show Regions* is de-selected.
    iii. Verify *Show Points* is de-selected.
    iv. Verify *Progress of Computations* is checked.
    v. Click OK.

8. Save your progress.

G. Configure STK to Calculate the Antenna Gain Differences

1. Select Analysis in the STK toolbar and select *Analysis Workbench*.
2. Click on the *Calculation* tab.
3. Select *Facility-Interferer-Transmitter-Int_Xmtr-To-Satellite-My_Satellite-Receiver-Receiver1* in the left window.
    a. Click on the ( ) button to open the *Add Calculation Component* window.

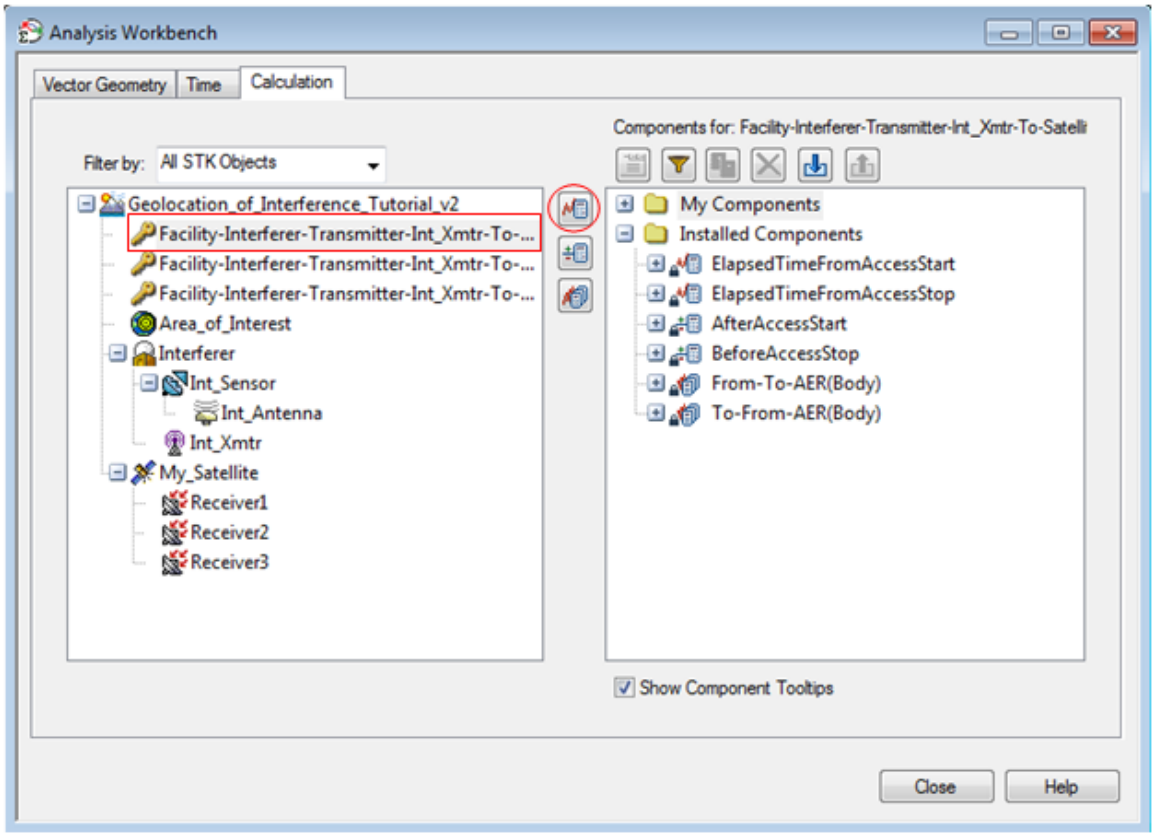

b. For the *Type* line, click *Select*.
c. Highlight Data Element and click OK.
d. Type "Gain_Rcvr1" for the *Name*.

e. In the *Select Data Element* window, click on the + button next to Link Information.
f. Scroll down and highlight Rcvr Gain.
g. **Make sure the *Use Samples* box is de-selected. (If you skip this step, STK will take hours to run the calculations!)**
h. The *Edit Component Properties* window should look like this:

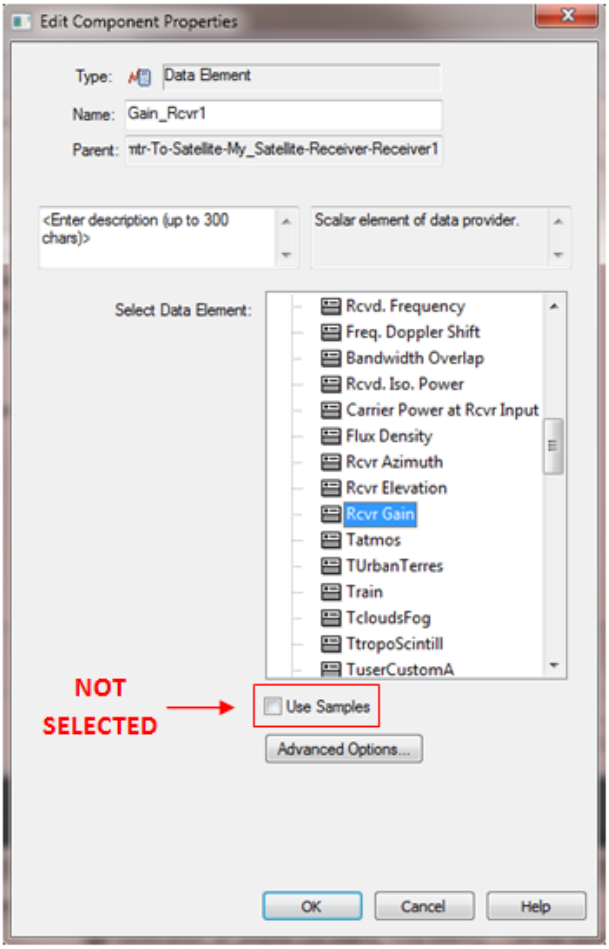

i. Click OK.
j. If you left click once to highlight "*Facility-Interferer-Transmitter-Int_Xmtr-To-Satellite-My_Satellite-Receiver-Receiver1*" you should see "Gain_Rcvr1" in the right window under *My Components*.

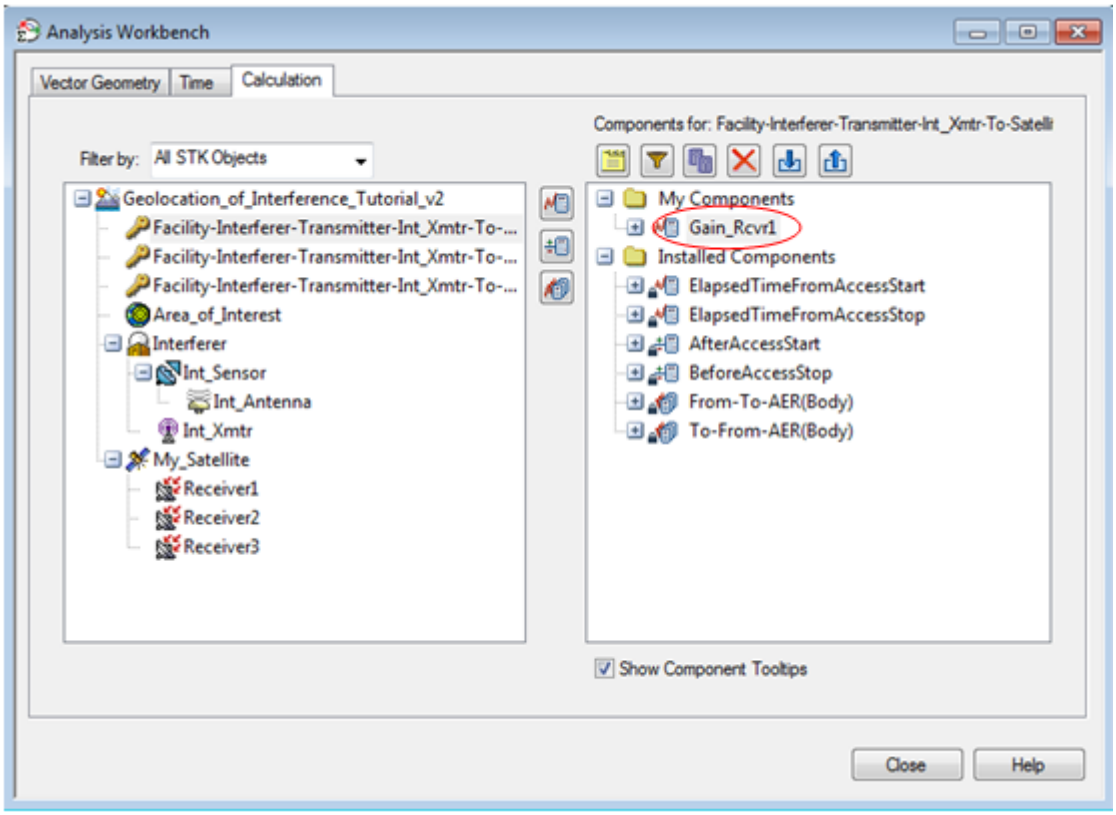

4. Select *Facility-Interferer-Transmitter-Int_Xmtr-To-Satellite-My_Satellite-Receiver-Receiver2* in the left window.
    a. Click on the ( ) button to open the *Add Calculation Component* window.

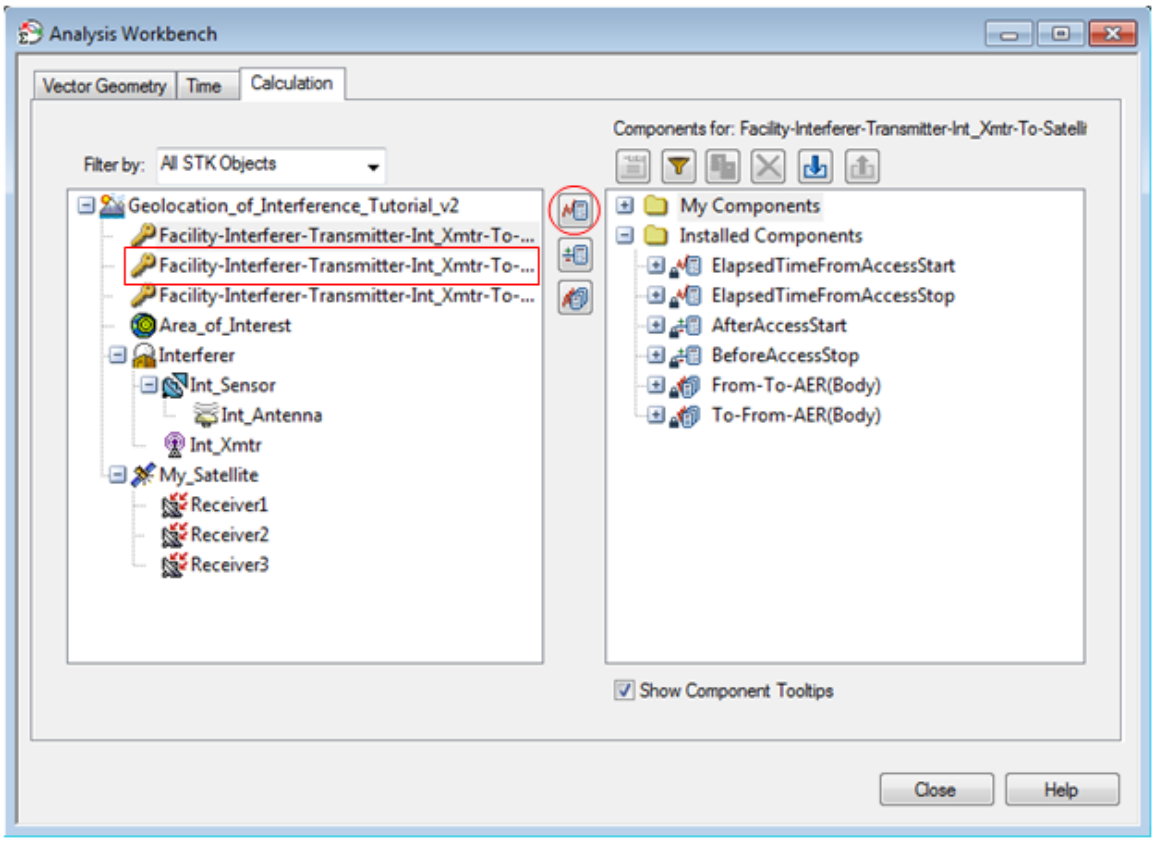

b. For the *Type* line, click *Select*.
c. Highlight Data Element and click OK.
d. Type "Gain_Rcvr2" for the *Name*.
e. In the *Select Data Element* window, click on the + button next to Link Information.
f. Scroll down and highlight Rcvr Gain.
g. **Make sure the *Use Samples* box is de-selected. (If you skip this step, STK will take hours to run the calculations!)**
h. Click OK.
i. If you left click once to highlight "*Facility-Interferer-Transmitter-Int_Xmtr-To-Satellite-My_Satellite-Receiver-Receiver2"* you should see "Gain_Rcvr2" in the right window under *My Components*.

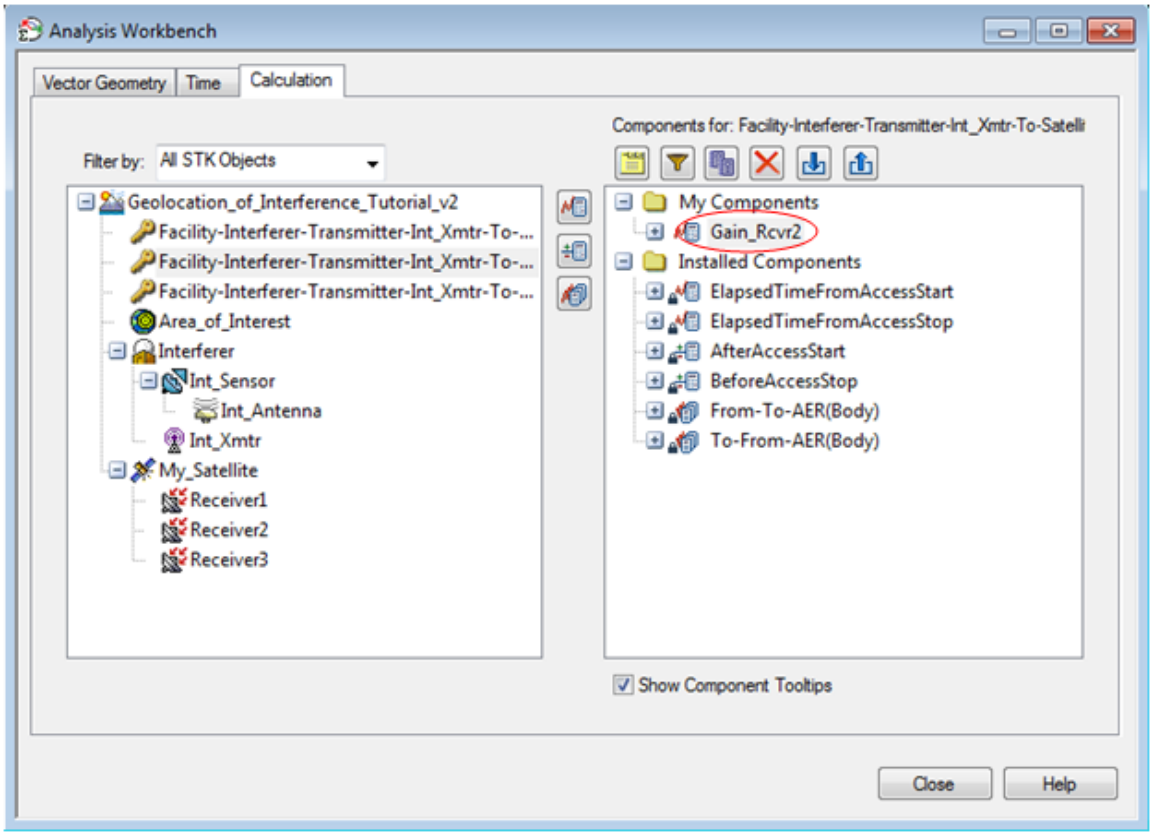

5. Select *Facility-Interferer-Transmitter-Int_Xmtr-To-Satellite-My_Satellite-Receiver-Receiver3* in the left window.
    a. Click on the ( ) button to open the *Add Calculation Component* window.

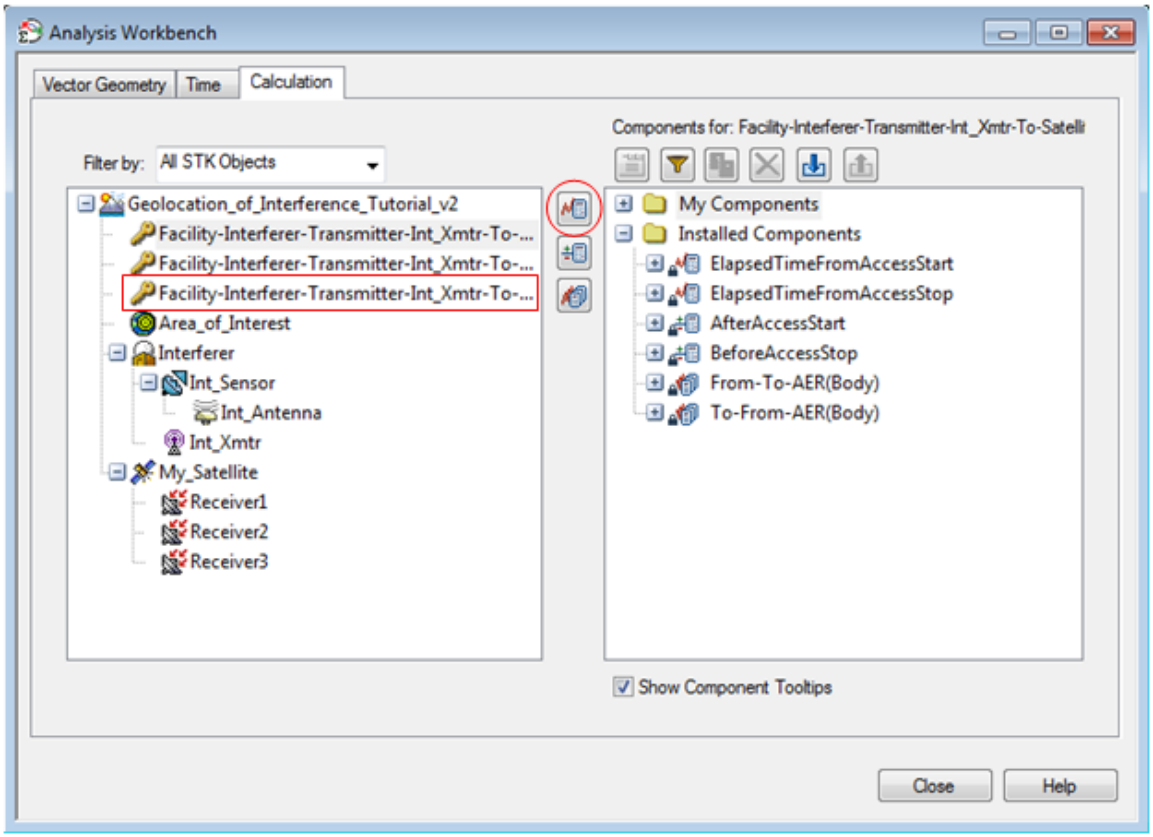

b. For the *Type* line, click *Select*.
c. Highlight Data Element and click OK.
d. Type "Gain_Rcvr3" for the *Name*.
e. In the *Select Data Element* window, click on the + button next to Link Information.
f. Scroll down and highlight Rcvr Gain.
g. **Make sure the *Use Samples* box is de-selected. (If you skip this step, STK will take hours to run the calculations!)**
h. Click OK.
i. If you left click once to highlight "*Facility-Interferer-Transmitter-Int_Xmtr-To-Satellite-My_Satellite-Receiver-Receiver3"* you should see "Gain_Rcvr3" in the right window under *My Components*.

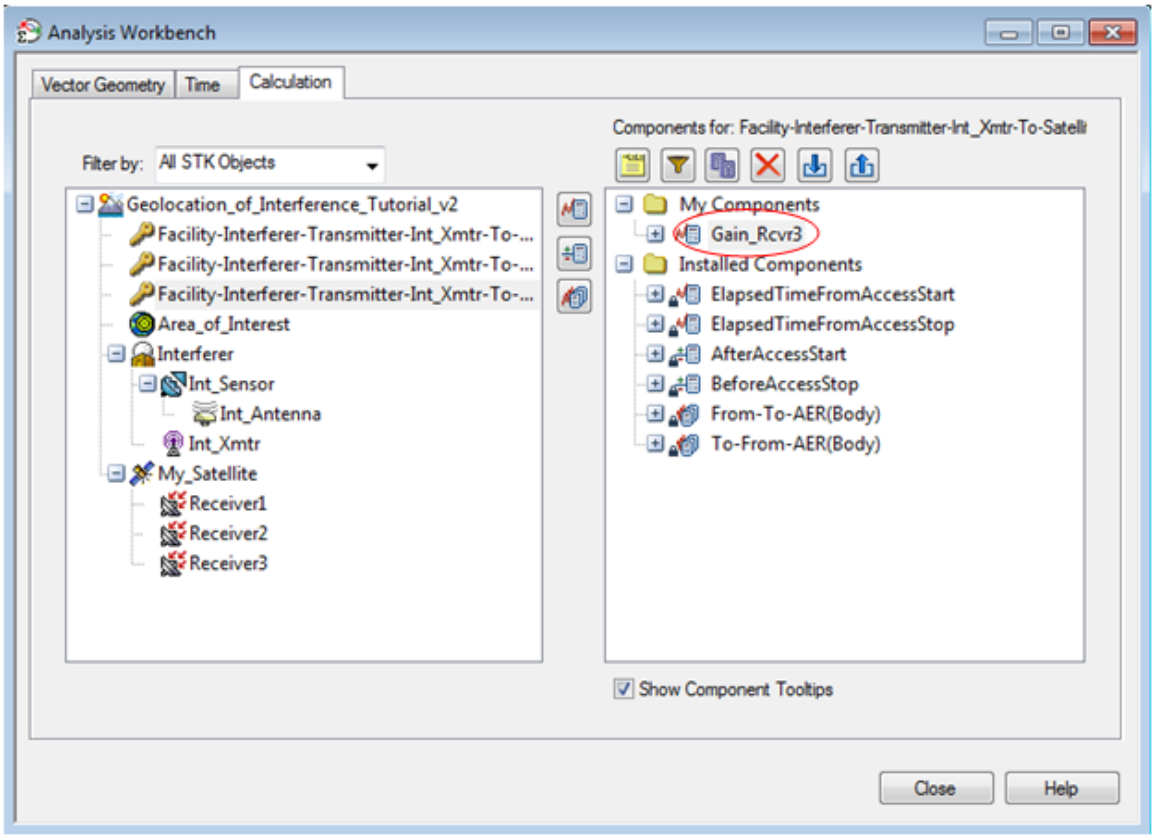

6. Save your progress.
7. Select "Int_Xmtr" in the *Analysis Workbench* left window.
    a. Click on the ( ) button to open the *Add Calculation Component* window.
    b. For the *Type* line, click Select.
    c. Highlight Function(x,y) and click OK.
    d. Type "DeltaGain_1-2" for the *Name*.
    e. Verify the *Function* is a*x + b*y.
    f. Under *Arguments*, select the ( ) next to *x*.
        i. In the left window, scroll up and highlight *Facility-Interferer-Transmitter-Int_Xmtr-To-Satellite-My_Satellite-Receiver-Receiver1*.
        ii. Select "Gain_Rcvr1" in the right window and click OK.
    g. Under *Arguments*, select the ( ) next to *y*.
        i. In the left window, scroll up and highlight *Facility-Interferer-Transmitter-Int_Xmtr-To-Satellite-My_Satellite-Receiver-Receiver2*.
        ii. Select "Gain_Rcvr2" in the right window and click OK.
    h. Verify the *Units* for *x* and *y* are dB.
    i. Under *Coefficients*:
        i. Verify that the coefficient for *a* is 1.
        ii. Change the coefficient for *b* to -1.

j. The *Edit Component Properties* should look like this:

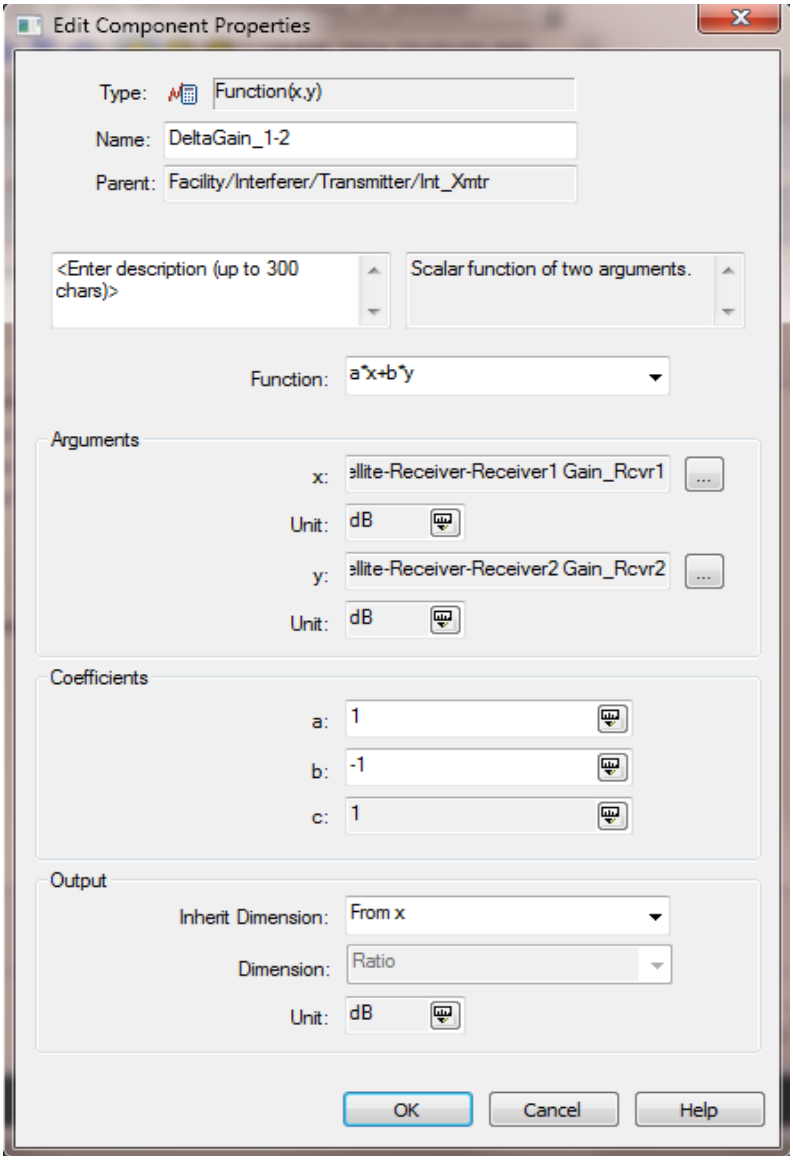

k. Click OK.

8. Save your progress.
9. With "Int_Xmtr" still selected in the *Analysis Workbench* left window:
   a. Click on the ( ) button to open the *Add Calculation Component* window.
   b. For the *Type* line, click Select.
   c. Highlight Function(x,y) and click OK.
   d. Type "DeltaGain_1-3" for the *Name*.
   e. Verify the *Function* is a*x + b*y.
   f. Under *Arguments*, select the ( ) next to *x*.

i. In the left window, scroll up and highlight *Facility-Interferer-Transmitter-Int_Xmtr-To-Satellite-My_Satellite-Receiver-Receiver1*.
ii. Select "Gain_Rcvr1" in the right window and click OK.

g. Under *Arguments*, select the (…) next to *y*.
i. In the left window, scroll up and highlight *Facility-Interferer-Transmitter-Int_Xmtr-To-Satellite-My_Satellite-Receiver-Receiver3*.
ii. Select "Gain_Rcvr3" in the right window and click OK.

h. Verify the *Units* for *x* and *y* are dB.
i. Under *Coefficients*:
i. Verify that the coefficient for *a* is 1.
ii. Change the coefficient for *b* to -1.

j. Click OK.

10. With "Int_Xmtr" still selected in the *Analysis Workbench* left window:
a. Click on the (…) button to open the *Add Calculation Component* window.
b. For the *Type* line, click Select.
c. Highlight Function(x,y) and click OK.
d. Type "DeltaGain_2-3" for the *Name*.
e. Verify the *Function* is a*x + b*y.
f. Under *Arguments*, select the (…) next to *x*.
i. In the left window, scroll up and highlight *Facility-Interferer-Transmitter-Int_Xmtr-To-Satellite-My_Satellite-Receiver-Receiver2*.
ii. Select "Gain_Rcvr2" in the right window and click OK.

g. Under *Arguments*, select the (…) next to *y*.
i. In the left window, scroll up and highlight *Facility-Interferer-Transmitter-Int_Xmtr-To-Satellite-My_Satellite-Receiver-Receiver3*.
ii. Select "Gain_Rcvr3" in the right window and click OK.

h. Verify the *Units* for *x* and *y* are dB.
i. Under *Coefficients*:
i. Verify that the coefficient for *a* is 1.
ii. Change the coefficient for *b* to -1.

j. Click OK.

11. Now, if you highlight "Int_Xmtr" in the *Analysis Workbench* left window, you should see the following elements:

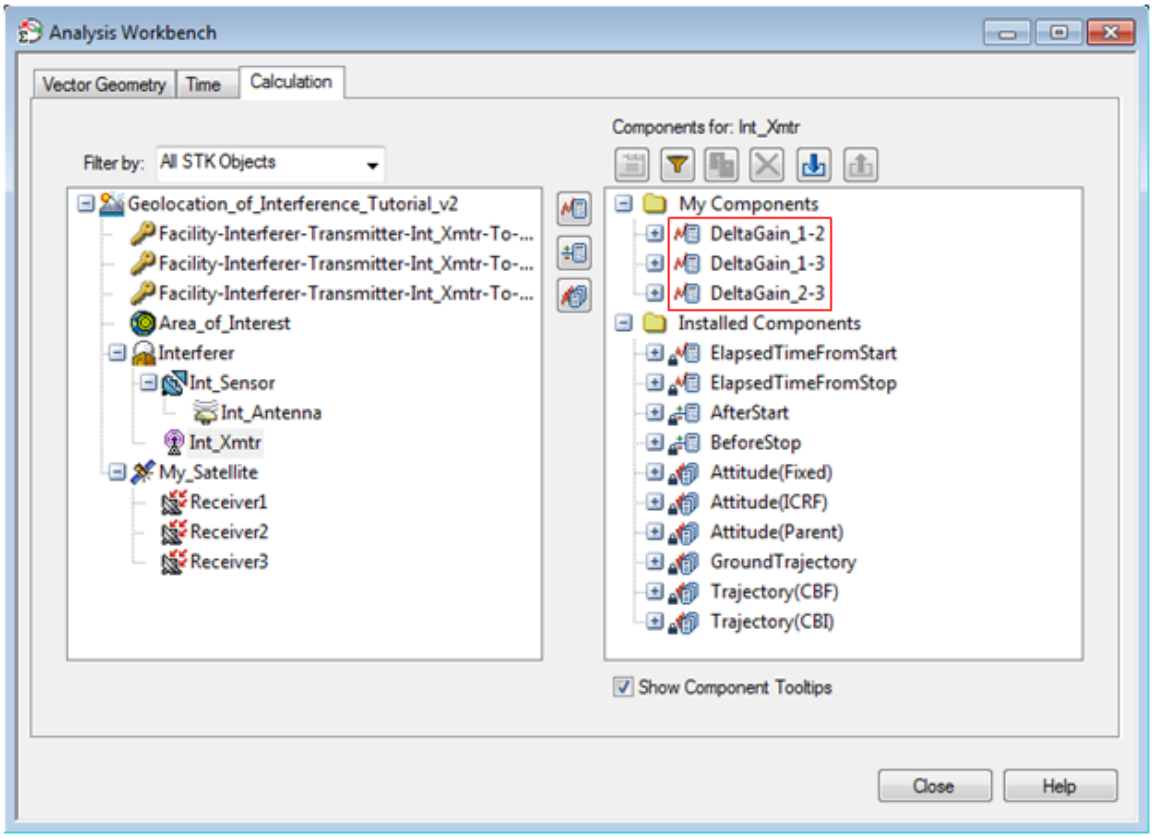

12. Click Close.
13. Save your progress.

H. Configure STK to Display Difference Contours

1. Highlight "CoverageOfAOI" in the *Object Browser*.
2. Select Insert from the STK toolbar and select *Default Object*.
3. Select *Figure of Merit* from the menu.
4. Click *Insert*.
5. Rename the "FigureOfMerit1" object to "DeltaGain_1-2".
6. Double click on "DeltaGain_1-2" to open its Properties page.
    a. In the *DeltaGain_1-2 : Basic Definition* window:
        i. Click on *Type* and select Scalar Calculation from the drop down menu.
        ii. Click the (...) button next to *Scalar*.
            1. Scroll down in the left window and highlight "Int_Xmtr".
            2. Select "DeltaGain_1-2" in the right window and click OK.
    b. In the *DeltaGain_1-2 : 2D Graphics Animation* window:
        i. Verify *Hide all Animation and Static Graphics* is not checked.
        ii. Verify *Show Animation Graphics* is not checked.
    c. In the *DeltaGain_1-2 : 2D Graphics Static* window:
        i. Verify *Show Static Graphics* is checked.

ii. Verify Filled Area in the *Show Points As* section is selected with 50% Translucency.
iii. Verify Show Contours in the *Display Metric* section is selected.
iv. Verify *Do not show areas where FOM value exceeds max contour level* is checked.
v. Verify *Color Method* is set to Explicit.
vi. Verify Natural Neighbor Sampling under *Contour Interpolation* is checked and set to Medium Sampling.
vii. Click OK.

7. Select "DeltaGain_1-2" by clicking on it once with the left mouse button.
8. Press "CTRL + C".
9. Select "CoverageOfAOI" by clicking on it once with the left mouse button.
10. Press "CTRL + V" two times.
11. Rename one of the *FigureOfMerit* objects "DeltaGain_1-3".
12. Double click on "DeltaGain_1-3" to open its Properties page.
    a. In the *DeltaGain_1-3 : Basic Definition* window:
        i. Click on *Type* and select Scalar Calculation from the drop down menu.
        ii. Click the ( ) button next to *Scalar*.
            1. Scroll down in the left window and highlight "Int_Xmtr".
            2. Select "DeltaGain_1-3" in the right window and click OK.
13. Rename the remaining *FigureOfMerit* object to "DeltaGain_2-3".
14. Double click on "DeltaGain_2-3" to open its Properties page.
    a. In the *DeltaGain_2-3 : Basic Definition* window:
        i. Click on *Type* and select Scalar Calculation from the drop down menu.
        ii. Click the ( ) button next to *Scalar*.
            1. Scroll down in the left window and highlight "Int_Xmtr".
            2. Select "DeltaGain_2-3" in the right window and click OK.
15. Save your progress.
16. Right click on "CoverageOfAOI".
    a. Scroll down to *CoverageDefinition* in the drop down menu.
        i. Select *Compute Accesses* **(this may take a minute to compute)**.
17. Your *Object Browser* window should look as follows:

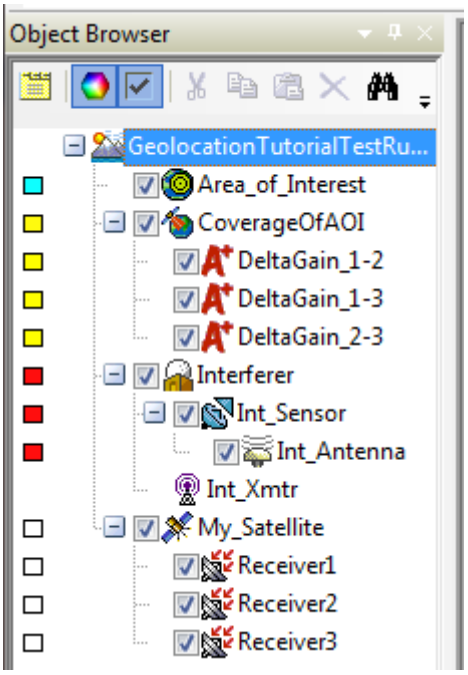

18. Save your progress.

I. Test the Model

1. Right click on "CoverageOfAOI" in the *Object Browser* window and select Report & Graph Manager from the drop down menu.
    a. Change the *Object Type* to Access.
    b. Left click once to highlight "*Facility-Interferer-Transmitter-Int_Xmtr-To-Satellite-My_Satellite-Receiver-Receiver1*".
        i. Under *Installed Styles* in the right window, scroll down and select Link Budget – Detailed.
        ii. Click *Generate*.
        iii. Scroll to the right in the *Detailed Link Budget* window and stop at the Rcvr Gain (dB) column.
        iv. Record this number as G_1 (32.8677 dB).
        v. Close the *Detailed Link Budget*.
    c. Left click once to highlight "*Facility-Interferer-Transmitter-Int_Xmtr-To-Satellite-My_Satellite-Receiver-Receiver2*".
        i. Under *Installed Styles* in the right window, scroll down and select Link Budget – Detailed.
        ii. Click *Generate*.
        iii. Scroll to the right in the *Detailed Link Budget* window and stop at the Rcvr Gain (dB) column.
        iv. Record this number as G_2 (30.7031 dB).
        v. Close the *Detailed Link Budget*.
    d. Left click once to highlight "*Facility-Interferer-Transmitter-Int_Xmtr-To-Satellite-My_Satellite-Receiver-Receiver3*".

i. Under *Installed Styles* in the right window, scroll down and select Link Budget – Detailed.
ii. Click *Generate*.
iii. Scroll to the right in the *Detailed Link Budget* window and stop at the Rcvr Gain (dB) column.
iv. Record this number as G_3 (35.4421 dB).
v. Close the *Detailed Link Budget*.

2. Close the *Report & Graph Manager* window.
3. Use the Microsoft Excel calculator below to compute the differences in the Gain Measurements from each Receiver (if using Microsoft Word, double click anywhere inside the table to activate it):
   a. Enter the values for G_1, G_2, and G_3 (Step 1 above) in the corresponding yellow cells under *Signal Strength Measurements*.
   b. Verify the *Desired Resolution* cell is set to 1.0.
   c. The three values in the green *Difference Contours* cells represent the computed contours for the antenna pairs. The *Plot* cells will be used in the next steps.

Signal Strength Measurements (dB)		
G1	G2	G3
32.8677	30.7031	35.4421

Desired Resolution (dB)
1.0

Difference Contours		
G1 - G2	G1 - G3	G2 - G3
2.1646	-2.5744	-4.7390

Plot		
G1 - G2	G1 - G3	G2 - G3
1.6646	-3.0744	-5.2390
3.6646	-1.0744	-3.2390

4. Double click on the "DeltaGain_1-2" Figure of Merit Object to open its Properties page.
5. In the *DeltaGain_1-2 : 2D Graphics Static* window:
   a. Enter 1.6646 (from the *Plot G1-G2* cell in the calculator above) as the *Start* value.
   b. Enter 3.6646 (from the *Plot G1-G2* cell in the calculator above) as the *Stop* value.
   c. Enter 1 as the *Step* value.
   d. Click *Add Levels*.
   e. Verify there are now **two** levels in the *Level Attributes* section. (If there are **three** levels, select and remove the level that does not contain the $G_x - G_y$ difference contour. This should be the greatest numerical value of the three levels and is probably located at the lowest position in the *Level Attributes* list. This is an occasional bug in STK!)
   f. Double click on the color box next to 1.6646 dB in the *Level Attributes* section and change the color to Red.

g. Click OK **(this may take a few minutes to complete and for the window to close)**.
h. You should now see a red contour line in the "Area_of_Interest" in the *2D Graphics Window*.

6. In the *DeltaGain_1-3 : 2D Graphics Static* window:
   a. Enter -3.0744 (from the *Plot G1-G3* cell in the calculator above) as the *Start* value.
   b. Enter -1.0744 (from the *Plot G1-G3* cell in the calculator above) as the *Stop* value.
   c. Enter 1 as the *Step* value.
   d. Click *Add Levels*.
   e. Verify there are now **two** levels in the *Level Attributes* section. (If there are **three** levels, select and remove the level that does not contain the $G_x - G_y$ difference contour. This should be the greatest numerical value of the three levels and is probably located at the lowest position in the *Level Attributes* list. This is an occasional bug in STK!)
   f. Double click on the color box next to -3.0744 dB in the *Level Attributes* section and change the color to Red.
   g. Click OK **(may take a few minutes to complete and for the window to close)**.
   h. You should now see a red contour line in the "Area_of_Interest" in the *2D Graphics Window*.
7. In the *DeltaGain_2-3 : 2D Graphics Static* window:
   a. Enter -5.239 (from the *Plot G2-G3* cell in the calculator above) as the *Start* value.
   b. Enter -3.239 (from the *Plot G2-G3* cell in the calculator above) as the *Stop* value.
   c. Enter 1 as the *Step* value.
   d. Click *Add Levels*.
   e. Verify there are now **two** levels in the *Level Attributes* section. (If there are **three** levels, select and remove the level that does not contain the $G_x - G_y$ difference contour. This should be the greatest numerical value of the three levels and is probably located at the lowest position in the *Level Attributes* list. This is an occasional bug in STK!)
   f. Double click on the color box next to -5.239 dB in the *Level Attributes* section and change the color to Red.
   g. Click OK **(may take a few minutes to complete and for the window to close)**.
   h. You should now see a red contour line in the "Area_of_Interest" in the *2D Graphics Window*.
8. The intersection of the three contour lines is the geolocation:

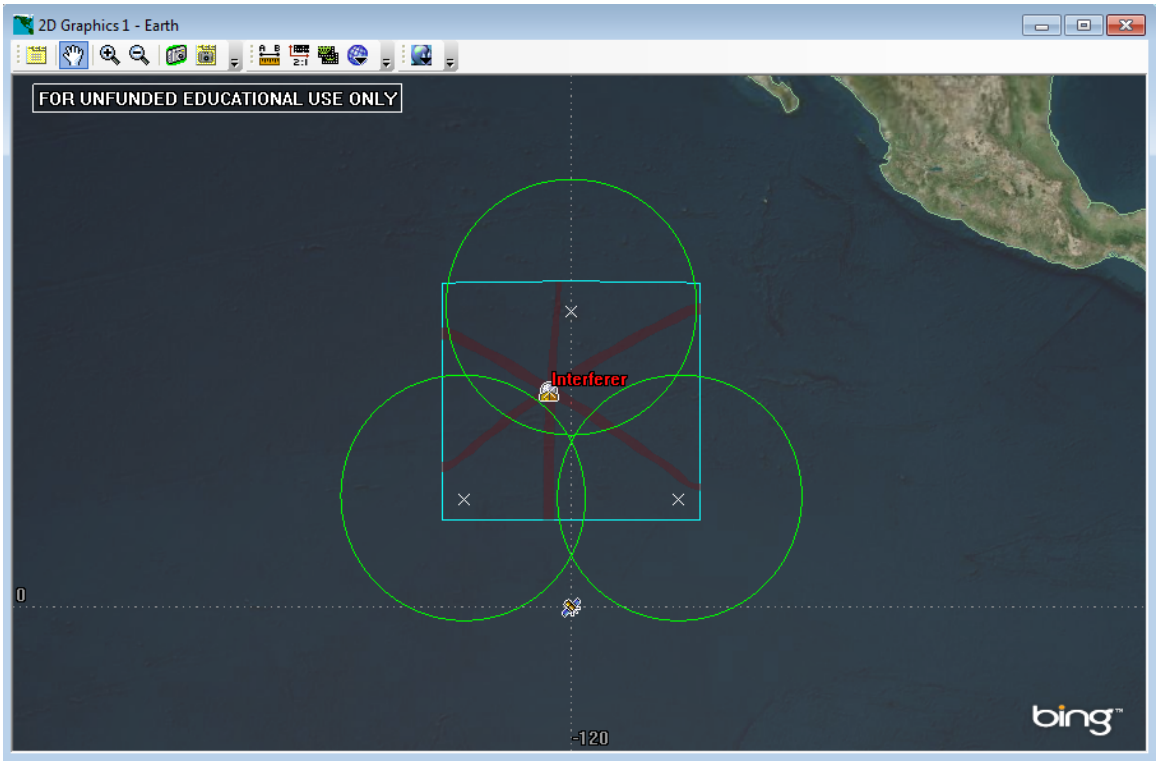

9. Save your progress.

J. Adapt the Model to a Real-world Scenario

Having comfortably completed the tutorial thus far, it is a relatively simple matter to adapt the model to a completely different set of specifications. What follows is a sample checklist that walks the user back through the tutorial to assist in successfully changing it to meet the user's needs.

1. Before altering the scenario, it is necessary to save a copy of the working scenario. In STK, simply changing the Scenario File name will not actually make a separate copy of the scenario. In order to maintain the integrity of the scenario created by in the tutorial, you have to copy all of the STK files to a new folder and then change the Scenario File name:
    a. Select File from the STK toolbar and click on *Save As*.
    b. In the *Save As* window, click on the *Up One Level* ( ) button.
    c. Click on the *New Folder* ( ) button and name the folder My_Scenario (or a name of your choosing).
    d. Still in the *Save As* window, double click on My_Scenario.
        i. In the *File name* area, name the new scenario My_Scenario and click *Save*.
2. Make changes to Part A – Create the Scenario.

a. Double click on "My_Scenario" in the *Object Browser* window to open its Properties page.
b. In this window, you can change the *Analysis Period* of your scenario.
c. You can also click on *Description* to provide a plain English description of your scenario parameters.

3. Make changes to Part B – Model the Satellite.
    a. Change the satellite parameters as required.
4. Make changes to Part C – Configure the Satellite Receiver Model.
    a. Be sure to change all applicable parameters for each antenna you are modeling. Some things you may need to change include:
        i. Frequency
        ii. Antenna Type
        iii. Antenna Frequency
        iv. Antenna Beamwidth
        v. Antenna Orientation
5. Make changes to Part D – Create an Area Target.
    a. Change the points to the new area of interests created by the intersection of the antenna fields of view in your scenario.
6. Make changes to Part E – Model a Transmitter. Since the transmitter object is mainly used for STK to close the communication link and calculate Link Budget parameters, the location and parent object of this transmitter are essentially arbitrary. You can still use it to verify that your adapted model is functioning properly when you are done making changes.
    a. Change the frequency and modulation to match the parameters used for the Receiver object in Part C.
    b. Click on the *Access* icon ( ) and verify STK is computed the accesses between your Transmitter object and your Receiver objects.
7. Make changes to Part F – Create a Coverage Definition.
    a. Verify the *Selected Region* is your Area Target.
    b. Verify the *Grin Constraint Options* Transmitter is still your transmitter.
    c. Verify the *Assigned Assets* are your receivers.
8. Make changes to Part G – Configure STK to Calculate the Antenna Gain Differences.
    a. You may have to re-create the necessary *Scalar Data Elements* and *Scalar Functions* using your own objects.
9. Make changes to Part H – Configure STK to Display Difference Contours.
    a. Verify that each FOM object is still using the correct *Scalar* component.
    b. Right click on your Coverage Definition object, scroll down to *CoverageDefinition* and select *Clear Accesses*.
    c. Then select *Compute Accesses*.
10. Make changes to Part I – Test the Model.
    a. Run the Link Budget – Detailed report for each of your receivers and record the Rcvr Gain values.
    b. Use the provided calculator to compute the Difference Contours for your Desired Resolution.

c. Change each FOM object to display the contours. Verify that your Transmitter object is located in the intersection of the three Difference Contours.

Now the model is ready to geolocate *unknown* interfering transmitters. When interference is detected, simply enter the signal strength measurements for each antenna into the provided calculator and plot the difference contours.

LIST OF REFERENCES

[1] G. Maral and M. Bousquet, *Satellite Communications Systems*, 4th ed. West Sussex, England: John Wiley & Sons, 2002.

[2] J. R. Wertz, D. F. Everett, and J. J. Puschell, Eds., *Space Mission Engineering:The New SMAD*, Hawthorne, CA: Microcosm Press, 2011.

[3] "Basic Satellite Communications System Image." [Online]. Available: http://www.radio-electronics.com/info/satellite/communications_satellite/communications_satellite.gif.

[4] A. C. Clarke, "Extra-terrestrial relays," *Wireless World*, vol. LI, no. 11, pp. 305–308, Oct. 1945.

[5] The President's National Security Telecommunications Advisory Committee, "NSTAC report to the president on commercial satellite communications mission assurance," U.S. Department of Homeland Security, Washington, DC, Nov. 2009.

[6] D. L. Oltrogge and H. Rashid, "Effective strategies for satellite communications RFI mitigation," presented at the 2012 IEEE First AESS European Conference on Satellite Telecommunications (ESTEL), Rome, Italy, 2012.

[7] *Joint Spectrum Interference Resolution (JSIR) Procedures*, Chairman of the Joint Chiefs of Staff Manual (CJCSM 3320.02D), June 3, 2013.

[8] B. R. Elbert, *Introduction to Satellite Communication*, 3rd ed. Norwood, MA: Artech House, 2008.

[9] H. H. Loomis, "Geolocation of electromagnetic emitters," Naval Postgraduate School, Monterey, CA, Rep. NPS-EC-00-003, 2007, p. 1

[10] I. Progri, *Geolocation of RF Signals Principles and Simulations*, 1st ed. New York, NY: Springer Science + Business Media, 2011, pp. 3–5.

[11] FCH Ltd., "C band single antenna footprint." [Online]. Available: http://www.fchorizon.com/images/telstar10.jpg.

[12] S. Quayle, "Ku band single antenna footprint" [Online]. Available: http://www.stevequayle.com/imgs/telstar5_ku_footprint.b.jpg.

[13] J. Christensen, "ITU regulations for Ka-band satellite networks" [Online]. Available: http://www.itu.int/en/Pages/default.aspx.

[14] K. Singarajah, “Overview of Ka-band satellite system developments & key regulatory issues,” presented at the ITU Conference on Prospects for Use of the Ka-Band by Satellite Communication Systems, Almaty, Kazakhstan, Sept. 2012.

[15] Ground Control Global Satellite Communications, “Global Xpress coverage map.” [Online]. Available: http://www.groundcontrol.com/Global_Xpress_Coverage_Map.htm. [Accessed: 17-Jul-2013]

[16] Analytic Graphics Inc., Systems Tool Kit 10.0.2 Software Help, July 2013.

[17] Boeing, “WGS payload block diagram.” [Online]. Available: http://www.boeing.com/boeing/defense-space/space/bss/factsheets/702/wgs/wgs_factsheet.page.

[18] M. Hayes and M. Robusto, *Locating and resolving source of satellite interference to improve spectrum efficiency*, unpublished.

[19] Math-Prof.com. “Hexagon Area Calculator.” [Online]. Available: http://www.math-prof.com/AreaVolume/Hexagon.aspx

[20] inmarsat, “Global Xpress” [Online]. Available: http://www.inmarsat.com/about-us/our-satellites/global-xpress/.

[21] Boeing, “Transformational wideband communication capabilities for the warfighter” [Online]. Available: http://www.boeing.com/boeing/defense-space/space/bss/factsheets/702/wgs/wgs_factsheet.page

[22] ViaSat, “About ViaSat” [Online]. Available: http://www.viasat.com/company/about/about-viasat.

[23] ViaSat, “ViaSat-1 launch” [Online]. Available: http://www.viasat.com/viasat-1-launch.

[24] “ViaSat-1.” [Online]. Available: http://en.wikipedia.org/wiki/ViaSat-1.

[25] Lockheed Martin, “MUOS Fact Sheet.” [Online]. Available: http://www.lockheedmartin.com/content/dam/lockheed/data/space/documents/MUOS/B1369220_MUOS%20Factsheet.pdf.

INITIAL DISTRIBUTION LIST

1. Defense Technical Information Center
   Ft. Belvoir, Virginia

2. Dudley Knox Library
   Naval Postgraduate School
   Monterey, California